REPORT DOCUMENTATION PAGE

Form Approved
OMB No. 0704-0188

1. AGENCY USE ONLY *(Leave Blank)*	2. REPORT DATE	3. REPORT TYPE AND DATES COVERED
	June 1990	Final 0688-0690

4. TITLE AND SUBTITLE
A Theoretical Investigation Into the Inelastic Behavior of Metal-Matrix Composites

5. FUNDING NUMBERS

6. AUTHOR(S)
William F. Ward

7. PERFORMING ORGANIZATION NAME(S) AND ADDRESS(ES)
USASD
FBH, IN 46216

Georgia Institute of Technology
School of Mechanical Engineering
Atlanta, GA 30332

8. PERFORMING ORGANIZATION REPORT NUMBER

9. SPONSORING/MONITORING AGENCY NAME(S) AND ADDRESS(ES)

10. SPONSORING/MONITORING AGENCY REPORT NUMBER

11. SUPPLEMENTARY NOTES

12a. DISTRIBUTION/AVAILABILITY STATEMENT

12b. DISTRIBUTION CODE

13. ABSTRACT *(Maximum 200 words)*

Various self-consistent analysis have been proposed and used to approximately evaluate the elastic stiffness and elastic-plastic behavior of metal-matrix composites. Such analysis have generally relied on very simple theoretical models for the matrix inelastic stress-strain response. This was perhaps substantiated on the basis of a lack of combined stress state experiments. Weng (1988) successfully approximated the inelastic behavior of spherical particle-reinforced utilizing a modified self-consistent model called the equivalent inclusion-average stress (EIAS) method. Noting the overly stiff response of the basic EIAS model, he developed the "secant modulus" method to correct for the overconstraining power of the matrix. The purpose of this thesis is to reexamine the problem in the context of more sophisticated nonlinear kinematic hardening rules for the matrix. An EIAS method which incorporates a tangent stiffness formulation based on incremental plasticity is proposed. It is shown that this method is comparable to Weng's secant modulus method. A β parameter and χ function are proposed to correct (continued)

14. SUBJECT TERMS	15. NUMBER OF PAGES
Metal-matrix composites, plasticity, inelasticity, boron-aluminum equivalent inclusion-average stress (EIAS) method	130
	16. PRICE CODE

17. SECURITY CLASSIFICATION OF REPORT	18. SECURITY CLASSIFICATION OF THIS PAGE	19. SECURITY CLASSIFICATION OF ABSTRACT	20. LIMITATION OF ABSTRACT
UNCLASS	UNCLASS	UNCLASS	

REPORT DOCUMENTATION PAGE

Part 13. Abstract (continued):

for the constraining power of the matrix due to eigenstrain accumulation and anisotropy due to fiber reinforcement. The proposed EIAS method-tangent stiffness formulation with the β parameter and χ function produces satisfactory results when compared to existing experimental data for the Boron-Aluminum system.

A THEORETICAL INVESTIGATION INTO THE INELASTIC BEHAVIOR OF METAL-MATRIX COMPOSITES

A THESIS
Presented to
The Academic Faculty
By

Captain William F. Ward
United States Army

In Partial Fulfillment
of the Requirements for the Degree
Master of Science in Mechanical Engineering

Georgia Institute of Technology
June, 1990

TABLE OF CONTENTS

Table of Contents (continued)

ACKNOWLEDGEMENTS

I would like to thank the United States Army and the United States Military Academy for providing me with the opportunity to prove myself in the academic arena. Also, to my fellow graduate students, thanks for your support and friendship. I am eternally grateful to my advisor, Dr. McDowell, without whom none of this work would have been possible. Last, but definitely not least, I want to thank my lovely wife Erin for her unending support and understanding.

LIST OF FIGURES

List of Figures (continued)

SUMMARY

Various self-consistent analyses have been proposed and used to approximately evaluate the elastic stiffness and elastic-plastic behavior of metal matrix composites. Such analyses have generally relied on very simple theoretical models for the matrix inelastic stress-strain response. This was perhaps substantiated on the basis of a lack of combined stress state experiments. Recent biaxial loading experiments conducted by Dvorak and Bahei-El-Din on unidirectional, fiber-reinforced Boron-Aluminum resulted in the apparent inapplicability of prior self-consistent approaches based on (i) the measurement of "flats" on the composite yield surface and (ii) nonnormality of the plastic strain increment with respect to the yield surface. Dvorak and Bahei-El-Din (1987) introduced a new theory, the so-called Bimodal Theory of Fibrous Composites, in response to these apparent deficiencies.

Weng (1988) successfully approximated the inelastic behavior of spherical particle-reinforced composites utilizing a modified self-consistent model called the equivalent inclusion-average stress (EIAS) method. Noting the overly stiff response of the basic EIAS model, he developed the "secant modulus" method to correct for the overconstraining power of the matrix.

The purpose of this thesis is to reexamine the problem in the context of more

sophisticated nonlinear kinematic hardening rules for the matrix. An EIAS method which incorporates a tangent stiffness formulation based on incremental plasticity is proposed. It is shown that this method is comparable to Weng's secant modulus method. A β parameter and χ function are proposed to correct for the constraining power of the matrix due to eigenstrain accumulation and anisotropy due to fiber reinforcement. The proposed EIAS method-tangent stiffness formulation with the β parameter and χ function produces satisfactory results when compared to existing experimental data for the Boron-Aluminum system.

CHAPTER I

INTRODUCTION

Metal matrix composites (MMCs) represent an important component of today's materials technology. With their ductile matrices and high-strength fibers, MMCs offer high strength/weight ratios, superior resistance to corrosive environments, and the potential for high-temperature applications. Therefore, in spite of their high production costs and specialized fabrication techniques, designers prefer MMCs over the more widely employed resin matrix composites (Pindera and Lin, 1989) for many applications.

In order to take full advantage of the many attractive features offered by MMCs, it is necessary to understand and be able to accurately model their response in the nonlinear range. While researchers have enjoyed reasonable success in modeling the inelastic response of spherical particle-reinforced composites (Tandon and Weng, 1984; Weng, 1988), the formulation of constitutive relations for continuous fiber-reinforced composites has been frustrated by the lack of reasonably simple solutions which would describe the fiber-matrix interaction and its effect on plastic deformation. Progress has been made only in special cases where certain limitations are placed on the loading conditions or constituent materials (Dvorak and Bahei-El-

Din, 1982).

Experimental evidence indicates that the failure strain of the composite will be of the same order of magnitude as that of the elastic fiber (approximately 0.009 for boron, for example) which signifies that the deformation of MMCs is limited to the range of small strains. In this situation, plasticity analysis of MMCs is best accomplished using the micromechanics approach, which not only produces the effective response of the composite, but also provides an indication of the state of stress in the composite's constituent phases. Micromechanical theories calculate the overall response of the composite from the constituent properties and from their mutual constraints which are given by microstructural geometry (Dvorak and Bahei-El-Din, 1982).

Several different micromechanical approaches have been employed previously to model the inelastic response of MMCs. These range from mixture theories for unidirectional fiber-reinforced composites (c.f. Murakami and Hegemier, 1986) and self-consistent schemes (c.f. Hill, 1965a; 1965b; 1965c) to finite element analyses of a repeating unit cell (c.f. Dvorak, Roa, and Tarn, 1974). The most recent developments in the constitutive theory of the nonlinear response of unidirectional MMCs, based on the micromechanics approach, include the models proposed by Dvorak and Bahei-El-Din (1982, 1987) and Aboudi (1986), among others (Teply and Dvorak, 1985 and 1988).

Dvorak and Bahei-El-Din have made significant contributions to the plasticity

analysis of fibrous composites. These contributions include micromechanical models which derive the overall response from uniform local fields (averaging models), as well as models which approximate the actual nonuniform local fields and arrive at upper and lower bound solutions (bounding models) (Bahei-El-Din and Dvorak, 1989). Perhaps their most significant contribution in this area came as a result of experiments performed on unidirectionally reinforced B/Al tubes in order to characterize the elastic-plastic behavior of composites under combined stress states. Based on their observations, they developed and proposed the "bimodal plasticity theory of fibrous composites" (Dvorak, 1987). The bimodal theory deals primarily with the determination of composite yield surfaces and in that respect may be regarded as an application of classical incremental plasticity theory to heterogeneous composites.

The bimodal theory submits that the elastic-plastic response of MMCs reinforced by aligned, continuous fibers can be described in terms of two distinct modes. In the matrix-dominated mode, the composite deforms primarily by plastic slip in the matrix, on planes which are parallel to the fiber axis. In the fiber-dominated mode, both phases deform together as a heterogeneous medium in the elastic and plastic range. This theory admits two distinct overall deformation modes which may exist in binary elastic-plastic fibrous composite systems under certain loading conditions. To each mode there corresponds a segment of the composite yield surface which reflects the onset of yielding of the matrix phase in that particular

mode, the envelope of these two segments comprises the composite yield surface. They derived constitutive equations for the matrix-dominated mode of deformation while the response of the fiber-dominated mode of deformation is approximated by a self-consistent model. The two deformation modes give different branches of the composite yield surface which identify the state of stress that activates a particular mode, and indicate the conditions for mode transition in a given composite system. The matrix-dominated mode is found to exist in systems reinforced by fibers of high longitudinal shear stiffness, such as boron. Systems reinforced with more compliant fibers, such as graphite, appear to deform exclusively in the fiber-dominated mode (Dvorak and Bahei-El-Din, 1987).

Dvorak and Bahei-El-Din concede that some observed phenomena cannot be fully explained by the theory and appear to violate some of the classical assumptions of plasticity theory (eg. Drucker's hypothesis). For instance, they observed "flats" in the composite yield surfaces and non-normality of the plastic strain rate vector to the composite yield surface (Dvorak, 1987; Dvorak and Bahei-El-Din, 1988).

Another recent work which stimulated application of the Equivalent Inclusion-Average Stress (EIAS) method in this thesis was that of Weng (1988). Weng's work focussed on application to particle-reinforced composites, but the idea of relaxing constraint in the EIAS method during plastic flow is especially relevant to our analysis of fibrous-reinforced composites.

In a two-phase composite containing spherical inclusions, two distinct modes

of plastic deformation may take place. The first one is that the matrix will remain elastic, and the inclusions are the plastically deforming phase. The second one is that the inclusions will remain elastic and the matrix is the plastically deforming one. As the constraining power

imposed on the deformation of the inclusions is exercised by their surrounding matrix, these two types of composites will exhibit different constraining effects. In the former case, as the matrix remains elastic, its constraint power will remain constant and be may aptly represented by its elastic stiffness tensor. Weng terms this type of composite, with plastically deforming inclusions, a composite of the first kind. In the second case, the continuous plastic flow of the matrix phase will lead to a weakening constraint power and, therefore, the equation describing the deformation of the inclusions must incorporate such an effect. This type of composite, with the matrix being the plastically deforming phase, is termed a composite of the second kind. Since this thesis focuses on composites of the second kind, we will direct our attention to Weng's treatment of the same.

Weng's methods for analyzing composite plasticity are based on Mori-Tanaka's concept of average stress in the matrix, in conjunction with Eshelby's solution of an ellipsoidal inclusion. Hence, an "interaction strain" is introduced in addition to Eshelby's transformation strain to enhance description of inclusion interaction effects at higher volume fractions. This method will heretofore be referred to as the equivalent inclusion-average stress or EIAS method. Weng presents two solution

procedures for solving the problem of composite plasticity for composites of the second kind. The first method is an EIAS method with elastic constraint. In this method, plastic strain in the matrix is treated as a negative eigenstrain in the comparison material. The comparison material has the same elastic moduli as the matrix material and remains elastic throughout the solution procedure. This causes an overconstraining effect, resulting in an overly stiff composite response in the plastic regime (Weng, 1988).

Weng's second solution procedure is a novel EIAS method with a secant moduli formulation. Since he intended to apply his theory for monotonic, proportional loading, he employed the deformation theory of plasticity instead of an incremental theory to model behavior of the matrix. With a ductile matrix material, there is decreasing constraining power of the matrix material as plastic flow increases. To account for this decreasing constraint, Weng utilizes the "secant modulus" approach to calculate the stiffness of the comparison material. The secant modulus accounts for both plasticity and the weakening constraint power of the matrix; therefore, negative eigenstrains are not used to account for the plastic strain in the matrix as with the original EIAS method with elastic constraint. However, ε^*, Eshelby's transformation strain, is still used to account for inclusion-matrix misfit which is inherent in the EIAS approach. Weng notes that for spherical particle-reinforced composites, this method produces much better results than the EIAS method with elastic constraint (1988).

The purpose of this thesis is to develop a constitutive model which predicts the overall response of the composite under quite generally incrementally applied uniform macroscopic stresses or strains in terms of the constituent properties and the geometry of the microstructure. Utilizing Weng's analysis of the composite of a second kind as a starting point, we develop three material models for analyzing the plasticity of fibrous composites. Each model represents a refinement of the previous in order to achieve a better approximation of experimental data.

First, we provide a detailed development of the EIAS method with elastic constraint. This model is nearly the same presented by Weng (1988), but we use the Eshelby tensor of elasticity for circular, cylindrical fibers instead of the tensor for spherical particle reinforcement. Also, we use an incremental plasticity theory instead of the deformation plasticity theory to calculate the increment of plastic matrix strain. This will allow us to subject our model to both proportional and nonproportional loading histories, as well as to cyclic loading histories. The results with this type of model as applied to fibrous composites coincide with Weng's results in essence. The model performs well in the elastic regime but is overly stiff in the plastic regime (Weng, 1988).

Secondly, we develop a model similar to Weng's EIAS secant modulus formulation; however, instead of using the secant modulus to account for the weakening constraint power of the matrix, we introduce a tangent stiffness method. This method uses the instantaneous value of the matrix plastic hardening modulus to

estimate the instantaneous tangent stiffness of the comparison material in the EIAS approach. Our use of an incremental plasticity theory to compute the increment of plastic matrix strain instead of the deformation theory of plasticity used by Weng motivates the introduction of the tangent stiffness approach. We call this model the EIAS Method-Tangent Stiffness Formulation. We also applied this method to spherical particle-reinforced composites and compared our results to those of Weng's using his secant moduli approach. Our results are comparable to Weng's, but we feel that our model more closely approximates experimental data, especially at lower fiber volume fractions.

Thirdly, in light of the unsatisfactory results achieved with the above two models for unidirectional composites, we propose a theoretically-based modification of the constraint power in the EIAS formulation which, when used in combination with the EIAS method-tangent stiffness formulation, produces satisfactory predictions for the inelastic behavior of unidirectional, continuous fiber-reinforced composites.

Finally, keeping in mind the experimental observations of Dvorak and Bahei-El-Din regarding violation of normality for B/Al continuous fiber-reinforced composites, we offer some explanations, based on our theoretical investigation. These studies lead us to conclude that a micromechanically-based theory is essential for describing the elastic-plastic behavior of important classes of fiber-reinforced composites. Non-associativity is required for any phenomenological model, in general, owing to shear localization in the matrix near reinforcement interfaces in

addition to the strong tendency for the plastic strain rate in the matrix material to rotate toward the direction perpendicular to reinforcement to relax constraint development.

As a result of our investigations, we propose a composite material model which enables fully incremental solutions based on an EIAS method with eigenstrain relaxation as opposed to a purely rate form of the EIAS. Our original contributions to the analysis of fibrous MMCs include the tangent stiffness formulation for estimating the comparison matrix material in the EIAS method; the β parameter which relaxes the constraint effect of the comparison material by reducing the rate of eigenstrain accumulation; and the χ function which allows the inelastic behavior of the composite to transition to matrix- dominated behavior as the matrix plastic strain rate vector rotates and aligns itself with the reinforcement direction.

CHAPTER II

EIAS METHOD WITH ELASTIC CONSTRAINT

2.1 Eigenstrain Terminology

An eigenstrain is a collective term given (Mura, 1987) to such nonelastic strains as plastic strains and misfit strains. It is a "ficticious" quantity which defines the level of misfit related to the applied loading level, mismatch of elastic constants and matrix plastic strain. Eigenstress is a generic term given to self-equilibrated, internal stresses caused by one or several of these eigenstrains in bodies which are not subject to any externally applied body forces or surface tractions. Eigenstress fields develop when eigenstrains are incompatible.

A finite subdomain Ω, with a prescribed eigenstrain ε_{ij}^{*}, in a homogeneous material domain D with no prescribed eigenstrain is called an inclusion (see Figure 1). The elastic moduli of Ω and D are assumed to be the same when inclusions are under consideration.

If Ω has different elastic moduli than D, then Ω is called an inhomogeneity. In this situation, an applied stress is perturbed by the presence of the inhomogeneity, and a stress perturbance field exists. An eigenstress field approximates the perturbed stress field by considering a corresponding fictitious eigenstrain ε_{ij}^{*} in Ω in a

homogeneous material.

2.2 Fundamental Equations of Elasticity with Eigenstrains

In this section, the equations of linear elasticity are reviewed with particular reference to solving eigenstrain problems (Mura, 1987; Taya and Arsenault, 1989). These problems consist of solving for the displacement u_i, strain ε_{ij}, and stress σ_{ij} at an any point $x(x_1,x_2,x_3)$ when a free body D is subjected to a given distribution of eigenstrain ε_{ij}^*. A body is free when there are no externally applied surface tractions or body forces.

2.2.1 Hooke's Law

For infinitesimal deformations, the total strain ε_{ij} is the sum of the elastic strain e_{ij} and eigenstrain ε_{ij}^*,

$$\varepsilon_{ij} = e_{ij} + \varepsilon_{ij}^* . \tag{2-1}$$

Hooke's Law relates the elastic strain to the stress σ_{ij} by

$$\sigma_{ij} = C_{ijkl} e_{kl} = C_{ijkl}(\varepsilon_{kl} - \varepsilon_{kl}^*) . \tag{2-2}$$

C_{ijkl} are the elastic moduli. In D-Ω where the ε_{ij}^* are zero, equation **(2-2)** becomes

$$\sigma_{ij} = C_{ijkl} \varepsilon_{kl} . \tag{2-3}$$

In this work, we will focus on isothermal behavior such that the eigenstrains are

2.2.2 Equilibrium Conditions

When calculating eigenstresses, the domain D must be assumed free of any external force and surface constraints. If these conditions for D are not satisfied, superposition of the eigenstress field of D on appropriate boundary value problem can be used to construct the applied stress field.

The equilibrium equations are

$$\sigma_{ij,j} = 0 \qquad (i,j = 1,2,3) \; . \tag{2-4}$$

The boundary conditions for free external surface tractions are

$$\sigma_{ij} n_j = 0 \; , \tag{2-5}$$

where n_i is the exterior unit normal vector on the boundary of the domain D. In most cases, D is considered an infinitely extended body and the boundary conditions in (2-5) are replaced by $\sigma_{ij}(\mathbf{x}) \to 0$ as $\mathbf{x} \to \infty$.

2.3 Eshelby's Equivalent Inclusion Problem

As stated earlier, an inclusion is defined as a sub-domain Ω in domain D, where eigenstrain $\varepsilon_{ij}^{*}(\mathbf{x})$ is given in Ω and is zero in D-Ω. The elastic moduli in Ω and D-Ω are assumed to be the same. The remaining domain D-Ω is referred to as the matrix.

Eshelby devised a method to solve three-dimensional elasticity problems for inclusions (or inhomogeneities) of ellipsoidal shape embedded in an infinite elastic

body or matrix. Consider first an inclusion problem where an ellipsoidal domain (denoted by Ω) is subjected to uniform non-elastic strain (or eigenstrain) ε_{ij}^{*} (see Figure 1). Such an inclusion embedded in an infinite elastic body with elastic moduli C_{ijkl} causes stress fields within and outside the inclusion. Eshelby suggested a method for obtaining the solution of the stress field within Ω (Eshelby, 1957) and outside Ω (Eshelby, 1959). The procedure for obtaining the stress field outside Ω is very difficult, but that for the stress field inside Ω is simplified because it is uniform for a given uniform eigenstrain ε_{ij}^{*}. In the absence of applied loading, the perturbance stress inside Ω due to misfit is given by Eshelby as

$$\sigma_{ij}^{pt} = C_{ijkl}(\varepsilon_{kl}^{pt} - \varepsilon_{kl}^{*}) , \tag{2-6}$$

where ε_{kl}^{pt} is the perturbance strain in Ω and is related to the eigenstrain, ε_{mn}^{*}, by

$$\varepsilon_{kl}^{pt} = S_{klmn}\varepsilon_{mn}^{*} . \tag{2-7}$$

From **(2-6)** and **(2-7)**, it is clear that the perturbance stress inside the inclusion can be readily calculated for a given eigenstrain, ε_{ij}^{*}.

S_{ijkl} is the Eshelby tensor for the matrix material and is a function of the geometry of the ellipsoidal inclusion and the matrix Poisson's ratio if the matrix is isotropic. The ε_{kl}^{*} are the uniform eigenstrains in the inclusion associated with the misfit. Per Eshelby, uniformity of eigenstrains requires uniformity of the remotely applied stresses. S_{ijkl} is given in terms of the Green's function G_{mnpq} as

$$S_{ijkl} = \frac{1}{8\pi} C_{pqkl} \int_{-1}^{1} d\bar{\zeta}_3 \int_{0}^{2\pi} (G_{ipjq}(\bar{\xi}) + G_{jpiq}(\bar{\xi})) d\theta \qquad (2\text{-}8)$$

where the integration is performed over the unit sphere.

This form of S_{ijkl} admits any form of anisotropy of the matrix, although the Green's function must be available for the matrix. The above equation reduces to

$$S_{ijkl} = \frac{1}{8\pi} C_{pqkl} (\bar{G}_{ipjq} + \bar{G}_{jpiq}) \qquad (2\text{-}9)$$

The $\bar{G}$'s are presently available for isotropic and transversely isotropic matrices. For other anisotropies, they may be determined numerically.

The integration for S_{ijkl} is performed in a natural coordinate system which defines the volume of an ellipsoidal inhomogeniety. For the case of circular, cylindrical fibers, one axis of the ellipse goes to infinity while the other two are equal. For a more detailed development of the Eshelby tensor, see Appendix A.

A practical and important application of Eshelby's equivalent inclusion method is the case of an "inhomogeneity problem." When the elastic moduli of an ellipsoidal inclusion differ from those of the surrounding matrix, the inclusion is called an ellipsoidal inhomogeneity. Fibers and precipitates are examples of inhomogeneities. An elastic material containing inhomogeneities is free from any stress field unless a load is applied. On the other hand, a material containing inclusions is subjected to a self-equilibrated, internal stress (eigenstress) field, even if it is free from all external

load is applied. On the other hand, a material containing inclusions is subjected to a self-equilibrated, internal stress (eigenstress) field, even if it is free from all external tractions. Eshelby first pointed out that the stress perturbance in an inclusion relative to the applied stress due to the presence of an inhomogeneity can be simulated by an eigenstress caused by an inclusion when the eigenstrain is chosen properly. This eigenstress is called the perturbance stress, σ_{ij}^{pt}, and the equivalency will be called the equivalent inclusion method.

When a composite consisting of a matrix with stiffness tensor C_{ijkl} and a single inhomogeneity with a stiffness tensor C_{ijkl}^{*} is subjected to the uniform applied stress σ_{ij}^{o}, the actual (or total) stress field σ_{ij}^{t} in the inhomogeneity (see Figure 2(a)) is given by

$$\sigma_{ij}^{t} = \sigma_{ij}^{o} + \sigma_{ij}^{pt} = C_{ijkl}^{*}(\varepsilon_{kl}^{o} + \varepsilon_{kl}^{pt}) \tag{2-10}$$

where σ_{ij}^{pt} and ε_{kl}^{pt} are the stress and strain perturbances introduced by the existence of the inhomogeniety, and ε_{kl}^{o} is the strain of the matrix (without the inhomogeneity) corresponding to σ_{ij}^{o}.

This inhomogeneity problem can be reduced to the inclusion problem insofar as the disturbances of the stress and strain are concerned. In the equivalent inclusion method, we must introduce an eigenstrain in Ω in order to reproduce the effect of the presence of the inclusion. The composite is treated as though it consists of pure matrix material (elastic constants C_{ijkl}). There are no eigenstrains introduced in D-Ω.

Hence, in Ω, we have

$$\sigma^{o}_{ij}+\sigma^{pt}_{ij}=C^{*}_{ijkl}(\varepsilon^{o}_{kl}+\varepsilon^{pt}_{kl}) \qquad \textit{actual}$$
$$=C_{ijkl}(\varepsilon^{o}_{kl}+\varepsilon^{pt}_{kl}-\varepsilon^{*}_{kl}) \quad \textit{equivalent inclusion problem} \tag{2-11}$$

where ε_{kl}^{*} is the eigenstrain. Equation **(2-11)** is the governing equation of misfit (see Figure 2(b)) for a single inhomogeneity.

It is obvious from equations **(2-10)** and **(2-11)** that the perturbance stress in the inclusion is given by equation **(2-6)**. Then, the perturbance strain ε_{kl}^{pt} is related to the unknown eigenstrain ε_{kl}^{*} by equation **(2-7)**. The perturbance stress in Ω is

$$\sigma^{pt}_{ij} = C_{ijkl}\left(\varepsilon^{pt}_{kl} - \varepsilon^{*}_{kl}\right). \tag{2-12}$$

Note that $\sigma_{ij}^{pt} \to 0$ and $\varepsilon_{kl}^{pt} \to 0$ as $|x_i| \to \infty$, such that σ_{ij}^{pt} is self-equilibrated, i.e. $\sigma_{ij,j}^{pt}=0$.

If the matrix has uniform plastic strain, ε_{ij}^{pm}, then we may treat ε_{ij}^{pm} as a negative eigenstrain, i.e.,

$$\varepsilon^{**}_{ij} = -\varepsilon^{pm}_{ij} + \varepsilon^{*}_{ij}. \tag{2-13}$$

In the context of the elastic Eshelby solution, the matrix plastic strain must be enforced homogeneously in D and then treated as a negative eigenstrain in Ω (Weng, 1988; Mura, 1987). In metal-matrix composites for which the matrix is elastic-plastic and the fibers are elastic, plastic strain occurs in the matrix. We must then modify **(2-11)** as follows (Weng, 1988):

$$C^*_{ijkl}\left(\varepsilon^o_{kl} + \varepsilon^{pt}_{kl} + \varepsilon^{pm}_{kl}\right) = C_{ijkl}\left(\varepsilon^o_{kl} + \varepsilon^{pt}_{kl} + \varepsilon^{pm}_{kl} - \varepsilon^*_{kl}\right)$$
$$= C_{ijkl}\left(\varepsilon^o_{kl} + \varepsilon^{pt}_{kl} - \varepsilon^{**}_{kl}\right), \qquad \text{(2-14)}$$

where it is understood that ε_{kl}^{pm} is the matrix plastic strain. The left side of **(2-14)** represents the actual stress in the inclusion assuming the inclusion deforms compatibly with the matrix plastic strain (i.e. $u_i^+ = u_i^-$). The right side is the associated equivalent inclusion problem. The perturbance strain in this case is

$$\varepsilon^{pt}_{kl} = S_{klmn}(\varepsilon^*_{mn} - \varepsilon^{pm}_{mn}) \; . \qquad \text{(2-15)}$$

It is noted here that the equivalent inclusion problem employs the assumption of elastic constraint of the matrix on the fiber which means that the problem treats the matrix as if no plastic strain had occurred. This may be reasonable in the sense that after plastic straining, misfit accommodation is by virtue of elastic unloading processes, i.e. within the yield surface, at each successive increment of deformation. Weng (1988) pointed out that this procedure overestimates the constraint power of the matrix at significant levels of matrix plasticity.

2.4 Interaction of Inclusions

The development of the inhomogeneous inclusion problem was based on Eshelby's equivalent inclusion concept for a single inclusion in an infinitely extended matrix material. This approach needs to be modified when it is used to analyze fibrous composite systems. In a fibrous composite, each fiber is an inclusion.

Depending on the volume fraction, the fibers, or inclusions, tend to interact causing additional stresses in Ω which augment the perturbance stress, σ_{ij}^{pt}. These additional stresses are called interaction stresses, in general, and are represented by σ_{ij}^{I}.

Strictly speaking, we cannot just assume for finite D that $\sigma_{ij}^{pt}n_j=0$ on the boundary of D as is the case with a single inclusion in an infinite matrix. In general, we may think of σ_{ij}^{I} as an image stress, analogous to image stresses due to finite boundaries in dislocation mechanics, for example. Then, equation **(2-14)** becomes, in Ω,

$$\begin{aligned} C^{*}_{ijkl}\left(\varepsilon^{o}_{kl}+\varepsilon^{pt}_{kl}+\varepsilon^{pm}_{kl}+\varepsilon^{I}_{kl}\right) &= C_{ijkl}\left(\varepsilon^{o}_{kl}+\varepsilon^{pt}_{kl}+\varepsilon^{pm}_{kl}+\varepsilon^{I}_{kl}-\varepsilon^{*}_{kl}\right) \\ &= C_{ijkl}\left(\varepsilon^{o}_{kl}+\varepsilon^{pt}_{kl}+\varepsilon^{I}_{kl}-\varepsilon^{**}_{kl}\right). \end{aligned} \qquad \textbf{(2-16)}$$

Here, ε_{kl}^{I} and σ_{kl}^{I} are regarded as an averaged image or interaction strain and stress, respectively, over the complete volume. Then we must specify how ε_{kl}^{I} is to be calculated.

2.4.1 The Mori-Tanaka Method

The Mori-Tanaka Method assumes that the inclusions are randomly distributed. Then, per a rule of mixtures type formulation, in the absence of remote applied loading,

$$f\langle\sigma_{ij}\rangle_f + (1 - f)\langle\sigma_{ij}\rangle_m = 0. \qquad \textbf{(2-17)}$$

Here, $\langle\sigma_{ij}\rangle_f \equiv$ the average internal (self-equilibrated) stress perturbation in the

inclusion;

$\langle\sigma_{ij}\rangle_m \equiv$ the average internal (self-equilibrated) stress perturbation in the matrix;

and $f \equiv$ the volume fraction of inclusions.

The total stress inside an inclusion is

$$\sigma_{ij} = \sigma_{ij}^{pt} + \langle\sigma_{ij}\rangle_m \tag{2-18}$$

where

$$\sigma_{ij}^{pt} = C_{ijkl}(\varepsilon_{kl}^{pt} - \varepsilon_{kl}^{*} + \varepsilon_{kl}^{pm}) \tag{2-19}$$

and

$$\varepsilon_{kl}^{pt} = S_{klmn}(\varepsilon_{mn}^{*} - \varepsilon_{mn}^{pm}). \tag{2-20}$$

Here, σ_{ij}^{pt} is the stress corresponding to the infinite body solution, i.e. a single inclusion in a matrix of infinite extent.

Since the inclusion can be placed anywhere in the matrix, the average internal stress in an inclusion is

$$\langle\sigma_{ij}\rangle_f = \sigma_{ij}^{pt} + \langle\sigma_{ij}\rangle_m . \tag{2-21}$$

Substituting for $\langle\sigma_{ij}\rangle_f$ in **(2-17)** and simplifying, we have

$$f\left(\sigma_{ij}^{pt} + \langle\sigma_{ij}\rangle_m\right) + (1 - f)\langle\sigma_{ij}\rangle_m = 0$$

$$f\sigma_{ij}^{pt} = -\langle\sigma_{ij}\rangle_m \tag{2-22}$$

$$or\ \langle\sigma_{ij}\rangle_m = -f\sigma_{ij}^{pt}.$$

Utilizing this result in combination with

$$\langle \sigma_{ij} \rangle_f = -\frac{1}{f}\langle \sigma_{ij} \rangle_m + \langle \sigma_{ij} \rangle_m \tag{2-23}$$

which was obtained by dividing through by f in (2-17), we have

$$\langle \sigma_{ij} \rangle_f = (1 - f)\sigma_{ij}^{pt}. \tag{2-24}$$

Let us define the average interaction stress, i.e.

$$\sigma_{ij}^{I} \equiv \langle \sigma_{ij} \rangle_m . \tag{2-25}$$

Therefore, according to the Mori-Tanaka Method, the interaction (or image) stress is

$$\sigma_{ij}^{I} = -f\sigma_{ij}^{pt} . \tag{2-26}$$

2.4.2 The Image Stress Approach

Mura (1987) presents the concept of an image stress, σ_{ij}^{I}, where the internal stress is equal to the sum of the image stress and the perturbance stress, σ_{ij}^{pt}, in Ω, i.e.

$$\sigma_{ij} = \sigma_{ij}^{I} + \sigma_{ij}^{pt} . \tag{2-27}$$

Consider a finite material domain D in which are embedded n number of ellipsoidal inclusions. Also, assume there exists some finite ellipsoidal domain, D^{*},

which encloses the inclusion, Ω, and has dimensions on the order of the fiber spacing (see Figure 3(a)). The domain, D^*, is of the same ellipsoidal character as Ω in terms of orientation and shape (see Figure 3(b)). It can be shown that σ_{ij}^{pt} by itself (i.e. a single inclusion in an infinite body) does not satisfy the traction boundary condition $\sigma_{ij}^{pt}n_j=0$ on δD^*. Hence, the image stress may be viewed as a corrective term to satisfy equilibrium in D^* and the traction boundary conditions on δD^*, i.e.

$$\begin{aligned} \sigma_{ij,j}^{I} &= 0 \quad in\ D^*, \\ (\sigma_{ij}^{I} + \sigma_{ij}^{pt})n_j &= 0 \quad on\ \delta D^*. \end{aligned} \tag{2-28}$$

Recall that $\sigma_{ij,j}^{pt}=0$ from the equivalent inclusion problem. This ensures some measure of consideration of the finite distance between fibers.

The average value of σ_{ij}^{I} over the volume D^* can be shown to be

$$\langle \sigma_{ij}^{I} \rangle = -\frac{1}{V_{D^*}} \int_{V_{D^*}} \sigma_{ij}^{pt} dV = -\frac{1}{V_{D^*}} \int_{\Omega} \sigma_{ij}^{pt} dD^* \tag{2-29}$$

by Tanaka-Mori's Theorem (Mura, 1987). V_{D^*} is the volume of the domain D^*, and the integration is performed over the volume of the inclusion Ω.

For uniform eigenstrains in Ω, σ_{ij}^{pt} is constant in Ω and hence

$$\begin{aligned} \langle \sigma_{ij}^{I} \rangle &= -\frac{\Omega}{V_{D^*}} \sigma_{ij}^{pt} = -f^* \sigma_{ij}^{pt} \\ \sigma_{ij}^{I} &= C_{ijkl} \varepsilon_{kl}^{I} . \end{aligned} \tag{2-30}$$

Here, Ω is the volume of the inhomegeneity, and $\Omega/V_{D^*} = f^*$, the fiber volume

fraction in D^*. In our analysis, we then assume that

$$\langle \sigma_{ij}^I \rangle = \sigma_{ij}^I , \tag{2-31}$$

in both phases. Likewise, for strain,

$$\langle \varepsilon_{ij}^{pt} \rangle = \frac{\Omega}{V_{D^*}} \varepsilon_{ij}^{pt} = f^* S_{ijkl} (\varepsilon_{kl}^* - \varepsilon_{kl}^{pm}) \tag{2-32}$$

and

$$\langle \varepsilon_{ij}^I \rangle = -f^* \left(\varepsilon_{ij}^{pt} - \varepsilon_{ij}^* + \varepsilon_{ij}^{pm} \right), \tag{2-33}$$

where it is understood that the brackets refer to the average over the volume D^*.

Utilizing this result and attributing to the bracketed quantities which follow the definition of average over the entire volume of the finite domain D, we are able to determine an expression for the image stress in terms of the perturbance stress for the entire composite. The image strain, ε_{kl}^I, is related to the image stress, σ_{ij}^I, by

$$\varepsilon_{kl}^I = C_{klij}^{-1} \sigma_{ij}^I = \langle \varepsilon_{ij}^I \rangle . \tag{2-34}$$

From (2-19), (2-33), and $\sigma_{ij}^I = -f^* \sigma_{ij}^{pt}$, we have

$$\sigma_{ij}^I = -f \sigma_{ij}^{pt} = C_{ijkl} \left[-f (\varepsilon_{kl}^{pt} - \varepsilon_{kl}^* + \varepsilon_{kl}^{pm}) \right] . \tag{2-35}$$

The quantity in brackets on the right side of the equation is ε_{kl}^I as can be seen from (2-33). Note that we are now using f, the composite fiber volume fraction, instead of f^*. Recognizing this and solving for ε_{kl}^I, we have

$$\varepsilon_{ij}^{I} = -fC_{ijkl}^{-1}\sigma_{kl}^{pt} . \tag{2-36}$$

We can clearly see that **(2-34)** and **(2-36)** are both expressions for ε_{kl}^{I}. Equating the right sides of these equations and multiplying both sides by C_{ijkl}, we see that

$$\sigma_{ij}^{I} = -f\sigma_{ij}^{pt} \tag{2-37}$$

and therefore the average interaction strain in **(2-33)** is consistent with **(2-30)**. One notes that the above expression for the image stress is identical to that obtained by the Mori-Tanaka method, which may be expected for a two-phase composite with uniform eigenstrains and ellipsoidal inclusions as pointed out by Norris (1989).

2.5 Average Stress and Strain in the Composite

Stress-strain analysis usually requires some assumption about the relationship of the applied stress to the actual stress in the composite. A usual approach is to take the average of all the stresses over the entire volume of the composite, i.e.

$$\bar{\sigma}_{ij} = \frac{1}{V_D}\int_{V_D}\sigma_{ij}dV . \tag{2-38}$$

Since the various stresses are assumed uniform in the EIAS approach, we have

$$\bar{\sigma}_{ij} = (1 - f)(\sigma_{ij}^{o} + \sigma_{ij}^{I}) + f(\sigma_{ij}^{o} + \sigma_{ij}^{I} + \sigma_{ij}^{pt}). \tag{2-39}$$

Hence, the average stress in the composite is equal to the matrix volume fraction times the average matrix stress plus the fiber volume fraction times the average fiber

stress. Simplifying (2-39), we have

$$\bar{\sigma}_{ij} = \sigma^{o}_{ij} + \sigma^{I}_{ij} + f\sigma^{pt}_{ij} . \tag{2-40}$$

In section 2.4, we showed that

$$\sigma^{I}_{ij} = -f\sigma^{pt}_{ij} . \tag{2-41}$$

Therefore,

$$\bar{\sigma}_{ij} = \sigma^{o}_{ij} . \tag{2-42}$$

Hence, the applied stress, σ_{ij}^{o}, is equal to the average stress. This should be intuitively obvious based on the foundations of the EIAS approach.

Applying a similar volume averaging approach to determine the average strain in the composite, we have

$$\bar{\varepsilon}_{ij} = \varepsilon^{pm}_{ij} + (1-f)(\varepsilon^{o}_{ij}+\varepsilon^{I}_{ij}) + f(\varepsilon^{o}_{ij}+\varepsilon^{I}_{ij}+\varepsilon^{pt}_{ij}). \tag{2-43}$$

Therefore, the average strain in the composite is equal to the sum of the matrix plastic strain (corresponding to a homogeneous stress-free deformation), the matrix volume fraction times the average matrix strain, and the fiber volume fraction times the average fiber strain. After simplification, we have

$$\begin{aligned} \bar{\varepsilon}_{ij} &= \varepsilon^{pm}_{ij} + \varepsilon^{o}_{ij} + \varepsilon^{I}_{ij} + f\varepsilon^{pt}_{ij} \\ &= (1 - f)\varepsilon^{pm}_{ij} + \varepsilon^{o}_{ij} + f\varepsilon^{*}_{ij} . \end{aligned} \tag{2-44}$$

Note that we have foregone any consideration of variational principles for

defining the strain of the aggregate. These considerations are not essential when dealing with a work-hardening matrix.

2.6 Final Form of the EIAS Method with Elastic Constraint

At this point we are ready to combine the concepts of the equivalent inclusion problem with those of image and average stresses to produce the final constitutive relationships for our model based on the treatment of matrix plastic strain as a negative eigenstrain in the fiber.

For better description of finite fiber volume interaction effects, the image stress is included on both sides of **(2-14)**. Repeating **(2-16)**, in Ω,

$$\begin{aligned} & C^*_{ijkl}(\varepsilon^o_{kl} + \varepsilon^{pt}_{kl} + \varepsilon^{pm}_{kl} + \varepsilon^I_{kl}) \\ & = C_{ijkl}(\varepsilon^o_{kl} + \varepsilon^{pt}_{kl} + \varepsilon^{pm}_{kl} + \varepsilon^I_{kl} - \varepsilon^*_{kl}) \ . \end{aligned} \tag{2-45}$$

The left side of **(2-45)** represents the actual stress in the fiber whereas the right side represents the corresponding equivalent inclusion problem for the same stress.

2.7 Rate Form of the EIAS Approach

We may consider the solution of the elastoplastic problem as the sum of the solutions of a sequence of elastically constrained plastic deformations, subjecting each increment to the equivalent inclusion solution.

Adopting a rate form of equation (2-45), we have

$$C^{*}_{ijkl}(\dot{\varepsilon}^{o}_{kl} + \dot{\varepsilon}^{pt}_{kl} + \dot{\varepsilon}^{pm}_{kl} + \dot{\varepsilon}^{I}_{kl}) = C_{ijkl}(\dot{\varepsilon}^{o}_{kl} + \dot{\varepsilon}^{pt}_{kl} + \dot{\varepsilon}^{pm}_{kl} + \dot{\varepsilon}^{I}_{kl} - \dot{\varepsilon}^{*}_{kl}) , \tag{2-46}$$

where

$$\dot{\varepsilon}^{pt}_{kl} = S_{klmn}(\dot{\varepsilon}^{*}_{mn} - \dot{\varepsilon}^{pm}_{mn}) ,$$
$$\dot{\varepsilon}^{I}_{kl} = -f(\dot{\varepsilon}^{pt}_{kl} - \dot{\varepsilon}^{*}_{kl} + \dot{\varepsilon}^{pm}_{kl}) , \tag{2-47}$$
$$and\ \dot{\varepsilon}^{o}_{kl} = C^{-1}_{klij}\dot{\sigma}^{o}_{ij} .$$

The matrix plastic strain rate, $\dot{\varepsilon}_{ij}^{pm}$, is given by the incremental elastoplastic flow rule

$$\dot{\varepsilon}^{pm}_{ij} = 0 \quad if\ F < 0\ or\ F = 0\ and\ \frac{\partial F}{\partial \sigma^{m}_{ij}}\dot{\sigma}^{m}_{ij} < 0,$$
$$\dot{\varepsilon}^{pm}_{ij} = \frac{1}{h}(\dot{\sigma}^{m}_{kl}n_{kl})n_{ij} \quad if\ F = 0\ and\ \frac{\partial F}{\partial \sigma^{m}_{ij}}\dot{\sigma}^{m}_{ij} \geq 0. \tag{2-48}$$

Here, F ≡ the matrix yield function, and $\dot{\sigma}_{ij}^{m} = \dot{\sigma}_{ij}^{o} + \dot{\sigma}_{ij}^{I}$ is the average matrix stress rate. The unit normal vector to the yield surface is given by

$$n_{ij} = \frac{\partial F}{\partial \sigma^{m}_{ij}}\left(\frac{\partial F}{\partial \sigma^{m}_{kl}}\frac{\partial F}{\partial \sigma^{m}_{kl}}\right)^{-\frac{1}{2}} . \tag{2-49}$$

The quantity h is the plastic hardening modulus of the matrix. Hence, we may restate (2-48) as

$$\dot{\varepsilon}_{ij}^{pm} = \frac{1}{h}\left[\dot{\sigma}_{kl}^{o} - fC_{klmn}(\dot{\varepsilon}_{mn}^{pt} - \dot{\varepsilon}_{mn}^{*} + \dot{\varepsilon}_{mn}^{pm})\right] n_{kl} n_{ij}$$

$$\text{if } n_{ij}\dot{\sigma}_{ij}^{m} \geq 0 \text{ and } F = 0, \tag{2-50}$$

$$\dot{\varepsilon}_{ij}^{pm} = 0 \qquad \text{otherwise.}$$

The quantity enclosed in brackets is the matrix stress rate, $\dot{\sigma}_{ij}^{m}$. Appendix B outlines the two incremental plasticity theories used to calculate the matrix plastic strain increment in this thesis.

Substituting (2-47) into (2-46), we have

$$\begin{aligned} &C_{ijkl}^{*}\Big\{C_{klmn}^{-1}\dot{\sigma}_{mn}^{o} + S_{klmn}(\dot{\varepsilon}_{mn}^{*} - \dot{\varepsilon}_{mn}^{pm}) + \dot{\varepsilon}_{kl}^{pm} \\ &- f\left[S_{klmn}(\dot{\varepsilon}_{mn}^{*} - \dot{\varepsilon}_{mn}^{pm}) - \dot{\varepsilon}_{kl}^{*} + \dot{\varepsilon}_{kl}^{pm}\right]\Big\} = \\ &C_{ijkl}\Big\{C_{klmn}^{-1}\dot{\sigma}_{mn}^{o} + S_{klmn}(\dot{\varepsilon}_{mn}^{*} - \dot{\varepsilon}_{mn}^{pm}) + \varepsilon_{kl}^{pm} \\ &-f\left[S_{klmn}(\dot{\varepsilon}_{mn}^{*} - \dot{\varepsilon}_{mn}^{pm}) - \dot{\varepsilon}_{kl}^{*} + \dot{\varepsilon}_{kl}^{pm}\right] - \dot{\varepsilon}_{kl}^{*}\Big\} . \end{aligned} \tag{2-51}$$

In this equation, $\dot{\sigma}_{mn}^{o}$ is the applied stress rate (or increment) and the unknowns are $\dot{\varepsilon}_{kl}^{*}$ and $\dot{\varepsilon}_{kl}^{pm}$.

2.8 Solution Procedure for the EIAS Method with Elastic Constraint

Equation (2-51) above is the governing equation for solution of the EIAS problem with full elastic constraint. Since an incremental plasticity theory is used to calculate the increment of matrix plastic strain, an incremental form of (2-51) is adopted for solution of the problem. Equation (2-51) is rewritten for ease of

programming as follows:

$$A_{ijmn}\Delta\sigma^{o}_{mn} + B_{ijmn}\Delta\varepsilon^{pm}_{mn} = D_{ijmn}\Delta\varepsilon^{*}_{mn} \tag{2-52}$$

where the coefficient matrices A_{ijmn}, B_{ijmn}, and D_{ijmn} are

$$\begin{aligned}
A_{ijmn} &= C^{*}_{ijkl}C^{-1}_{klmn} - C_{ijkl}C^{-1}_{klmn} = \Delta C_{ijkl}C^{-1}_{klmn} \\
B_{ijmn} &= -C^{*}_{ijkl}S_{klmn} + fC^{*}_{ijkl}S_{klmn} + C_{ijkl}S_{klmn} - fC_{ijkl}S_{klmn} \\
&\quad + fC_{ijmn} - C_{ijmn} + C^{*}_{ijmn} - fC^{*}_{ijmn} \\
&= (1 - f)(\Delta C_{ijmn} - \Delta C_{ijkl}S_{klmn}) \\
D_{ijmn} &= C_{ijkl}S_{klmn} - fC_{ijkl}S_{klmn} - C^{*}_{ijkl}S_{klmn} + fC^{*}_{ijkl}S_{klmn} \\
&\quad - fC^{*}_{ijmn} + fC_{ijmn} - C_{ijmn} \\
&= (1 - f)(-\Delta C_{ijkl}S_{klmn} - C_{ijmn}) - fC^{*}_{ijmn} ,
\end{aligned} \tag{2-53}$$

where $\Delta C_{ijmn} = C_{ijmn}^{*} - C_{ijmn}$.

These matrices are calculated based on the material properties of the particular composite system of interest, and they only have to be calculated once for a given loading history. Therefore, the subroutine which performs these calculations (called COEFMAT for material coefficients) is located outside the calculation "loop", which significantly reduces calculation time.

The program was written for "load controlled" conditions as the applied stress increment, $\Delta\sigma_{ij}^{o}$, is the input to the program. A separate program capable of producing proportional as well as nonproportional loading histories was written to

create the loading history input file.

As stated above, the two unknowns in the problem are the increment of eigenstrain, $\Delta\varepsilon_{kl}^{*}$, and the increment of matrix plastic strain, $\Delta\varepsilon_{kl}^{pm}$. The plastic strain increment, $\Delta\varepsilon_{kl}^{pm}$ is calculated based on the current stress state (and increment) using an incremental plasticity theory outlined in Appendix B. With $\Delta\sigma_{ij}^{o}$ and $\Delta\varepsilon_{kl}^{pm}$ known, $\Delta\varepsilon_{kl}^{*}$ can be easily calculated by multiplying the left side of **(2-52)** by the inverse of the coefficient matrix D_{ijmn} (i.e., D_{ijmn}^{-1}). Then, the complete state of stress and strain for the composite and its constituents can be calculated for that particular instant in the loading history. Updating of the stress and strain was accomplished in the program by a subroutine called UPDATE. Once the update was performed and values were written to a data file, the program reads the next applied stress increment from the input file and the cycle continues until the loading history is exhausted.

This program is particularly efficient in that no iteration is required. This is accomplished as follows. From **(2-50)**, we have the matrix flow rule

$$\begin{aligned}\dot{\varepsilon}_{ij}^{pm} &= \frac{1}{h}\left[\dot{\sigma}_{kl}^{o} - fC_{klmn}(\dot{\varepsilon}_{mn}^{pt} - \dot{\varepsilon}_{mn}^{*} + \dot{\varepsilon}_{mn}^{pm})\right]n_{kl}n_{ij} \\ &= \dot{\lambda}n_{ij} = \frac{1}{h}\left(\dot{\sigma}_{kl}^{m}n_{kl}\right)n_{ij}.\end{aligned} \tag{2-54}$$

Taking the scalar product of both sides of **(2-54)** with n_{ij}, we have

$$\dot{\varepsilon}_{ij}^{pm}n_{ij} = \dot{\lambda} = \frac{1}{h}\left[\dot{\sigma}_{kl}^{o} - fC_{klmn}\left(\dot{\varepsilon}_{mn}^{pt} - \dot{\varepsilon}_{mn}^{*} + \dot{\varepsilon}_{mn}^{pm}\right)\right]n_{kl}. \tag{2-55}$$

From the EIAS method, equation **(2-52)**,

$$A_{ijmn}\dot{\sigma}^{o}_{mn} + B_{ijmn}\dot{\varepsilon}^{pm}_{mn} = D_{ijmn}\dot{\varepsilon}^{*}_{mn} \quad . \tag{2-56}$$

Solving for $\dot{\varepsilon}_{ij}^{*}$,

$$\dot{\varepsilon}^{*}_{ij} = D^{-1}_{mnij}\left(A_{mnpq}\dot{\sigma}^{o}_{pq} + B_{mnpq}\dot{\varepsilon}^{pm}_{pq}\right) \quad . \tag{2-57}$$

By substituting **(2-57)** into the flow rule, we may rewrite the plastic strain rate in **(2-54)** explicitly in terms of the applied stress rate $\dot{\sigma}_{ij}^{o}$ as

$$\dot{\varepsilon}^{pm}_{ij} = \dot{\lambda} n_{ij}, \tag{2-58}$$

where

$$\dot{\lambda} = \frac{\left[\dot{\sigma}^{o}_{kl} - f\left(C_{klmn}S_{mnpq} - C_{klpq}\right)D^{-1}_{rspq}A_{rstu}\dot{\sigma}^{o}_{tu}\right]n_{kl}}{\left[h + f\left(C_{klmn}S_{mnpq} - C_{klpq}\right)D^{-1}_{rspq}B_{rstu}n_{tu}n_{kl} + f\left(C_{klmn} - C_{klpq}S_{pqmn}\right)n_{mn}n_{kl}\right]}. \tag{2-59}$$

This noninterative form makes the program especially practical for application in finite element type programs, for example. Readers are referred to Appendix C for a flowchart of this program, called BALNIT (for **B**oron/**AL**uminum-No **IT**eration).

CHAPTER III

EIAS METHOD - TANGENT STIFFNESS FORMULATION

3.1 EIAS Method with a Tangent Stiffness Formulation

Based on his work with spherical inclusions in a plastically deforming matrix, Weng (1988) concluded that the constraint power of the EIAS method with elastic constraint renders it much too stiff in the elastic-plastic range. Weng introduced a modified Eshelby formulation based on the secant modulus for the deformation theory of plasticity in order to weaken the constraint power of the matrix in the EIAS method. For incremental elasto-plasticity and general loading paths, we cannot use the secant modulus approach directly. However, it is possible to construct an analogous approximate Eshelby relation based on the tangent modulus. It is important to emphasize that the EIAS method (Weng, 1988; Mura, 1987) based on elastic constraint, which treats plastic strain as an eigenstrain, is not generally applicable to significant matrix inelastic deformation of reinforced materials. Even though the method may be applied unambiguously to the case of viscoplastic matrix behavior, it is nonetheless overly stiff.

To introduce a tangent stiffness formulation, we note that the matrix plastic strain rate is not explicitly required as in the previous case. The plastic hardening

modulus h, based on the plastic internal state of the matrix material, is uniquely related to the tangent stiffness, C_{ijkl}^{T}.

For deviatoric matrix plasticity, we may write

$$\dot{\sigma}_{ij}^{m} = C_{ijkl}\left[\dot{\varepsilon}_{kl}^{m} - \frac{1}{h}(\dot{\sigma}_{mn}^{m} n_{mn}) n_{kl}\right] = C_{ijkl}\left[\dot{\varepsilon}_{kl}^{m} - \dot{\varepsilon}_{kl}^{pm}\right]. \tag{3-1}$$

Solving for the matrix strain rate $\dot{\varepsilon}_{ij}^{m}$ during plastic flow,

$$\begin{aligned} \dot{\varepsilon}_{ij}^{m} &= \left[C_{ijkl}^{-1} + \frac{1}{h} n_{ij} n_{kl}\right] \dot{\sigma}_{kl}^{m} \\ &= \left(C_{ijkl}^{T}\right)^{-1} \dot{\sigma}_{kl}^{m} . \end{aligned} \tag{3-2}$$

We may write the modified Eshelby rate-type equation based on tangent stiffness as:

$$C_{ijkl}^{*}\left(\dot{\varepsilon}_{kl}^{o} + \dot{\varepsilon}_{kl}^{pt} + \dot{\varepsilon}_{kl}^{I}\right) = C_{ijkl}^{T}\left(\dot{\varepsilon}_{kl}^{o} + \dot{\varepsilon}_{kl}^{pt} + \dot{\varepsilon}_{kl}^{I} - \dot{\varepsilon}_{kl}^{*}\right). \tag{3-3}$$

Since the effect of matrix plastic deformation is introduced through the tangent stiffness, we note that

$$\begin{aligned} \dot{\varepsilon}_{kl}^{pt} &= S_{klmn}^{T} \dot{\varepsilon}_{mn}^{*}, \\ \dot{\varepsilon}_{ij}^{I} &= -f(\dot{\varepsilon}_{ij}^{pt} - \dot{\varepsilon}_{ij}^{*}), \\ \text{and } \dot{\varepsilon}_{ij}^{o} &= \left(C_{ijkl}^{To}\right)^{-1} \dot{\sigma}_{kl}^{o} \end{aligned} \tag{3-4}$$

where the Mori-Tanaka theorem (Mura, 1987) is employed to arrive at the form of the interaction strain rate $\dot{\varepsilon}_{ij}^{I}$. It is important to note that a tangent stiffness method must be employed in the reference material relation between $\dot{\varepsilon}_{ij}^{o}$ and $\dot{\sigma}_{kl}^{o}$; strictly

speaking, C_{ijkl}^{To} should be based on the elastic-plastic state of a comparison matrix material at stress $\dot{\sigma}_{ij}^{o}$, but since $\dot{\epsilon}_{ij}^{o}$ and $\dot{\sigma}_{ij}^{o}$ are no longer uniquely related (as is the case for deformation theory), a formulation for C_{ijkl}^{To} will be introduced later.

The Eshelby tensor S_{klmn}^{T} in this case is based on the effective Poisson's ratio, $\bar{\nu}$, of the matrix which may be assumed of the form

$$\bar{\nu} = \nu + \frac{(0.5 - \nu)}{\left(1 + \frac{h}{2G}\right)} \tag{3-5}$$

where ν is the elastic Poisson's ratio of the matrix. Hence, $\bar{\nu}$ varies continuously from ν for $h \to \infty$ to 0.5 at $h = 0$. This form is based on the dependence of the tangent stiffness on the plastic modulus h. The tangent stiffness formulation is rather insensitive to the choice of the form of $\bar{\nu}$ so long as $\bar{\nu}$ is allowed to vary continuously between fully elastic and fully plastic limits.

The average stress rate in the matrix is given by

$$\dot{\sigma}_{ij}^{m} = \dot{\sigma}_{ij}^{o} + \dot{\sigma}_{ij}^{I} , \tag{3-6}$$

where

$$\dot{\sigma}_{ij}^{I} = -f\dot{\sigma}_{ij}^{pt} = -fC_{ijkl}^{T}\left(\dot{\epsilon}_{kl}^{pt} - \dot{\epsilon}_{kl}^{*}\right) \tag{3-7}$$

in the tangent stiffness formulation. The average composite stress and strain rate are given by

$$
\begin{aligned}
\bar{\dot{\sigma}}_{ij} &= (1 - f)(\dot{\sigma}^{o}_{ij} + \dot{\sigma}^{I}_{ij}) + f(\dot{\sigma}^{o}_{ij} + \dot{\sigma}^{I}_{ij} + \dot{\sigma}^{pt}_{ij}) \\
&= \dot{\sigma}^{o}_{ij} + \dot{\sigma}^{I}_{ij} + f\dot{\sigma}^{pt}_{ij} = \dot{\sigma}^{o}_{ij} \\
\bar{\dot{\varepsilon}}_{ij} &= (1 - f)(\dot{\varepsilon}^{o}_{ij} + \dot{\varepsilon}^{I}_{ij}) + f(\dot{\varepsilon}^{o}_{ij} + \dot{\varepsilon}^{I}_{ij} + \dot{\varepsilon}^{pt}_{ij}) \\
&= \dot{\varepsilon}^{o}_{ij} + f\dot{\varepsilon}^{*}_{ij} .
\end{aligned}
\tag{3-8}
$$

This approach requires no iteration and is very efficient; it does involve several additional matrix inversions, however, since the tangent stiffness must be updated at each time step. For an applied stress rate $\dot{\sigma}_{mn}{}^{o}$, we may write the Eshelby equation (3-3), after substitution, in the form

$$
\begin{aligned}
\Delta C_{ijkl}\left(C^{To}_{klmn}\right)^{-1}\dot{\sigma}^{o}_{mn} = \Big[&-\Delta C_{ijkl}S^{T}_{klmn} + \Delta C_{ijkl}S^{T}_{klmn}f \\
&- \Delta C_{ijmn}f - C^{T}_{ijkl}\delta_{km}\delta_{ln}\Big]\dot{\varepsilon}^{*}_{mn}
\end{aligned}
\tag{3-9}
$$

where $\Delta C_{ijkl} = C_{ijkl}{}^{*} - C_{ijkl}{}^{T}$ and δ_{km} is the Kronecker delta. Equation (3-9) is of the form

$$
A_{ijkl}\dot{\sigma}^{o}_{kl} = B_{ijmn}\dot{\varepsilon}^{*}_{mn} . \tag{3-10}
$$

Thus,

$$
\dot{\varepsilon}^{*}_{pq} = \left(B_{ijpq}\right)^{-1}A_{ijkl}\dot{\sigma}^{o}_{kl} . \tag{3-11}
$$

With $\dot{\varepsilon}_{ij}^{*}$ in hand, one may proceed to compute the rates of matrix stress and composite strain.

As before, the matrix plastic strain rate is given by

$$\dot{\varepsilon}_{ij}^{pm} = \frac{1}{h}\dot{\sigma}_{kl}^{m}n_{kl}n_{ij} \text{ for } F=0 \text{ and } \dot{\sigma}_{kl}^{m}n_{kl} \geq 0$$
$$\dot{\varepsilon}_{ij}^{pm} = 0 \qquad \text{otherwise} \tag{3-12}$$

where h is given in Appendix B for two incremental plasticity approaches. It is important to note that the matrix stress, plastic strain, and any associated state variables (e.g. backstress) must be updated to assign the current hardening modulus, h, in the tangent stiffness method.

3.2 Formulation for Comparison Matrix Material in the Tangent Stiffness Method

In the general tangent stiffness formulation, the comparison material may be assumed to have a compliance of the form

$$(C_{ijkl}^{To})^{-1} = f\beta\left\{(C_{ijkl}^{T})^{-1} - C_{ijkl}^{-1}\right\} + (C_{ijkl}^{T})^{-1} \tag{3-13}$$

or

$$(C_{ijkl}^{To})^{-1} = (1 + f\beta)(C_{ijkl}^{T})^{-1} - f\beta C_{ijkl}^{-1} \tag{3-14}$$

such that

$$\|(C^{To}_{ijkl})^{-1}\dot{\sigma}^{o}_{ij}\| \geq \|(C^{T}_{ijkl})^{-1}\dot{\sigma}^{o}_{ij}\| \quad for\ \beta \geq 0\ . \tag{3-15}$$

The equality holds if $f=0$ (i.e., the comparison material response is the actual matrix material response), if $\beta = 0$, or for purely elastic response of the matrix. Note that C_{ijkl} is the stiffness of the matrix.

Introduction of the constant β is necessitated by the fact that the response of the comparison material is not uniquely defined in the general elastic-plastic loading case. Due to the constraint associated with both the fiber geometry and higher fiber stiffness, the comparison matrix material generally has higher stress levels and, consequently, lower tangent stiffness. It should be emphasized that the concept of comparison material, and of the Eshelby approach for that matter, is rooted in linear elasticity; hence, the incremental elastic-plastic case obviously must invoke the spirit of the elastic approach but with additional consideration for the actual degree of constraint in the plastic regime. The parameter β affects the rate of eigenstrain accumulation only in the elastic-plastic regime. For $\beta = 0$, the degree of constraint on the matrix plastic deformation is low as is the rate of eigenstrain accumulation with composite strain accumulation. As β increases, the constraint on matrix plastic deformation and, correspondingly, the eigenstrain accumulation rate both increase. This leads to an increasing composite strain hardening rate with increasing β.

The introduction of the parameter β should therefore be viewed as a means of specifying the comparison matrix material behavior in the elastic-plastic regime in

the incremental approach. The secant modulus approach employed by Weng (1988), another approximate application of the Eshelby concept, does not involve such an assumption but is premised on applicability of the deformation theory of plasticity. Therefore, it is restricted to monotonic, proportional loading. In general, it is desirable to employ the incremental tangent stiffness approach for general loading paths. Moreover, even under proportional loading of the composite, the average matrix plastic strain rate varies nonproportionally for directionally reinforced composites if the applied loading is not coaxial with principal material directions. This is a first order consideration for unidirectional metal-matrix composites for which the plastic strain rate in virtually any off-axis loading situation rotates away from the fibers toward the direction of least constraint. For such composite materials with preferred directions of plastic flow which minimize constraint, it may be anticipated that β will be small since the flow will seek these orientations. Composites without preferred reinforcement directions (e.g. particulate reinforced) will require significantly higher values of β even though the average level of constraint may be lower since there are no preferred directions of plastic flow to minimize constraint. As a perhaps subtle but important consequence of the reinforced material's preferred orientation, one may expect the possible existence of a composite yield surface with an associative flow rule to depend on constraint anisotropy; the meaning of this term will become clear as this discussion proceeds. The term is related to the anisotropy of constraint hardening of the composite, i.e. creation of internal stress associated

with inhomogeneity. At the very least, such a formulation would be highly complex to model all observed effects (Wang, 1970). In general, this is due to the fact that the matrix plastic strain rate rotates in a complicated manner relative to the composite stress rate in response to changing constraint during the transition from elastic to fully plastic matrix response.

In this work, we will apply the tangent stiffness approach to two very different classes of elastic reinforcement in a ductile matrix. In the first case, we will consider a silica spherical particle-reinforced epoxy composite previously treated by Weng (1988) with the secant modulus approach. Then, we will consider unidirectional, continuous fiber-reinforced boron-aluminum under various loading conditions.

In recognition of the lack of constraint on matrix plastic deformation for fibrous composites loaded off-axis, we must also introduce a provision for transition to matrix plastic deformation-dominated behavior. As reported by Dvorak and Bahei-El-Din (1987), the off-axis behavior of certain unidirectional composites typified by high fiber transverse shear modulus is essentially dominated by matrix behavior in the plastic regime, nearly independent of fiber volume fraction. For composites with low fiber transverse shear modulus, the tendency for matrix shear localization and plastic strain rate rotation away from the fibers is not as great. Dvorak and Bahei-El-Din have defined these two types of unidirectional metal-matrix composites as matrix-dominated and fiber-dominated, respectively.

While the issue of defining the comparison material response (i.e. β) for the

must be accomplished via a transition to matrix-dominated deformation for off-axis loading. This transition behavior will depend both on the plastic tangent modulus of the matrix, h, and the projection of the direction of plastic straining in the principal direction of reinforcement anisotropy (i.e. the fiber direction), $\hat{e}_3$. To accomplish a decrease in the rate of eigenstrain accumulation (decreased misfit constraint) as plastic flow becomes fully developed and rotates away from the fiber direction, we may introduce an effective fiber stiffness

$$\hat{C}^{*}_{ijkl} = (C^{*}_{ijkl} - C^{T}_{ijkl})\chi + C^{T}_{ijkl} \tag{3-16}$$

to be used in the incremental EIAS approach instead of C_{ijkl}^{*} where

$$\chi = \exp\left[-\left\{\frac{h_o}{h}\left(1 - \frac{|\hat{e}_3 \cdot n_{ij}\hat{e}_i \otimes \hat{e}_j \cdot \hat{e}_3|}{\sqrt{2/3}}\right)\right\}^{N}\left(1 - \frac{a}{c}\right)\right] \tag{3-17}$$

and a and c are the minimum and maximum diameters, respectively of the ellipsoidal reinforcement. The maximum diameter, c, is assumed to be aligned with the $\hat{e}_3$ direction. Constant h_o is a small value of the plastic modulus h representative of the transition to asymptotic (e.g. past the initial yielding regime) matrix strain hardening. For the case of long fibers, $(a/c) \rightarrow 0$; $(h_0/h)^N$ then largely governs the transition to matrix-dominated behavior. As $(h_o/h)^N$ becomes much greater than 1, $\chi \rightarrow 0$ and $\hat{C}_{ijkl}^{*}$ $\rightarrow C_{ijkl}^{T}$. This is when matrix-dominated behavior is realized. Typically, N may be expected to be sufficiently large (i.e. N>2) to result in a continuous but rapid transition to matrix-dominated behavior. The transition to matrix-dominated behavior

matrix-dominated behavior. As $(h_o/h)^N$ becomes much greater than 1, $\chi \to 0$ and $\hat{C}_{ijkl}^{\bullet} \to C_{ijkl}^{T}$. This is when matrix-dominated behavior is realized. Typically, N may be expected to be sufficiently large (i.e. N>2) to result in a continuous but rapid transition to matrix-dominated behavior. The transition to matrix-dominated behavior is also affected by the magnitude of the projection of the matrix plastic strain rate in the fiber direction, $|\hat{e}_3 \cdot n_{ij} \hat{e}_i \otimes \hat{e}_j \cdot \hat{e}_3| = |n_{33}|$. Clearly, the transition is delayed and fiber dominance persists until the matrix plastic strain rate rotates sufficiently away from the fiber direction (i.e. $|n_{33}|$ small). This condition is met more rapidly for predominantly transverse loadings than for moderate off-axis loadings; hence, the composite response remains fiber-dominated ($\hat{C}_{ijkl}^{\bullet} \approx C_{ijkl}^{\bullet}$) longer for loading directions more nearly aligned with the fibers.

As $\hat{C}_{ijkl}^{\bullet} \to C_{ijkl}^{T}$, the eigenstrain rate diminishes correspondingly by virtue of **(3-9)**, reflecting the loss of constraint on the plastic deformation. For fibrous composites (i.e. low a/c) with a high fiber transverse shear modulus, the additional assumption $C_{ijkl}^{To} = C_{ijkl}^{T}$ ($\beta = 0$) is reasonable since this equality holds rigorously under both elastic and fully plastic, matrix-dominated conditions.

For fibrous systems with low fiber transverse shear modulus, it is necessary to assign $\beta > 0$ since the transition to matrix-dominated behavior is not realized due to the reduction of constraint anisotropy; hence, the comparison material response is slightly different from the actual matrix response. For such cases, the rotation of the matrix plastic strain rate relative to the fibers during loss of constraint anisotropy and

interface shear localization is expected to be less pronounced and associativity of a flow rule based on a composite yield surface is expected to be more realistic.

Note that for spherical particle reinforcement, (a/c)=1 and χ=1 which leads to $\hat{C}_{ijkl}^{\bullet} = C_{ijkl}^{\bullet}$. Only β affects constraint hardening in the plastic regime in this case, as constraint anisotropy does not enter as a consideration. The following discussion will serve to clarify this point.

A key idea in this formulation is the concept of constraint hardening. It may be obvious that for systems with aligned ellipsoidal reinforcement, the composite is at most elastically transversely isotropic if the matrix is elastically isotropic. It is well known that such fibrous systems exhibit significant levels of "constraint" on matrix deformation. A perhaps subtle but very important concept is that of constraint anisotropy which has been mentioned previously in connection with χ. From a formal standpoint, it is most instructive to view constraint in terms of its evolution with plastic flow of the matrix. After some level of matrix plastic straining, the anisotropic elastic-plastic state of the composite may be expressed as an isotropic tensor function of the unit vector $\hat{e}_3$ in the reinforcement direction and backstress α_{ij}^{m} associated with the matrix kinematic hardening. The symmetry classes represented by $\hat{e}_3$ and α_{ij}^{m} are transversely isotropic and orthotropic, respectively. We will refer to the orientations of $\hat{e}_3$ and α_{ij}^{m} as structural and microstructural, respectively. Since we wish to examine the role of plastic strain on constraint rate reduction, we may introduce the symmetric second rank tensor ψ_{ij} defined in ε_{ij}^{pm} space by

$$\psi_{ij} = \frac{\partial \sigma_{kk}^{m}}{\partial \varepsilon_{ij}^{pm}}, \tag{3-18}$$

where ψ_{ij} obviously is a vector in this space normal to the level surface $\sigma_{kk}^{m}(\varepsilon_{kl}^{pm})$, which may be viewed as a constraint surface valid for monotonic, proportional loading; $\sigma_{kk}^{m}(\varepsilon_{mn}^{pm})$ is the hydrostatic constraint stress in the matrix which relaxes as plastic strains are generated. Clearly, ψ_{ij} is the rate of increase of constraint stress with plastic strain. In general, we may assign ψ_{ij} the form

$$\psi_{ij} = \psi_{ij}(\hat{e}_3, \alpha_{kl}^{m}). \tag{3-19}$$

This may be expressed using the representation theorem in terms of the irreducible functionality basis of the pair $(\hat{e}_3, \alpha_{kl}^{m})$ (Wang, 1970). However, let us consider two special cases which are of much relevance to both particle and continuous fiber-reinforced composites.

First, for spherical particle reinforcement and elastic isotropy of both phases, there is no preferred structural orientation (no structural anisotropy) and hence

$$\psi_{ij} = \psi_{ij}(\alpha_{kl}^{m}). \tag{3-20}$$

For monotonic, proportional loading,

$$\alpha_{ij}^{m} = A(\|\varepsilon_{kl}^{pm}\|)\varepsilon_{ij}^{pm} \tag{3-21}$$

provided the matrix has at most only a purely hydrostatic initial residual stress. Hence,

$$\psi_{ij} = \psi_{ij}(\varepsilon_{kl}^{pm}). \tag{3-22}$$

Clearly, invoking the total derivative of $\sigma_{kk}^{m}(\varepsilon_{ij}^{pm})$,

$$\dot{\sigma}_{kk}^{m} = \frac{\partial \sigma_{kk}^{m}}{\partial \varepsilon_{ij}^{pm}} \dot{\varepsilon}_{ij}^{pm} = \psi_{ij} \dot{\varepsilon}_{ij}^{pm}. \tag{3-23}$$

The representation of ψ_{ij} is (Wang, 1970)

$$\begin{aligned} \psi_{ij} = {} & A_1(I_2,I_3)\varepsilon_{ij}^{pm} + A_2(I_2,I_3)\varepsilon_{ik}^{pm}\varepsilon_{kj}^{pm} \\ & + A_3(I_2,I_3)\delta_{ij}, \end{aligned} \tag{3-24}$$

where

$$I_2 = \varepsilon_{ij}^{pm}\varepsilon_{ij}^{pm} \text{ and } I_3 = \varepsilon_{ij}^{pm}\varepsilon_{jk}^{pm}\varepsilon_{ki}^{pm} \tag{3-25}$$

are the two non-zero invariants of ε_{ij}^{pm}.

Hence, in general,

$$\dot{\sigma}_{kk}^{m} = A'(I_2,I_3)\|\dot{\varepsilon}_{ij}^{pm}\| \tag{3-26}$$

since

$$\dot{\varepsilon}_{ij}^{pm} = \dot{\lambda}(\|\varepsilon_{kl}^{pm}\|)\varepsilon_{ij}^{pm} = \dot{\lambda}(I_2)\varepsilon_{ij}^{pm} \tag{3-27}$$

for monotonic, proportional loading and

$$\dot{\varepsilon}_{ij}^{pm}\delta_{ij} = 0. \tag{3-28}$$

The constraint stress development is therefore independent of loading direction, dependent only on the accumulation of plastic strain in the direction of loading. In other words, the constraint surface $\sigma_{kk}^{m}(\varepsilon_{ij}^{pm})$ is isotropic in plastic strain space.

For fibrous composites, on the other hand, structural anisotropy dominates; and we may consider the influence of α_{ij}^{m} to be small in comparison to that of $\hat{e}_3$ with respect to composite response. In this case, we introduce the dependency

$$\psi_{ij} = \psi_{ij}(\hat{e}_3, \alpha_{kl}^{m}) \tag{3-29}$$

and express the representation of ψ_{ij} with respect to the irreducible functionality basis of $\hat{e}_3$, i.e.

$$\psi_{ij} = \varphi\delta_{ij} + \xi\hat{e}_3\otimes\hat{e}_3 \tag{3-30}$$

where $\varphi > 0$, $\xi > 0$, and $\xi > \varphi$ such that $l_i\psi_{ij}l_j > 0$ for all vectors, l_i. It is understood that φ and ξ may depend on the invariants of α_{ij}^{m} and the joint invariants of α_{ij}^{m} and $\hat{e}_3$, but the terms in the representation based on these generators have been omitted as second order. In this case, the constraint hardening rate for monotonic loading is approximated by

$$\begin{aligned}\dot{\sigma}_{kk}^{m} = \psi_{ij}\dot{\varepsilon}_{ij}^{pm} &= \xi\|\dot{\varepsilon}_{kl}^{pm}\|n_{ij}\hat{e}_i\otimes\hat{e}_j:\hat{e}_3\otimes\hat{e}_3 \\ &= \xi\|\dot{\varepsilon}_{kl}^{pm}\|n_{33} = \xi\dot{\varepsilon}_{33}^{pm}.\end{aligned} \tag{3-31}$$

Consequently, the constraint surface evolves anisotropically. Moreover, the rate of

constraint hardening increases proportionally with $n_{ij}\hat{e}_i \otimes \hat{e}_j : \hat{e}_3 \otimes \hat{e}_3 = n_{33}$, the component of the unit normal vector of the plastic strain rate in the reinforcement direction.

Since

$$\| \dot{\varepsilon}_{ij}^{pm} \| = \frac{1}{h} (\dot{\sigma}_{ij}^{m} n_{ij}), \tag{3-32}$$

we may write (3-31) as

$$\frac{\dot{\sigma}_{kk}^{m}}{\dot{\sigma}_{ij}^{m} n_{ij}} = \xi n_{33} h^{-1} \tag{3-33}$$

which is the ratio of matrix constraint to projected deviatoric stress rates. Bear in mind that ξ depends on the magnitude of backstress as well. Note that this analysis, based on equation (3-29), did not rely on proportionality of the matrix plastic strain increment to achieve the result in equation (3-33).

We are now in a position to assess the form of constraint hardening introduced in the incremental Eshelby analysis based on these symmetry considerations. First, parameter β influences the comparison material response. For the form adopted, for a given value of β, C_{ijkl}^{To} depends uniquely on C_{ijkl}^{T} and hence h, the matrix plastic tangent modulus. The constraint hardening rate will therefore depend on the relevant structural/microstructural symmetry. For spherical particle reinforcement and proportionally applied tractions,

$$\frac{\dot{\sigma}^{m}_{kk}}{\dot{\sigma}^{m}_{ij} n_{ij}} = A'(I_2, I_3; \beta) h^{-1} \tag{3-34}$$

and for fiber reinforcement and proportionally applied tractions,

$$\frac{\dot{\sigma}^{m}_{kk}}{\dot{\sigma}^{m}_{ij} n_{ij}} = \xi(\alpha^{m}_{ij}, \hat{e}_3; \beta) n_{33} h^{-1}, \tag{3-35}$$

where the dependence of both ξ and A' on β is implicit. Interestingly, equation (3-35) indicates that $\dot{\sigma}_{kk}$ may become negative with monotonic plastic deformation only for the fibrous composite if $n_{33} < 0$; physically, this condition is that of a negative matrix plastic strain rate in the fiber direction. Clearly, the issue of distinct branches of stress-space composite yield criteria relating to matrix- and fiber-domination is related to the constraint anisotropy inherent in the structural symmetry class of transverse isotropy.

A related issue is that of χ, which is employed as a means of transitioning to matrix-dominated behavior in the incremental Eshelby approach, forcing the eigenstrain rate to vanish under fully plastic conditions. This is equivalent in principle, to the continuum slip model for the matrix-dominated mode suggested by Dvorak and Bahei-El-Din (1987) but is also quite different since a micromechanical framework is employed here rather than construction of a composite flow rule. The rate of change of the constraint in the Eshelby approach is assumed to additionally depend nonlinearly through ξ on h and n_{33}, i.e.

$$\frac{\dot{\sigma}_{kk}}{\dot{\sigma}^{m}_{ij} n_{ij}} = \xi(\alpha^{m}_{ij}, \mathcal{E}_3; \beta, h, n_{33}) n_{33} h^{-1}, \qquad (3\text{-}36)$$

where again implicit dependence on ß, h and n_{33} is expressed. Note that χ employs explicit dependence on h and n_{33} to correlate off-axis constraint weakening with plastic deformation. Note also that $\chi = 0$ for spherical particle reinforcement since the constraint hardening is isotropic in this case. See Appendix F for a more detailed discussion of constraint hardening in fiber-reinforced composites and development of the χ funtion.

3.3 Solution Procedure for the EIAS Method-Tangent Stiffness Formulation

Per the discussion in § **3.1** and **3.2**, the BALNIT program was modified accordingly. The BALNIT program incorporating the tangent stiffness method only was called TAN1. With the exceptions stated in § **3.1**, the solution procedure for TAN1 remains the same as BALNIT.

The TAN1 program was modified to include the ß parameter and the χ function. This program was called CSTAR since one of its key features is the modification of the fiber stiffness (C_{ijkl}^{*}) to lessen the constraining power. Again, the solution procedure remains the same with the exceptions stated in § **3.2.** Flowcharts for these programs are in Appendix C.

CHAPTER IV

DISCUSSION OF RESULTS

4.1 Introduction

Two composite systems were investigated - boron-aluminum (B/Al), a unidirectionally continuous fiber-reinforced MMC and a silica spherical particle-reinforced epoxy composite. The results as applicable to B/Al will be discussed first. Discussion of the results for the silica-epoxy composite are in § **4.7.**

4.2 Application to a Fibrous Reinforced Composite

Due to its good fiber/matrix bonding and very periodic microstructure with virtually no presence of voids, B/Al is in many ways a model material system which can be employed as a standard to test the accuracy of micromechanic composite models (Pindera and Lin, 1989). The constituent material properties for the B/Al system investigated are listed in Appendix E. These properties correspond to those used by Dvorak and Bahei-El-Din in their experimental work on B/Al (1988). Note the high transverse shear stiffness of the boron fibers. The Eshelby tensor for circular, cylindrical fibers and the nonlinear kinematic hardening rule utilized in this investigation are shown in Appendices A and B, respectively. The actual uniaxial

experimental behavior of the aluminum matrix material as shown in (Pindera and Lin, 1989) was used instead of the "in-situ" properties employed sometimes in development of micromechanics models. This in itself represents an issue and a possible advantage of the present model over other approaches, as will be discussed later. Uniaxial experimental data on B/Al, as presented by Pindera and Lin (1989), were utilized as a basis for determining the accuracy of our models. Although not specifically given, the fiber volume fraction of the composite used in the experiments appears to be approximately 48%. We were able to "back this out" using the constituent elastic properties, the composite modulus for the 0° test, and a rule of mixtures method.

Uniaxial histories were run on the three composite models (programs BALNIT, TAN1, and CSTAR) in the 0° and 90° orientations as well as three off-axis orientations, 10°, 15°, and 45°. These correspond to the orientations investigated experimentally by Pindera and Lin (1989). The results of the tests were plotted as $\bar{\sigma}_{zz}$ versus $\bar{\varepsilon}_{zz}$ where the zz-direction corresponds to the loading direction. Note that $\bar{\sigma}_{zz}$ and $\bar{\varepsilon}_{zz}$ represent the average composite stress and strain, respectively.

4.3 Analysis of Results using the EIAS Method with Elastic Constraint

Figures 4 and 5 show the results using the EIAS Method with Elastic Constraint. As expected, the results are extraordinarily stiff. The model does reasonably well in the elastic regime since the Eshelby approach is based on elastic

considerations. However, once past the point of initial yielding, continued accumulation of matrix plastic strain, which is treated as a negative eigenstrain, causes increased constraint and an overly stiff response. These results confirm what has been stated consistently in the literature, that unmodified self-consistent approaches are inadequate for modeling elastic-plastic behavior of composites, particularly for the case of the ductile matrix.

4.4 Analysis of EIAS Method-Tangent Stiffness Formulation

Figures 6 and 7 show the results of the tests using the EIAS Method-Tangent Stiffness Formulation with $\beta=0$ and without the χ function, i.e. $\hat{C}_{ijkl}^{*}=C_{ijkl}^{*}$ always. With $\beta=0$, the comparison material is the same as the matrix material. The model does reasonably well in approximating initial yielding behavior but does not capture the transition to asymptotic plastic flow. Without any correction for unwarranted eigenstrain accumulation, we see the composite stiffen in the plastic regime following initial yielding. These results demonstrate, however, that the tangent stiffness method has improved the model's ability to approximate initial yielding (i.e. the position and shape of the "knee" in the curve). However, eigenstrain accumulation or, conversely, excessive constraint hardening, still presents a problem. Extensive analysis was conducted to determine the effect of various values of β on the response and to determine if β alone would reduce the effects of excessive eigenstrain accumulation and bring the response more in line with the experimental data. These efforts proved

futile, as would be expected based on the discussion of constraint anisotropy in the previous section. A particular value of β would suffice only for a particular loading direction. It was evident that the χ function is necessary to model the change of constraint hardening for all orientations. The β factor is a comparison material parameter which should be unique to a particular composite system and should not change with each loading orientation for even continuous fiber-reinforced composites.

4.5 Analysis of Rotation of the Plastic Strain Rate Vector

Based on the literature, the inelastic response of the composite should asymptotically approach (or closely approximate) that of the pure matrix material for certain ranges of off-axis uniaxial loading directions relative to the fiber direction. This motivated an investigation of the rotation of the plastic strain rate vector, $\dot{\varepsilon}_{ij}^{pm}$, as a means of studying the transition from fiber-dominated to this so-called matrix-dominated behavior.

To help illustrate this point, we employed the tangent stiffness method with $\beta=0$ (no χ function) and plotted the matrix plastic strain in the fiber direction, ε_{33}^{pm}, versus the matrix plastic strain in the transverse direction, ε_{22}^{pm}, for several different monotonic, uniaxial loading orientations of interest. The directions 33 and 22 refer to the fixed material coordinate system, 33 being the direction of the aligned fibers. These results are shown in Figure 8. It is important to note that the tangent stiffness method accurately modeled the initial yielding regime. Therefore, it is accurate up

to approximately 0.2% strain. Therefore, the results shown in Figure 8 are also accurate for this same strain range. For the 0° orientation, relatively significant levels of positive ε_{33}^{pm} are generated while only limited levels of negative ε_{22}^{pm} are observed. This is in accordance with plastic incompressibility of the matrix. No $\dot{\varepsilon}_{ij}^{pm}$ rotation takes place in the 0° direction. In the 10° orientation, the response is initially very similar to that of the 0° orientation; however, rotation of $\dot{\varepsilon}_{ij}^{pm}$ causes generation of positive ε_{22}^{pm}, and we see the curve rotate towards positive ε_{22}^{pm}. In the 15° orientation, we observe behavior similar to the 10° orientation. Due to faster rotation of $\dot{\varepsilon}_{ij}^{pm}$, the curve turns more rapidly to the right, again demonstrating the increasing dominance (or positive magnitude) of ε_{22}^{pm}. The behavior of the 45° and 90° loading angles are essentially matrix-dominated from the outset. The negative values of ε_{33}^{pm} observed in the 90° direction are realized due Poisson's effect. Based on these results, we recognize the tendency of the matrix plastic strain rate vector to rotate and align itself with the 22-direction. Since predominance of ε_{22}^{pm} in the response is indicative of matrix-dominated behavior, we conclude that the transition to matrix-dominated behavior is related to the rotation of $\dot{\varepsilon}_{ij}^{pm}$. Only a micromechanical model can accurately predict this effect. It is very important to note that this effect is predicted <u>without</u> introduction of the χ function; χ merely serves to affect the eigenstrain rate past the initial yielding regime. Also, since the matrix plastic strain rate is nonproportional <u>even</u> <u>though</u> the tractions are applied proportionally, this casts grave doubts on the possibility of constructing a simple, associative flow rule

plasticity framework based on a composite yield surface, at least for composites which exhibit this transition to matrix-dominated behavior.

4.6 Analysis of the EIAS Method-Tangent Stiffness Formulation with β Parameter and χ Function

Figures 9 and 10 show the results of the tangent stiffness method including the χ function. $\beta=0$ was selected on the basis that the B/Al composite is expected to exhibit a matrix-dominated regime where the incremental composite response is essentially governed by that of the matrix. In the χ function, the parameters $h_o=180$ ksi and $N=4$ were selected to best fit the uniaxial test in the 45° orientation. Good results are realized in all orientations as the model now approximates a continuous transition to matrix-dominated, plastic deformation for off-axis loading. The χ function controls the rate of constraint hardening; therefore, we do not see increased constraint and the associated stiffening caused by eigenstrain accumulation as was the case with the model without the χ function. Comparing the 10° response to the 45° response, the reduction of constraint is more gradual in the 10° orientation; the model "recognizes" that the loading is more nearly aligned with the fiber direction and hence the response will remain fiber-dominated longer (i.e. it takes longer to realize matrix-dominated behavior).

It is important to point out that use of an incremental plasticity theory enabled us to conduct the rotation analysis of $\mathring{\varepsilon}_{ij}^{pm}$. The secant modulus method (Weng,

1988), in contrast, cannot support such studies because a backstress computation, inherent to an accurate incremental theory, is required to analyze $\dot{\varepsilon}_{ij}^{pm}$ rotation with some degree of accuracy. Also, it is anticipated that the constraint anisotropy issue will not be as pronounced for fibrous composites with low transverse elastic shear modulus; in this case, a combination of $\beta > 0$ and the χ function is most likely necessary.

The goal of concentric cylinder models which incorporate interface phases (Mikata and Taya, 1985) as well as the recently proposed "smear" model (Luo and Weng, 1989) both seek to describe the interface shear localization and loss of constraint by modifying the transformation strains. In contrast, our approach is to introduce an effective fiber stiffness; nonetheless, the goal is similar.

4.7 Application to Particle-Reinforced Composites

Next, we apply the tangent stiffness model to the elastic-plastic behavior of a silica particle-reinforced epoxy composite. The silica is elastic, and the epoxy is elastic-plastic. Both phases are assumed to be isotropic. The material properties are from Weng (1988) and are listed in Appendix E. The Eshelby tensor for spherical particle-reinforcement and the isotropic hardening plasticity theory employed to model the epoxy matrix behavior are given in Appendices A and B, respectively.

As stated in section 3.2, there is no structural anisotropy with spherical particle-reinforced composites. The fiber diameter ratio (a/c) = 1; therefore, χ =

1, and $\hat{C}_{ijkl}^{*} = C_{ijkl}^{*}$. Hence, only β affects constraint hardening. The EIAS Method-Tangent Stiffness Formulation with the β parameter for calculation of comparison matrix material response was used to calculate the uniaxial response of the composite with the same volume fractions as in Weng's work (1988).

Experimental data (Weng, 1988) were digitized and plotted with the results of the tangent stiffness model in Figures 11-13. The composite stress versus plastic strain is considered in these plots and is of course, orientation independent for each volume fraction of reinforcement.

The composite response was calculated with $\beta=0$ and $\beta=8$. The plot for $\beta=0$, Figure 11, represents behavior of the composite when the comparison matrix material response is the same as that of the actual matrix material. The results of the tangent stiffness model best fit Weng's secant modulus approach when $\beta=8$. These results are plotted in Figure 12, while the experimental results are shown in Figure 13.

Several points are noteworthy. First, the results agree relatively well with the experimental data. Second, the results are very similar to those of Weng who employed the EIAS method with a secant modulus based on the deformation theory of plasticity. It therefore appears that the tangent stiffness method is a reasonable extension of the secant modulus concept for the solution of incremental elastic-plastic problems involving complex cyclic loading paths. Refer to Appendix D for a more complete comparison of the two methods.

Due to the linear combination of β and f in **(3-14)**, the response stiffens for

a particular β as the volume fraction f increases. An increase in f leads to increased constraint and, consequently, a much stiffer response in the yielding regime. This fact is borne out by Figures 11 and 12. The stress versus plastic strain curves with $\beta=0$ are much flatter than those with $\beta=8$ for the same volume fraction of reinforcement.

Finally, our results with the tangent stiffness method with $\beta=8$ are stiffer than Weng's results, especially at lower volume fractions. One notes, however, that the actual experimental results are also stiffer than Weng's theoretical results (Weng, 1988).

The material response calculated using the EIAS model with elastic constraint, as shown by Weng (1988), is significantly stiffer than experimentally observed. This concurs with the results of our earlier calculations on B-Al fibrous composites.

CHAPTER V

CONCLUSIONS AND RECOMMENDATIONS

5.1 Summary of Composite Material Model

As a result of our theoretical study of the inelastic behavior of unidirectional, continuous fiber-reinforced metal-matrix composites, we developed a practical, computationally efficient micromechanical model which satisfactorily approximates experimental inelastic behavior of certain composites. This model is limited to two-phase composite systems where the matrix is the ductile phase but can be modified for any aspect ratio of aligned reinforcement by employing the appropriate Eshelby tensor. Material properties of the constituent phases must be input to the program. Detailed information regarding the stress and strain states of the composite as well as that of the individual phases can be obtained from the model.

The model employs a sophisticated nonlinear kinematic hardening rule to model the plastic flow of the matrix. Use of this incremental plasticity theory necessitates introduction of a tangent stiffness method instead of a secant stiffness method, which is restricted to deformation plasticity theory. Furthermore, use of an incremental theory facilitates consideration of nonproportional and/or cyclic loading histories.

The model employs two additional parameters, β and χ, to account for the constraint effects associated with eigenstrain accumulation and anisotropy due to fiber reinforcement. Although no exact function for the β parameter has been determined, intuitively it is a function of reinforcement volume fraction, fiber geometry, and elastic properties of the reinforcement. The β parameter is most singularly applicable to composite systems with little or no reinforcement or structural anisotropy while the χ function addresses cases of structural anisotropy, e.g. unidirectional, continuous fiber-reinforced systems.

5.2 Significant Findings

Due to the heterogeneous character of composites, the behavior of one constituent is not mutually exclusive of that of the others. This interaction of the phases renders analysis of the homogeneous aggregate very difficult, particularly in the plastic regime. In this thesis, we recognize the deficiencies of the EIAS method with elastic constraint and pursue sound methods of modifying the comparison material to collectively, and perhaps indirectly, take into account the first order effects. Our ultimate goal in this process was to effectively model the inelastic behavior of unidirectional, continuous fiber-reinforced composites.

In parallel to Weng's secant modulus method (1988), we introduced the tangent stiffness method. Our use of an incremental plasticity theory enabled us to instantaneously compute the matrix plastic hardening modulus which was used to

compute the "tangent stiffness modulus." This method produced equal, if not better, results than Weng's secant modulus method based on a comparison for a spherical particle-reinforced composite system, but failed to effectively approximate the experimental behavior for fibrous systems.

Recognizing that the overly stiff response was due to the overconstraining effects unique to fiber reinforcement, we focused on the realization that experimental results evidenced an eventual but complete transition to matrix-dominated behavior for all off-axis loadings, at least for the B/Al composite considered. From the analysis in § **4.5**, we identified the rotation of the matrix plastic strain rate vector as the primary cause for the transition to matrix-dominated behavior. Our χ function employs this rotation concept as a means to reduce the effect of fiber constraint anisotropy and represents a significant development above and beyond any methods currently in existence for modeling inelastic behavior of fibrous composites. By incorporating the χ function into the EIAS method-tangent stiffness formulation, we successfully approximated the behavior of a fibrous system.

We also introduced the β parameter as a means of accounting for the isotropic constraint effects in composites. This parameter is more relevant to composite systems with little or no reinforcement anisotropy (e.g. spherical particle-reinforced composites) instead of systems reinforced by unidirectional, continuous fibers. As stated in § **3.2**, fibrous composites may have distinct preferred directions of matrix plastic flow due to their aligned reinforcement whereas there are no such clearly

defined directions of flow in the spherical particle-reinforced composite. Additionally, the fibrous system with high fiber shear stiffness will tend to reduce constraint hardening rate through the phenomenon mentioned above, matrix plastic strain rate rotation, as well as interface shear localization. The particulate system cannot relieve constraint preferentially; therefore, it experiences additional constraint in the asymptotic plastic flow regime. Hence, the β parameter is required for the spherical particle-reinforced system, but it is not needed with the fibrous system considered.

Perhaps one of our most significant findings is that we have substantiated the experimental observations of B/Al behavior made by Dvorak (1987) which formed the basis of their bimodal plasticity theory of fibrous composites (Dvorak and Bahei-El-Din, 1987). Due to the plastic strain rate rotation exacerbated by the high boron fiber transverse shear stiffness, we support Dvorak and Bahei-El-Din's findings of non-normality of the plastic strain rate vector and "flats" in the composite yield surface. However, we feel that it is inadvisable to attempt to model a composite such as B/Al, which so clearly demonstrates both modes of deformation, with a normality flow rule based on a composite aggregate yield surface. This type of approach might be more successful when applied to a system with more compliant fibers in transverse shear. We find it particularly interesting that we have recovered Dvorak and Bahei-El-Din's anomalous results through an entirely different approach based on micromechanics.

Finally, we find it quite interesting that we were able to achieve good results

without consideration of the so-called "in-situ" behavior of the matrix. We utilized the actual uniaxial experimental behavior of the aluminum matrix material as shown in Pindera and Lin (1989) to determine the material parameters required to model matrix flow instead of the "in-situ" properties used by so many in the development of their micromechanics models (Pindera and Lin, 1989). This in itself represents a significant departure from contemporary approaches and may be viewed as an advantage of our model over these approaches, unless the "in-situ" behavior is (i) warranted based on different dislocation structure and/or (ii) determined to coincide with that actually employed in other models. Otherwise, the assumed matrix response in other models may be viewed as a kind of "first order fitting factor." As an example, Pindera and Lin (1989) adjusted the actual material properties to the so-called "in-situ" properties to allow for the effects of fabrication on the matrix material and so that their analytical results correlated with the experimental data. The matrix response is "backed out" by fitting the composite response. This "backing out" process is not required with our model.

5.3 Recommendations

As stated before, modeling of composite behavior is very complex because there are so many variables to take into consideration. For instance, shear-localization at the fiber-matrix interface is universally recognized as having a significant effect on the strength of fibrous composites, especially systems such as

B/Al which has a high fiber transverse shear modulus. However, we achieved acceptable results without specifically addressing this in our model. Perhaps we indirectly accounted for it in our introduction of χ for structural constraint anisotropy. Application of our model to systems reinforced by compliant fibers is outside the scope of this thesis. Therefore, we have several recommendations for future research to further test the validity of our model.

First, the EIAS model-tangent stiffness method with the χ function should be applied to a system reinforced by compliant fibers (eg. graphite) to determine how well it replicates experimental data. Certainly, we expect the χ function to play a different role for the compliant system.

Secondly, it would be interesting to conduct a similar plastic strain rate rotation analysis on this compliant system to see if it demonstrates both matrix- and fiber-dominated deformation modes. According to Dvorak and Bahei-El-Din, a system such as graphite-aluminum should deform only in the fiber-dominated mode (1987). If this is the case, plots of ε_{33}^{pm} versus ε_{22}^{pm} for uniaxial, monotonic loading in off-axis orientations should retain a higher degree of proportionality than that in Figure 8.

Finally, we stated that we utilized an incremental theory so that nonproportional and/or cyclic loading histories could be applied to our model. We did not report any such histories, but it would be interesting to see how our model correlates with the data recorded by Dvorak and Bahei-El-Din for nonproportional

loading experiments conducted on B/Al (1988).

REFERENCES

Aboudi, J. (1986). "Overall Finite Deformation of Elastic and Elastoplastic Composites." *Mechanics of Materials*, Vol. 5, 73-86.

Bahei-El-Din, Y.A. and Dvorak, G.J. (1989). "A Review of Plasticity Theory of Fibrous Composite Materials." *Metal Matrix Composites: Testing, Analysis and Failure Modes*, ASTM STP 1032, W.S. Johnson, ed., ASTM, Philadelphia.

Beneveniste, Y. (1987). "A New Approach to the Application of Mori-Tanaka's Theory in Composite Materials." *Mechanics of Materials*, Vol.6, 147-157.

Chaboche, J.L. (1978). "Description Thermodynamique et Phenomologique de la Viscoplaticité Cyclique avec Endommagement." Publication No. 1978-3, ONERA, France.

Chaboche, J.L. and Roussellier, G. (1983a). "On the Plastic and Viscoplastic Constitutive Relations-Part I: Rules Developed with Internal Variable Concept." ASME *Journal of Pressure Vessel Technology*. Vol.105, 153-158.

Chaboche, J.L. and Roussellier, G. (1983b). "On the Plastic and Viscoplastic Constitutive Relations-Part II: Application of the Internal Variables Concept to 316 Stainless Steel." ASME *Journal of Pressure Vessel Technology*. Vol.105, 159-164.

Christensen, R.M. (1979). *Mechanics of Composite Materials*. John Wiley & Sons, Inc., New York.

Dvorak, G.J. (1987). "Plasticity of Fibrous Composites." U.S. ARO Report 20061.1-EG.

Dvorak, G.J. and Bahei-El-Din, Y.A. (1979). "Elastic-Plastic Behavior of Fibrous Composites." *Journal of the Mechanics and Physics of Solids*, Vol. 27, 51-72.

Dvorak, G.J. and Bahei-El-Din, Y.A. (1982). "Plasticity Analysis of Fibrous Composites." *Journal of the Mechanics and Physics of Solids*, Vol. 49, 327-335.

Dvorak, G.J. and Bahei-El-Din, Y.A. (1987). "A Bimodal Plasticity Theory of Fibrous Composite Materials." *Acta Mechanica*, Vol. 69, 219-241.

Dvorak, G.J. and Bahei-El-Din, Y.A. (1988). "An Experimental Study of Elastic-Plastic Behavior of a Fibrous Boron-Aluminum Composite." *Journal of the Mechanics and Physics of Solids*, Vol. 36, No. 6, 655-687.

Dvorak, G.J., Rao, M.S.M., and Tarn, J.Q. (1974). "Generalized Initial Yield Surfaces for Unidirectional Composites." *Journal of Applied Mechanics*. Vol. 41, 249-253.

Dvorak, G.J. and Teply, J.L. (1985). "Periodic Hexagonal Array Models for Plasticity Analysis of Composite Materials." *Plasticity Today: Modelling, Methods and Applications*. W. Olszak Memorial Volume, A. Sawczuk and V. Blanchi, eds, Elsevier, 623.

Eshelby, J.D. (1957). "The Determination of the Elastic Field of an Ellipsoidal Inclusion, and Related Problems,". *Proceedings of the Royal Society, London*, Vol. A241, 376-396.

Eshelby, J.D. (1959). "The Elastic Field Outside and Ellipsoidal Inclusion." *Proceedings of the Royal Society, London*, Vol. A252A, 561.

Hill, R. (1963). "Elastic Properties of Reinforced Solids: Some Theoretical Principles." *Journal of the Mechanics and Physics of Solids*, Vol. 11, 357-372.

Hill, R. (1964). "Theory of Mechanical Properties of Fibre-Strengthened Materials: I. Elastic Behavior." *Journal of the Mechanics and Physics of Solids*, Vol. 12, 199-212.

Hill, R. (1965a). "Theory of Mechanical Properties of Fibre-Strengthened Materials: II. Inelastic Behavior," *Journal of the Mechanics and Physics of Solids*, Vol. 13, 189-198.

Hill, R. (1965b). "Theory of Mechanical Properties of Fibre- Strengthened Materials: III. Self-Consistent Model," *Journal of the Mechanics and Physics of Solids*, Vol. 13, 189-198.

Hill, R. (1965c). "A Self-Consistent Mechanics of Composite Materials." *Journal of the Mechanics and Physics of Solids*, Vol. 13, 213-222.

Luo, H.A. and Weng, G.J. (1989). "On Eshelby's Inclusion Problem in a Three-Phase Cylindrically Concentric Solid, and the Elastic Moduli of Fiber-Reinforced Composites." *Mechanics of Materials*. Vol. 8, 77-88.

McDowell, D.L. (1985). "An Experimental Study of the Structure of Constitutive Equations for Nonproportional Cyclic Plasticity." *Journal of Engineering Materials and Technology*, Vol. 107, 307-315.

McDowell, D.L. (1985). "A Two-Surface Model for Transient Nonproportional Cyclic Plasticity: Part 1 Development of Appropriate Equations." *Journal of Applied Mechanics*, Vol. 52, 298-302.

McDowell, D.L. (1985). "A Two-Surface Model for Transient Nonproportional Cyclic Plasticity: Part 2 Comparison of Theory with Experiments." *Journal of Applied Mechanics*, Vol. 52, 303-308.

McDowell, D.L. (1987). "Simple Experimentally Motivated Nonproportional Cyclic Plasticity Model." *ASCE Journal of Engineering Mechancis*, Vol. 113, No. 3, 378-397.

McDowell, D.L. and Moosbrugger, J.C. (1987). "A Generalized Rate-Dependent Bounding Surface Model." *Advances in Piping Analysis and Life Assessment for Pressure Vessels and Piping*, Chang, Gwaltney and McCawley, eds. PVP-Vol. 129, ASME, 1-11.

McDowell, D.L. and Moosbrugger, J.C. (1989). "On a Class of Kinematic Hardening Rules for Nonproportional Cyclic Plasticity." *Journal of Engineering Materials and Technology*. Vol. 111, 87-98.

Mikata, Y. and Taya, M. (1985). "A Four Concentric Cylinders Model for the Analysis of the Thermal Stress in a Continuous Coated Fiber Metal Matrix Composite." *Journal of Composite Materials*. Vol. 19, 554-578.

Mori, T. and Tanaka, K. (1973). "Average Stress in the Matrix and Average Elastic Energy of Materials with Misfitting Inclusions." *Acta Metallurgica*, Vol. 21, 571-574.

Mura, Toshio. (1987). *Micromechanics of Defects in Solids*. 2nd Ed. Boston: Martinus Nijhoff.

Murakami, H. and Hegemier, G.A. (1986). "A Mixture Model for Unidirectionally Fiber-Reinforced Composites." *Journal of Applied Mechanics*. Vol. 53, 765-773.

Norris, A.N. (1989). "An Examination of the Mori-Tanaka Effective Medium Approximation for Multiphase Composites." *Journal of Applied Mechanics*. Vol. 56, 83-88.

Pindera, M.-J. and Lin, M.W. (1989). "Micromechanical Analysis of the Elastoplastic Response of Metal Matrix Composites." *Journal of Pressure Vessel Technology*, Vol. 111, 183-190.

Tandon, G.P. and Weng, G.J. (1988). "A Theory of Particle-Reinforced Plasticity." *Journal of Applied Mechanics*, Vol. 55, 126-135.

Taya, Minoru and Arsenault, Richard. (1989). *Metal Matrix Composites: Thermomechancial Behavior*. New York: Pergamon Press.

Wang, C.C. (1970). "A New Representation Theorem for Isotropic Functions." Parts 1 and 2. *Archive for Rational Mechanics and Analysis*. Vol. 36, 166.

Weng, G.J. (1988). "Theoretical Principles for the Determination of Two Kinds of Composite Plasticity: Inclusions Plastic vs. Matrix Plastic." *ASME AMD*, Vol. 92, eds., Dvorak, G.J. and Laws, N., 193-208.

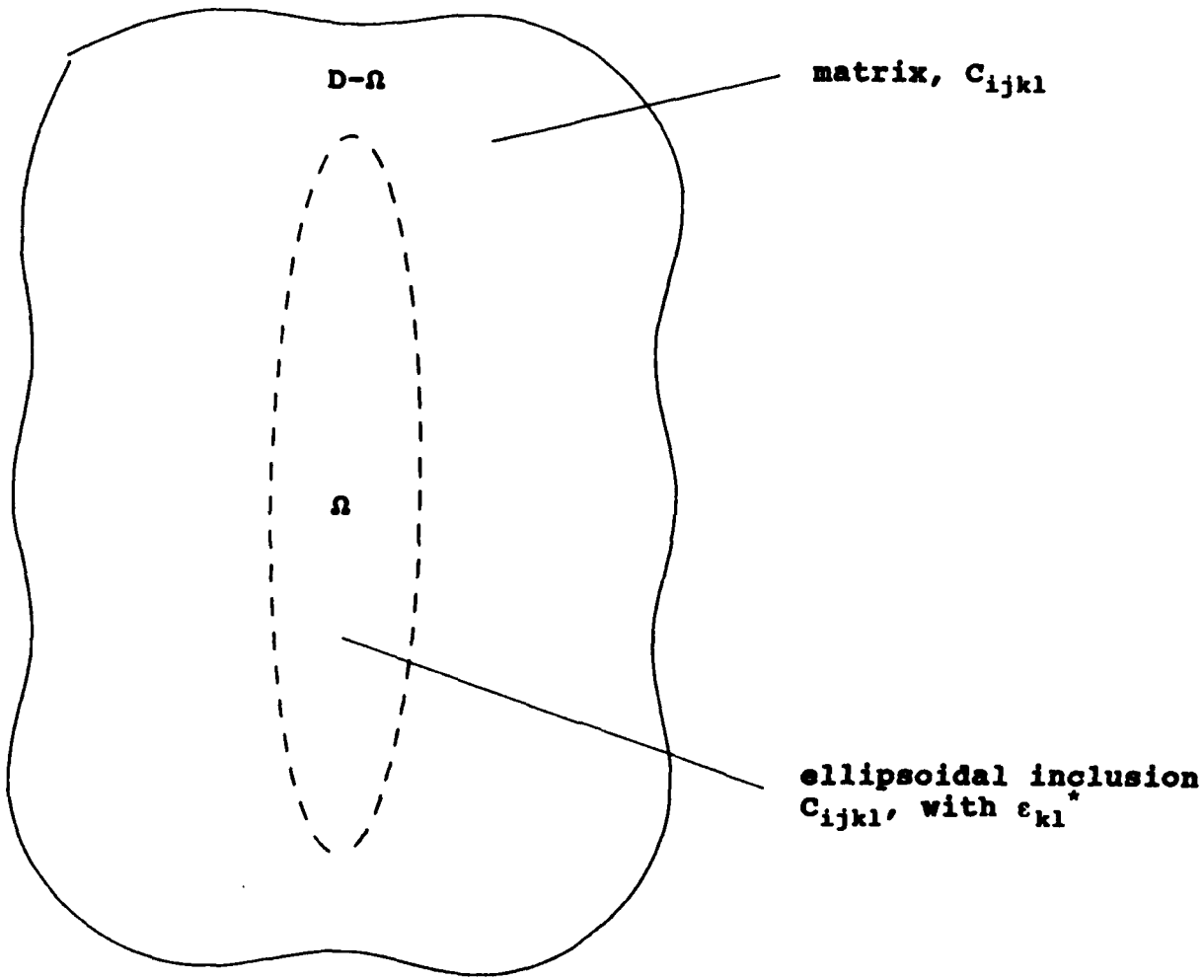

Figure 1. Ellipsoidal inclusion Ω, with eigenstrain ε_{kl}^*, embedded in the infinite material domain D (Taya and Arsenault, 1989).

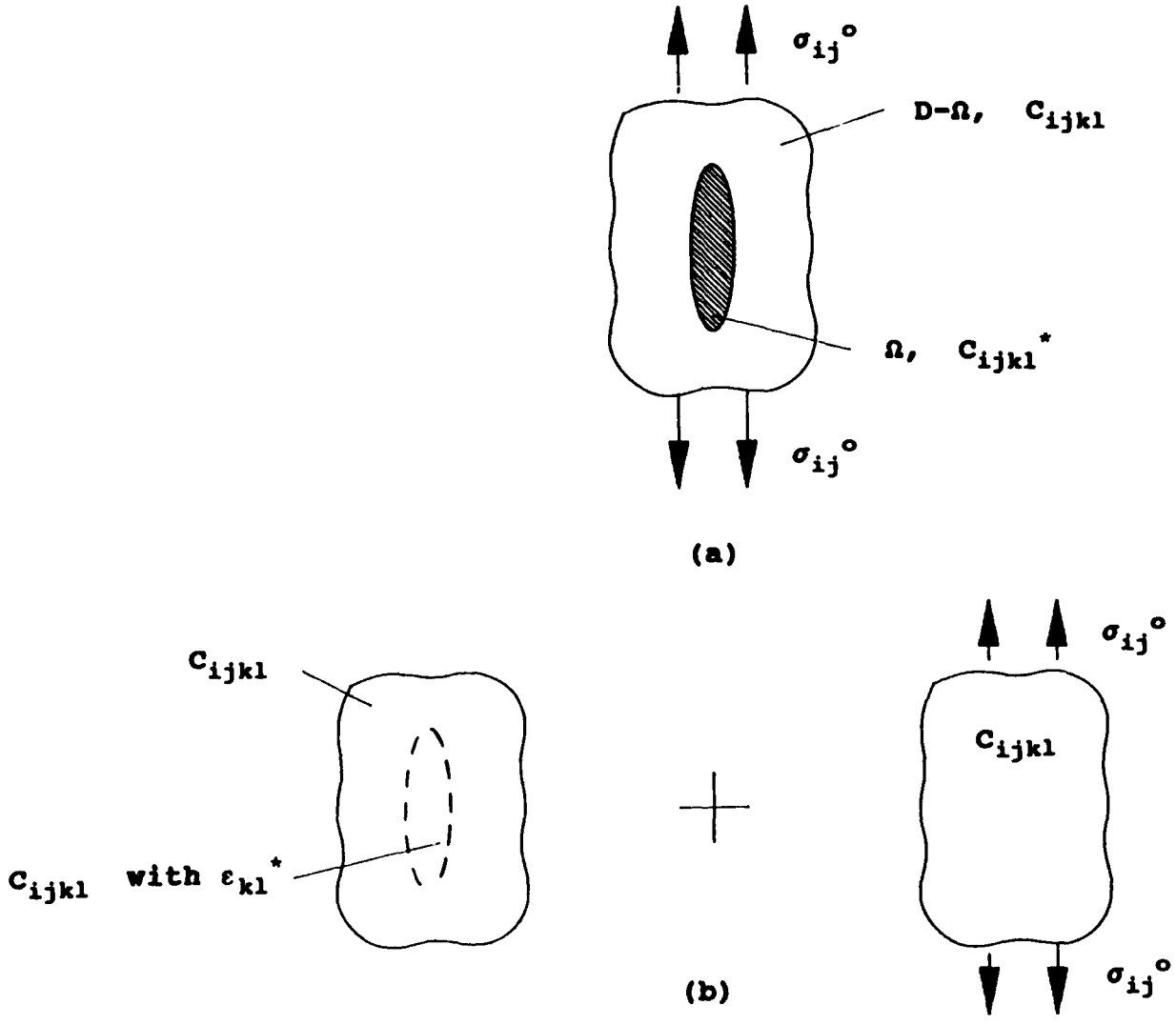

Figure 2. Infinite material domain D containing an ellipsoidal inhomogeneity, Ω, under applied stress σ_{ij}° (a) actual problem, (b) equivalent inclusion problem (Taya and Arsenault, 1989).

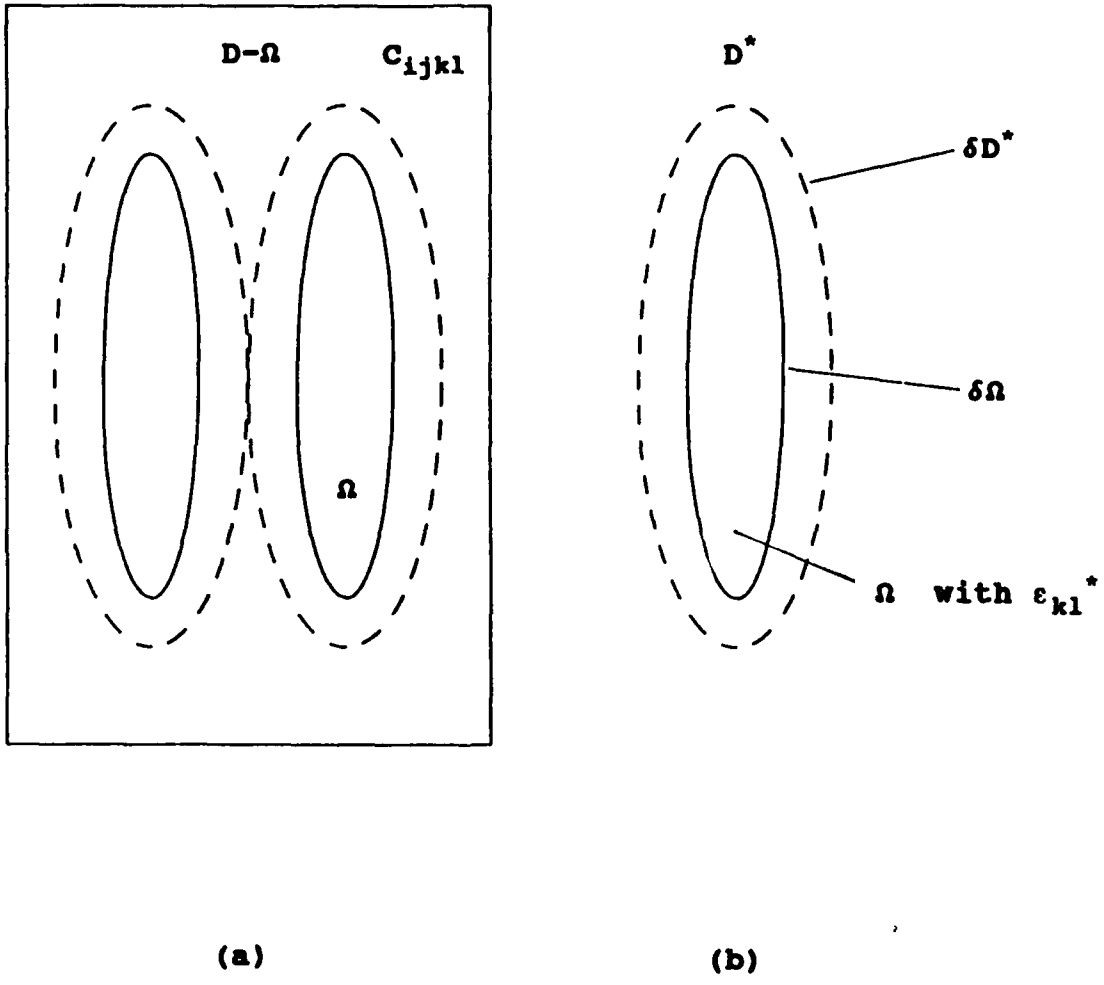

Figure 3. (a) n number of ellipsoidal inclusions, Ω, each with ε_{kl}^*, embedded in the finite material domain D; (b) a single inclusion, with ε_{kl}^*, enclosed by finite domain D^*.

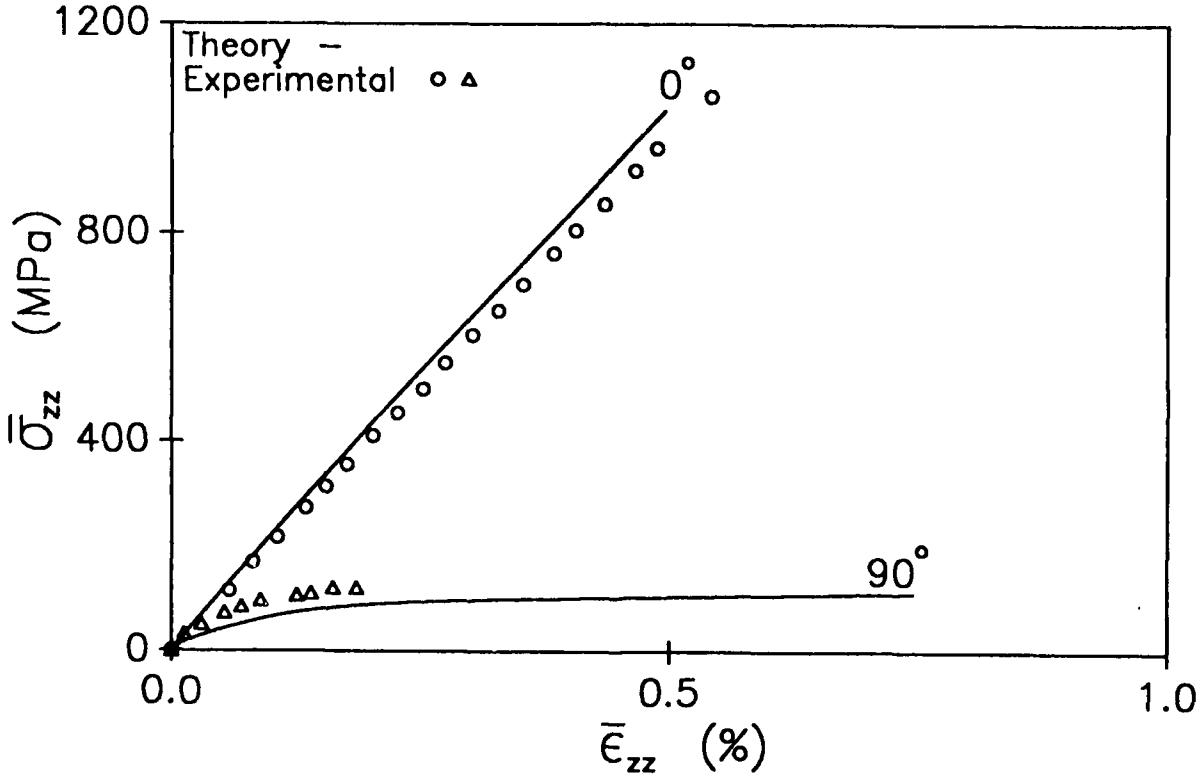

Figure 4. Results of the EIAS method with elastic constraint for B/Al - 0° and 90° orientations.

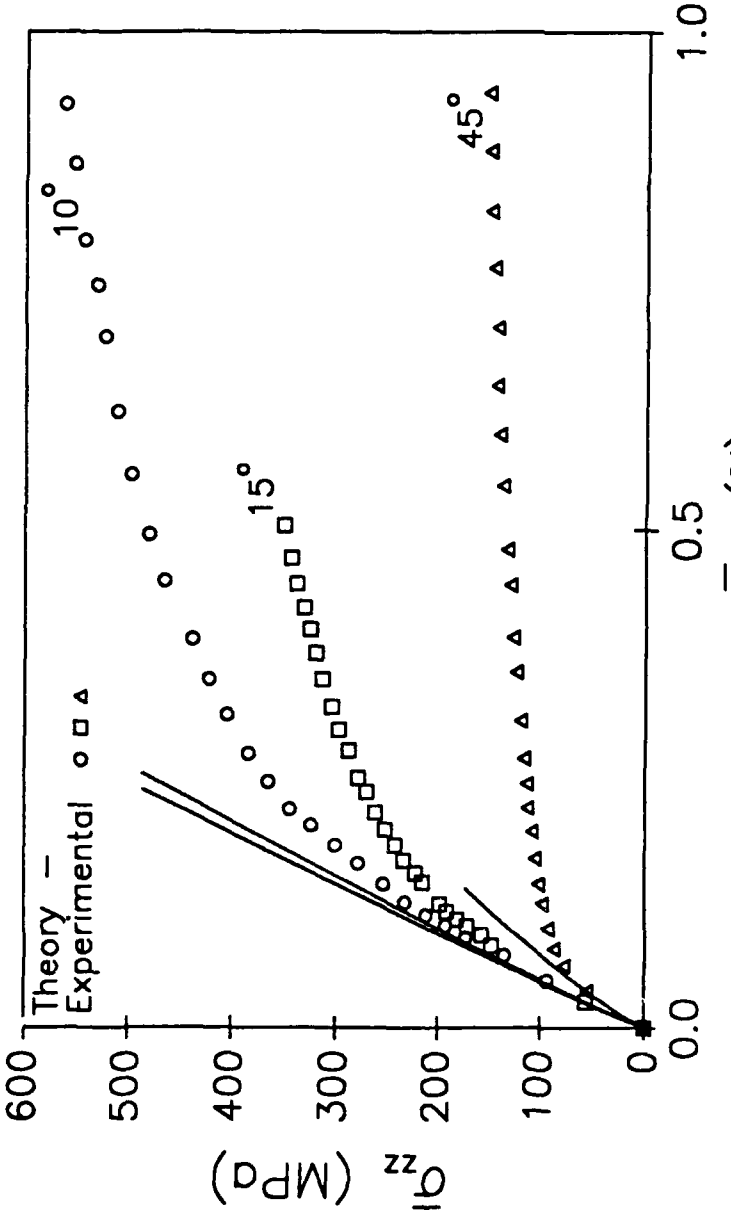

Figure 5. Results of the EIAS method with elastic constraint for B/Al - 10°, 15°, and 45° orientations.

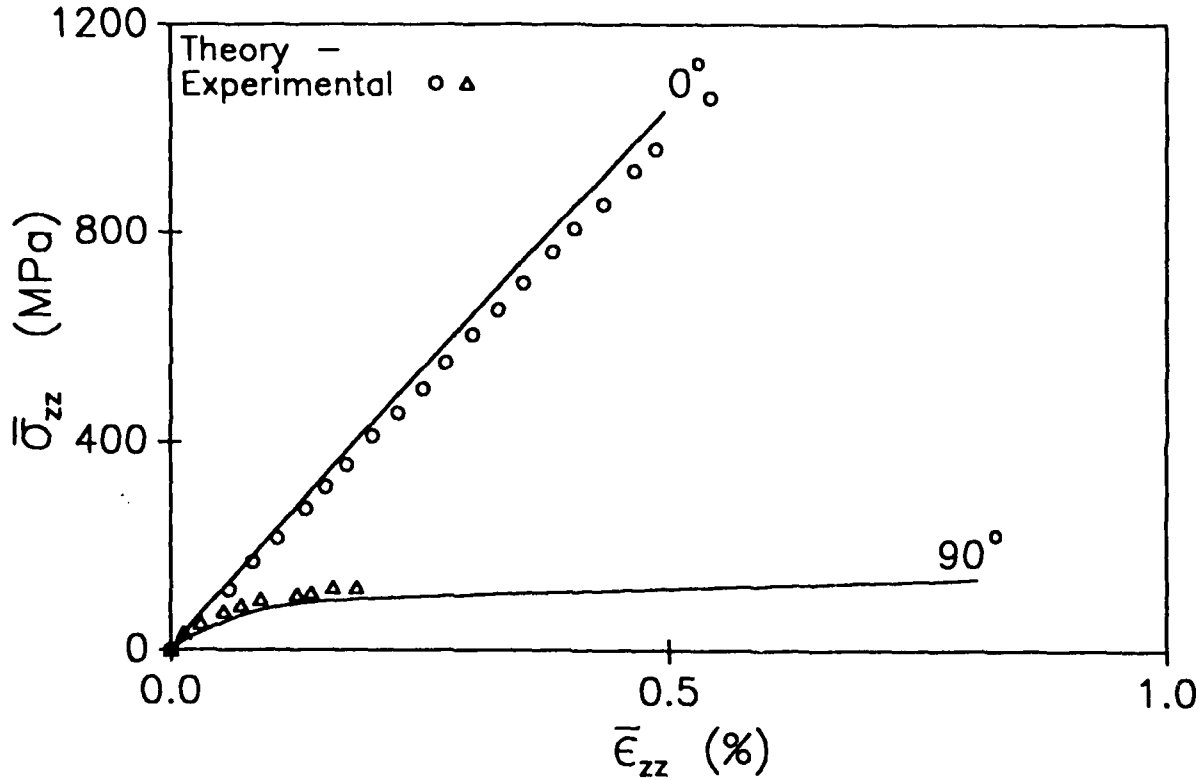

Figure 6. Results of the EIAS method-tangent stiffness formlualtion without β parameter or χ function for B/Al - 0° and 90° orientations.

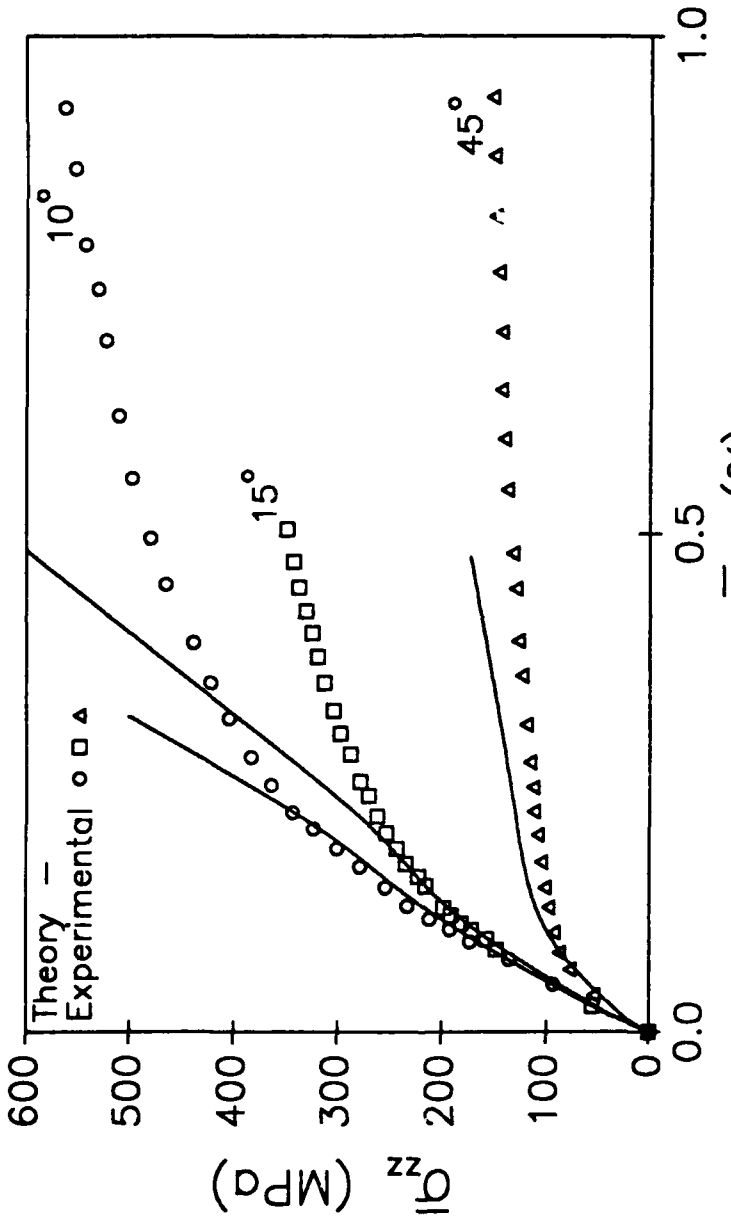

Figure 7. Results of the EIAS method-tangent stiffness formulation without β parameter or χ function for B/Al - 10°, 15°, and 45° orientations.

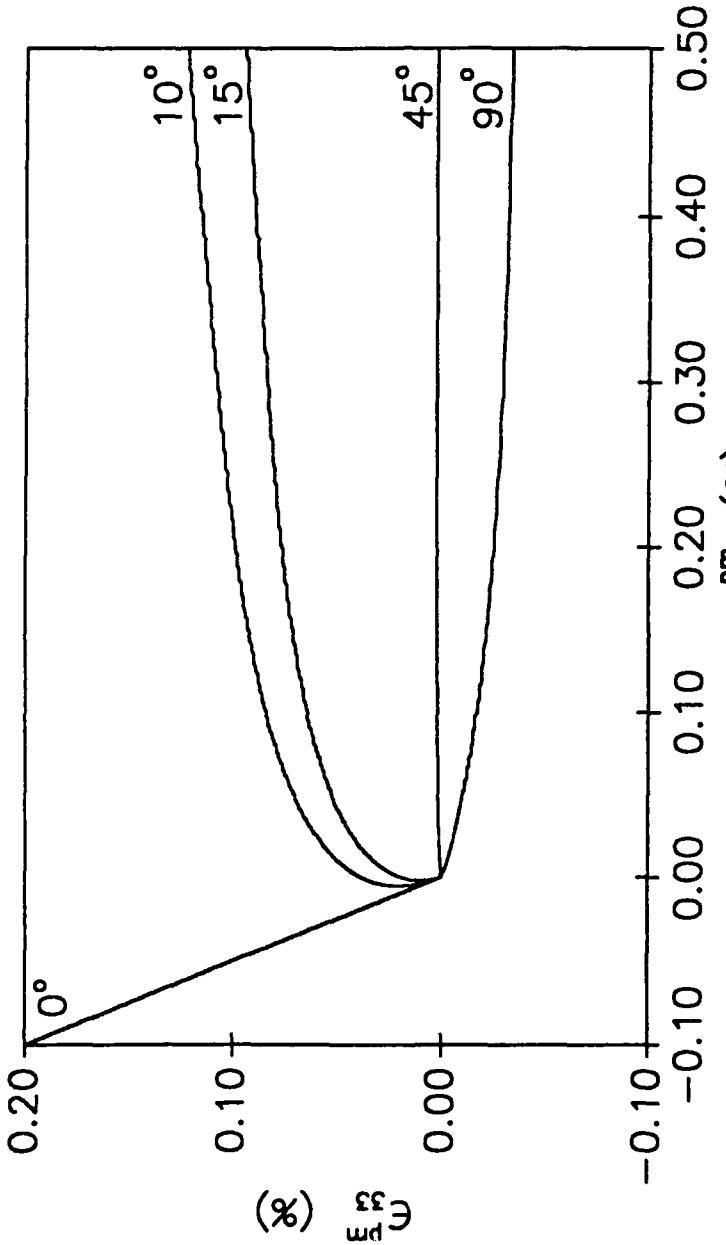

Figure 8. Analysis of matrix plastic strain rate rotation for 0°, 10°, 15°, 45°, and 90° orientations.

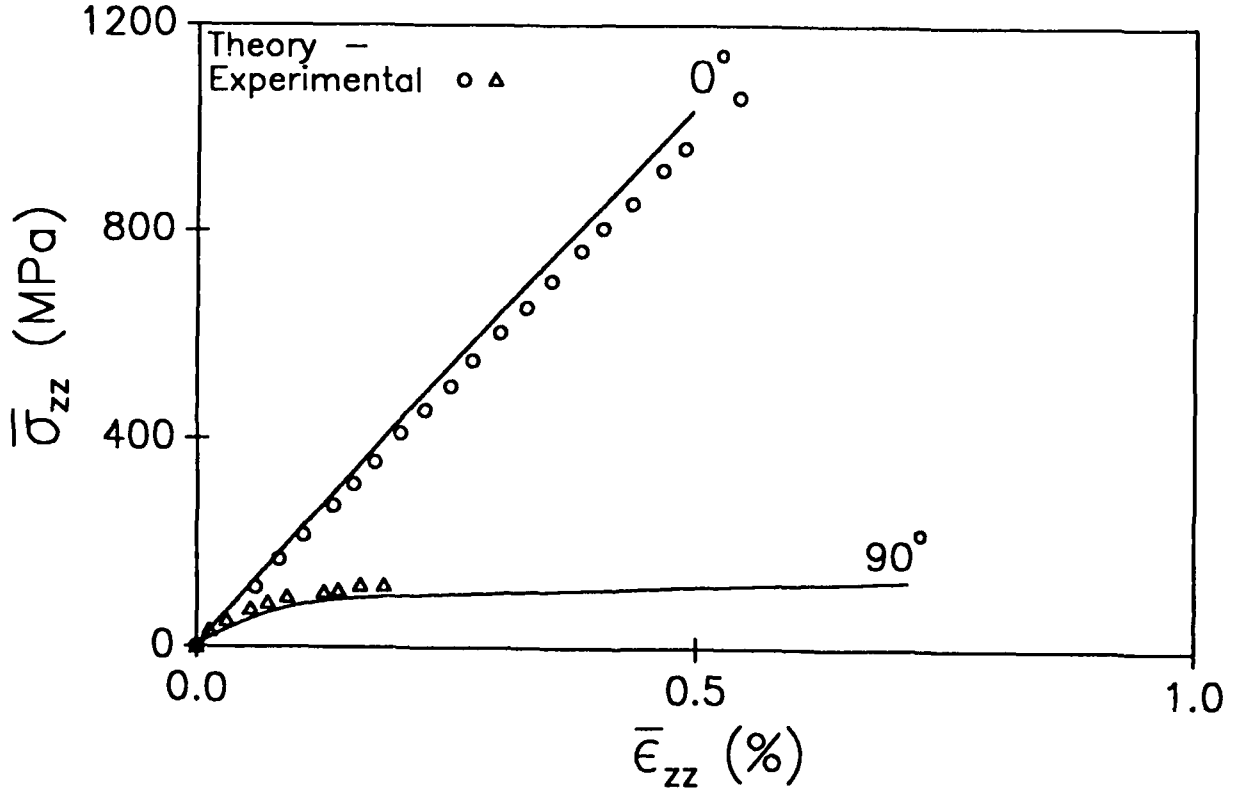

Figure 9. Results of the EIAS method-tangent stiffness formulation with $\beta=0$ and the χ function for B/Al - 0° and 90° orientations.

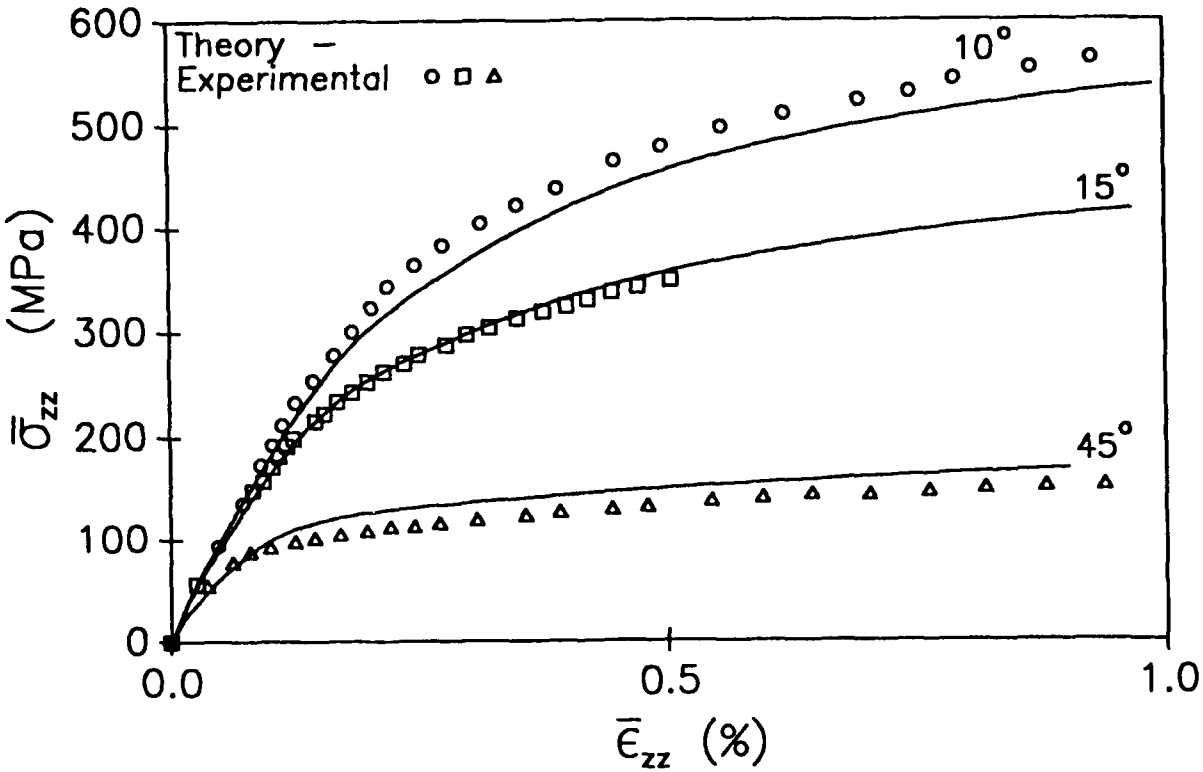

Figure 10. Results of the EIAS method-tangent stiffness formualtion with $\beta=0$ and the χ function for B/Al - 10°, 15°, and 45° orientations.

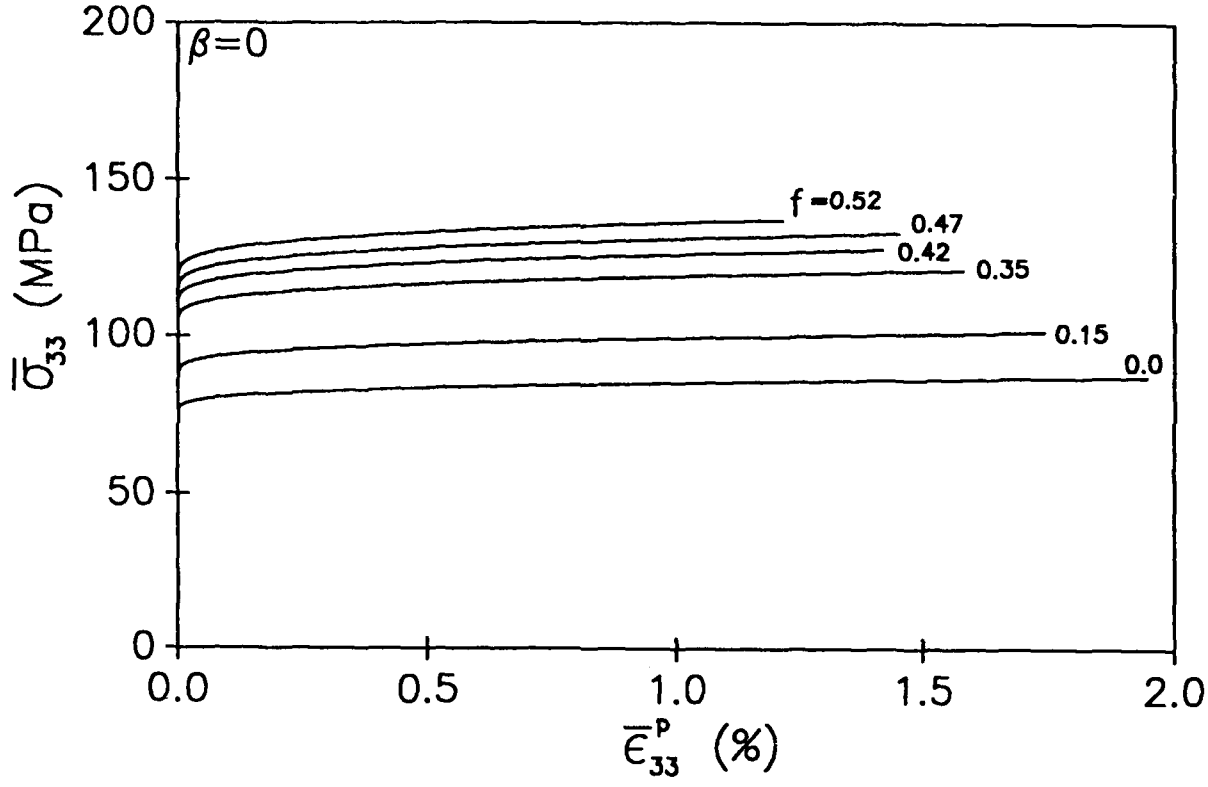

Figure 11. Results of the EIAS method-tangent stiffness formulation with $\beta=0$ for silica-epoxy spherical particle-reinforced composite.

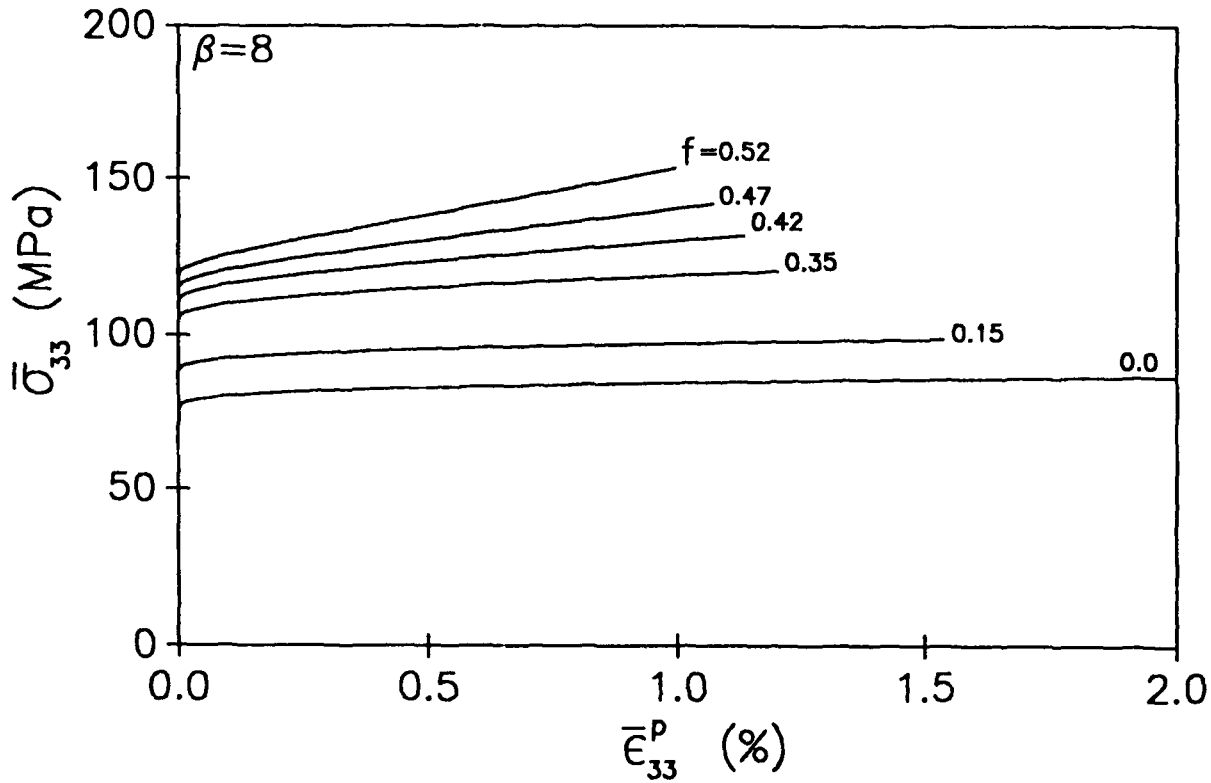

Figure 12. Results of the EIAS method-tangent stiffness formulation with β=8 for silica-epoxy spherical particle-reinforced composite.

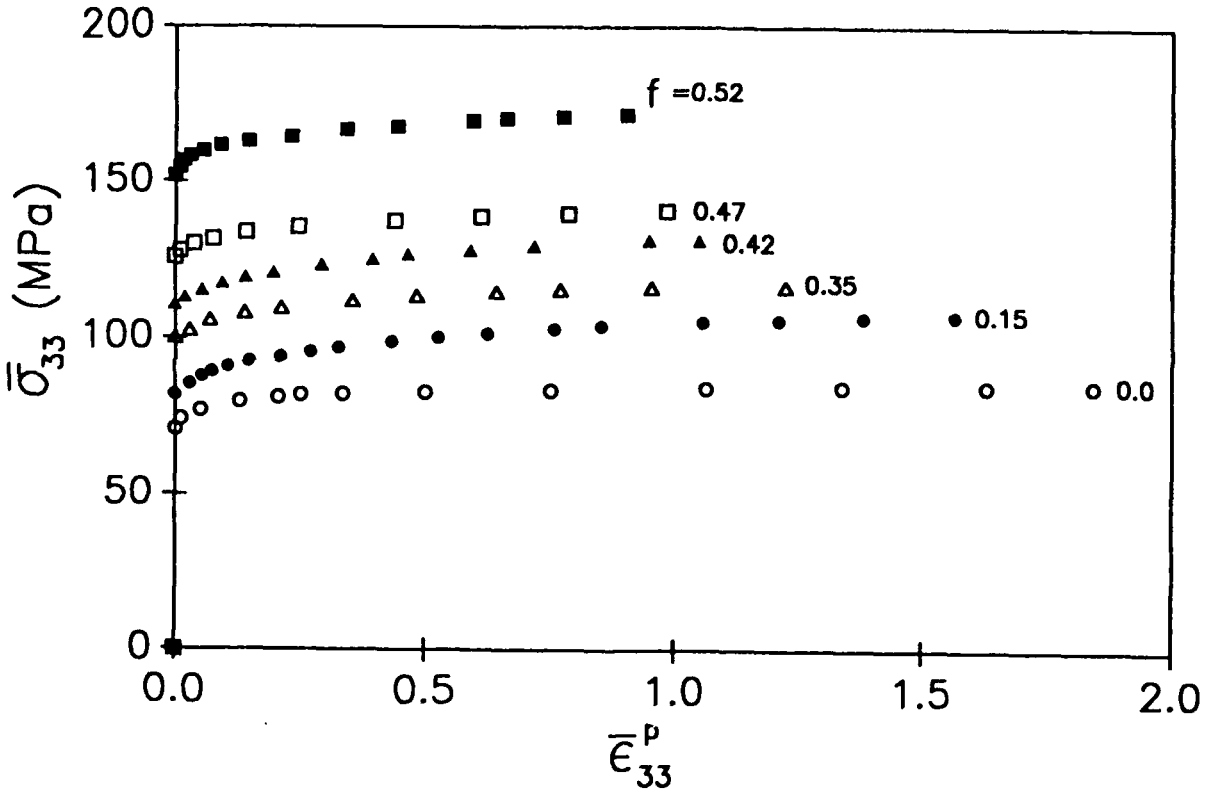

Figure 13. Weng's (1988) experimental results for silica-epoxy spherical particle-reinforced composite.

APPENDIX A

ESHELBY'S TENSOR OF ELASTICITY, S_{ijkl}

A.1 Introduction

In the context of the equivalent inclusion problem, the Eshelby tensor of elasticity, S_{ijkl}, relates the eigenstrain, ε_{kl}^{*}, to the perturbance strain, ε_{ij}^{pt}. In general, S_{ijkl} is a nonsymmetric tensor calculated based on the geometry of the composite reinforcement. Mura (1987) derives the Eshelby tensor in great detail for both isotropic and anisotropic inclusions. Since the composite systems analyzed in this thesis had isotropic inclusions, we show here the essentials to understand Mura's derivation of the Eshelby tensor for isotropic inclusions and give the equations of the Eshelby tensor for spherical and continuous fiber-reinforced composites. The problem and associated field equations are as set forth in **§ 2.1** and **§ 2.2** of the main thesis.

A.2 General Expressions of Elastic Fields for Given Eigenstrain Distributions

Eigenstrain is introduced as a description of misfit due to periodic inhomogeneity typical of reinforced composites. The corresponding eigenstresses are self-equilibrated.

Following Mura (1987), the fundamental linear elastic equations to be solved for given eigenstrain ε_{ij}^* are

$$C_{ijkl}u_{k,lj} = C_{ijkl}\varepsilon^*_{kl,j}, \tag{A-1}$$

where u_i is the displacement at an arbitrary point $\mathbf{x}(x_1,x_2,x_3)$. The body is assumed to be free of any external surface traction or body force such that $\sigma_{ij,j}=0$ everywhere within the body and $\sigma_{ij}n_j=0$ on the boundary. We will consider the body to be infinitely extended such that $\sigma_{ij} \to 0$ as $x_i \to \infty$ reproduces the traction free condition. In the case of periodic solutions, suppose $\varepsilon_{ij}^*(\mathbf{x})$ is given in the form of a single wave of amplitude $\varepsilon_{ij}^*(\xi)$, such as,

$$\varepsilon^*_{ij}(x) = \bar{\varepsilon}^*_{ij}(\xi)\exp(i\xi \bullet x), \tag{A-2}$$

where ξ is the wave vector corresponding to the given period of the distribution, and

$$i = \sqrt{-1} \text{ and } \xi \bullet x = \xi_k x_k, \tag{A-3}$$

since $\xi = \xi_i \hat{e}_i$. The solution of (A-1) corresponding to this distribution is obviously in the form of a single wave of the same period, i.e.

$$u_i(x) = \bar{u}_i(\xi)\exp(i\xi \bullet x). \tag{A-4}$$

Substituting (A-2) and (A-4) into (A-1), we have

$$C_{ijkl}\bar{u}_k\xi_l\xi_j = -iC_{ijkl}\bar{\varepsilon}^*_{kl}\xi_j, \tag{A-5}$$

which represents three equations for determining the three unknowns $\bar{u}_i$ for a given

ε_{ij}^{*}.

Using the notation

$$K_{ik}(\xi) = C_{ijkl}\xi_j\xi_l$$

$$X_i = -iC_{ijkl}\bar{\varepsilon}^{*}_{kl}\xi_j,$$

the displacement amplitude vector $\bar{u}_i$ is simply obtained as

$$\bar{u}_i(\xi) = X_j N_{ij}(\xi)/D(\xi), \tag{A-6}$$

where N_{ij} are the cofactors of the matrix $K_{ij}(\xi)$ and $D(\xi)$ is the determinant of $K_{ij}(\xi)$.

Substituting (A-6) into (A-4), we have

$$u_i(x) = -iC_{jlmn}\bar{\varepsilon}^{*}_{mn}(\xi)\xi_l N_{ij}(\xi)D^{-1}(\xi)\exp(i\xi\cdot x). \tag{A-7}$$

The corresponding equations for strain and stress are

$$\begin{aligned}
\varepsilon_{ij}(x) &= \frac{1}{2}(u_{i,j} + u_{j,i}) \\
&= \frac{1}{2}C_{klmn}\bar{\varepsilon}^{*}_{mn}(\xi)\xi_l\{\xi_j N_{ik}(\xi) \\
&\quad + \xi_i N_{ij}(\xi)\}D^{-1}(\xi)\exp(i\xi\cdot x), \qquad \text{(A-8)} \\
\sigma_{ij}(x) &= C_{ijkl}(\varepsilon_{kl} - \varepsilon^{*}_{kl}) \\
&= C_{ijkl}\{C_{pqmn}\bar{\varepsilon}^{*}_{mn}(\xi)\xi_q\xi_i N_{kp}(\xi)\exp(i\xi\cdot x) \\
&\quad - \varepsilon^{*}_{kl}(x)\}.
\end{aligned}$$

A.3 Method of Fourier Integrals

A more sophisticated distribution of eigenstrain than the single wave in equation (A-2) may be introduced. Of course, any distribution may be represented by the single wave solution in the Fourier series sense. If ε_{ij}^* is given in the Fourier integral form for an infinite domain, namely,

$$\varepsilon_{ij}^*(x) = \int_{-\infty}^{\infty} \bar{\varepsilon}_{ij}^*(\xi)\exp(i\xi \bullet x)d\xi, \tag{A-9}$$

where

$$\bar{\varepsilon}_{ij}^*(\xi) = (2\pi)^{-3} \int_{-\infty}^{\infty} \varepsilon_{ij}^*(x)\exp(-i\xi \bullet x)dx, \tag{A-10}$$

then the displacement, stress, and strain can be expressed as

$$\begin{aligned} u_i(x) &= -(2\pi)^{-3}\frac{\partial}{\partial x_l}\int_{-\infty}^{\infty}\int_{-\infty}^{\infty} C_{jlmn}\varepsilon_{mn}^*(x')\xi_l N_{ij}(\xi)D^{-1}(\xi) \\ &\quad \times\exp\{i\xi\bullet(x - x')\}d\xi dx', \\ \varepsilon_{ij}(x) &= (2\pi)^{-3}\int_{-\infty}^{\infty}\int_{-\infty}^{\infty}\frac{1}{2}C_{klmn}\varepsilon_{mn}^*(x') \\ &\quad \times \xi_l\{\xi_f N_{ik}(\xi) + \xi_i N_{jk}(\xi)\}D^{-1}(\xi) \\ &\quad \times \exp\{i\xi\bullet(x - x')\}d\xi dx', \end{aligned} \tag{A-11a}$$

and

$$\sigma_{ij}(x) = C_{ijkl}\Big[(2\pi)^{-3}\int_{-\infty}^{\infty}\int_{-\infty}^{\infty} C_{pqmn}\varepsilon^{*}_{mn}(x')\xi_q\xi_l N_{kp}(\xi)D^{-1}(\xi) \times \exp\{i\xi\bullet(x - x')\}d\xi dx' - \varepsilon^{*}_{kl}(x)\Big], \quad \text{(A-11b)}$$

for general eigenstrain distribution $\varepsilon_{ij}^{*}(x)$.

A.4 The Method of Green's Functions

When Green's functions $G_{ij}(x\text{-}x')$ are defined as

$$G_{ij}(x-x') = (2\pi)^{-3}\int_{-\infty}^{\infty} N_{ij}(\xi)D^{-1}(\xi)\exp\{i\xi\bullet(x-x')\}d\xi, \quad \text{(A-12)}$$

the displacement $u_i(x)$ in (A-11) can be rewritten as

$$u_i(x) = -\int_{-\infty}^{\infty} C_{jlmn}\varepsilon^{*}_{mn}(x')G_{ij,l}(x - x')dx', \quad \text{(A-13)}$$

where $G_{ij,l}(x\text{-}x') = \partial/\partial x_l\{G_{ij}(x\text{-}x') = -\partial/\partial x_l'\{G_{ij}(x\text{-}x')$.

The corresponding expressions for the strain and stress become

$$\varepsilon_{ij}(x) = -\frac{1}{2}\int_{-\infty}^{\infty} C_{klmn}\varepsilon^{*}_{mn}(x')\{G_{ik,lj}(x-x')+G_{jk,li}(x-x')\}dx', \quad \text{(A-14)}$$

and

$$\sigma_{ij}(x) = -C_{ijkl}\left\{\int_{-\infty}^{\infty} C_{pqmn}\varepsilon^{*}_{mn}(x')G_{kp,ql}(x-x')dx' + \varepsilon^{*}_{kl}(x)\right\}. \tag{A-15}$$

In 1963, Mura (1987) rewrote $\sigma_{ij}(\mathbf{x})$ in **(A-15)** in the form

$$\sigma_{ij}(x) = C_{ijkl}\int_{-\infty}^{\infty} e_{sth}e_{lnh}C_{pqmn}G_{kp,qt}(x-x')\varepsilon^{*}_{sm}(x')dx', \tag{A-16}$$

where e_{ijk} are permutation symbols. Since $e_{sth}e_{lnh} = \delta_{sl}\delta_{tn}-\delta_{sn}\delta_{tl}$, **(A-16)** becomes

$$\sigma_{ij}(x) = C_{ijkl}\int_{-\infty}^{\infty} C_{pqmn}(G_{kp,qn}\varepsilon^{*}_{ml} - G_{kp,ql}\varepsilon^{*}_{mn})dx'. \tag{A-17}$$

Following Mura (1987), it is shown that

$$C_{mnpq}G_{pk,qn}(x-x') = -\delta_{mk}\delta(x-x'), \tag{A-18}$$

where $\delta(\mathbf{x}-\mathbf{x}')$ is Dirac's delta function having the property

$$\int_{-\infty}^{\infty} \varepsilon^{*}_{ml}(x')\delta(x-x')dx' = \varepsilon^{*}_{ml}(x).$$

It is seen from **(A-18)** that the Green's function $G_{pk}(\mathbf{x}-\mathbf{x}')$ is the displacement component in the x_p-direction at point $\mathbf{x}$ when a unit body force in the x_k-direction is applied at point $\mathbf{x}'$ in the infinitely extended material. By this definition of the Green's function, we can derive **(A-13)** directly from **(A-1)**. As mentioned previously, the displacement u_i in **(A-1)** can be considered as a displacement caused by the body

force $-C_{ilmn}\varepsilon^{*}_{mn,l}$ applied in the x_i-direction. Since $G_{ij}(x-x')$ is the solution for a unit body force applied in the x_j-direction, the solution for the present problem is the product of G_{ij} and the body force $-C_{jlmn}\varepsilon^{*}_{mn,l}$, namely,

$$u_i(x) = -\int_{-\infty}^{\infty} G_{ij}(x-x')C_{jlmn}\varepsilon^{*}_{mn,l}(x')dx'. \qquad \textbf{(A-19)}$$

Integrating by parts and assuming that the boundary terms vanish, we have,

$$u_i(x) = \int_{-\infty}^{\infty} C_{jlmn}\varepsilon^{*}_{mn}(x')\frac{\partial}{\partial x'_l}G_{ij}(x - x')dx'. \qquad \textbf{(A-20)}$$

Expression **(A-19)** is preferable to **(A-20)**. When ε_{mn}^{*} is constant in Ω and zero in D-Ω (as per the Eshelby solution), it can be seen that the integrand in **(A-20)** vanishes except on the boundary of Ω since $\varepsilon_{mn}^{*}=0$ in D-Ω and $\varepsilon_{mn,l}^{*}=0$ in Ω.

A.5 Explicit Forms of the Green's Function for Isotropic Inclusions

An inclusion, containing eigenstrain ε_{ij}^{*}, is isotropic if it has the same elastic moduli as its surrounding domain. For isotropic materials, the integrands in equations **(A-11)** are

$$\begin{aligned} D(\xi) &= \mu^2(\lambda + 2\mu)\xi^6, \\ N_{ij}(\xi) &= \mu\xi^2\{(\lambda + 2\mu)\delta_{ij}\xi^2 - (\lambda + \mu)\xi_i\xi_j\}, \end{aligned} \qquad \textbf{(A-21)}$$

where $\xi^2=\xi_k\xi_k$ and λ and μ are Lame's elastic constants (μ is the shear modulus).

If we substitute the expressions in **(A-21)** into the integral expression for the Green's Function **(A-12)** and integrate, we obtain

$$G_{ij}(x) = \frac{1}{8\pi\mu|x|}\left\{2\delta_{ij} - \frac{\lambda + \mu}{\lambda + 2\mu}(\delta_{ij} - x_i x_j/|x|^2)\right\}$$
$$= \frac{1}{16\pi\mu(1-\nu)|x|}\left\{(3 - 4\nu)\delta_{ij} + x_i x_j/|x|^2\right\}, \qquad \textbf{(A-22)}$$

where $|x| = (x_i x_i)^{1/2}$, or

$$G_{ij}(x-x') = \frac{1}{4\pi\mu}\frac{\delta_{ij}}{|x-x'|} - \frac{1}{16\pi\mu(1-\nu)}\frac{\partial^2|x-x'|}{\partial x_i \partial x_j}, \qquad \textbf{(A-23)}$$

where ν is Poisson's ratio and $|x\text{-}x'| = (x_i\text{-}x_i')(x_i\text{-}x_i')$. Equation **(A-22)** or **(A-23)** is the form of the Green's function we need to obtain explicit expressions for the Eshelby tensor based on the geometry of the reinforcement.

From **(A-20)**, we have the following expression for the displacement in terms of the Green's function:

$$u_i(x) = -C_{jkmn}\varepsilon^*_{mn}\int_\Omega G_{ij,k}(x-x')dx', \qquad \textbf{(A-24)}$$

where Ω is an ellipsoidal inclusion given by the equation

$$\frac{x_1^2}{a_1^2} + \frac{x_2^2}{a_2^2} + \frac{x_3^3}{a_3^2} \le 1,$$

where a_1, a_2, and a_3 are the axes of the ellipsoid.

$G_{ij}(x\text{-}x')$ is from **(A-22)**.

After some manipulation, equation (A-24) can be rewritten as

$$u_i(x) = \frac{-\varepsilon^*_{jk}}{8\pi(1-\nu)}\int_\Omega g_{ijk}(\tilde{n})\frac{dx'}{|x'-x|^2}, \tag{A-25}$$

where

$$g_{ijk}(\tilde{n}) = (1-2\nu)(\delta_{ij}n_k + \delta_{ik}n_j - \delta_{jk}n_i) + 3n_in_jn_k. \tag{A-26}$$

The vector $\tilde{n}$ is the unit vector $(x'-x)/|x'-x|$.

When point x is located inside the inclusion, the integral in (A-25) can be explicitly performed. The volume element dx' in (A-25) can be written as $dx'=drdS=drr^2d\omega$, where $r = |x'-x|$ and $d\omega$ is a surface element of a unit sphere Σ centered at point x. Upon integration with respect to r, we have

$$u_i(x) = \frac{-\varepsilon^*_{jk}}{8\pi(1-\nu)}\int_\Sigma r(\tilde{n})g_{ijk}(\tilde{n})d\omega, \tag{A-27}$$

Following Mura (1987), the integral (A-27) may be transformed to

$$u_i(x) = \frac{x_m\varepsilon^*_{jk}}{8\pi(1-\nu)}\int_\Sigma \frac{\lambda_m g_{ijk}}{g}d\omega, \tag{A-28}$$

where

$$\lambda_1 = \frac{n_1}{a_1^2},\ \lambda_2 = \frac{n_2}{a_2^2},\ \lambda_3 = \frac{n_3}{a_3^2},$$

and

$$g = \sum_{i=1}^{3} \frac{n_i^2}{a_i^2}.$$

From $\varepsilon_{ij}(\mathbf{x})=\frac{1}{2}(u_{i,j}(\mathbf{x})+u_{j,i}(\mathbf{x}))$, the strain components become

$$\varepsilon_{ij}(\mathbf{x}) = \frac{\varepsilon^*_{mn}}{16\pi(1-\nu)}\int_{\Sigma}\frac{\lambda_i g_{jmn} + \lambda_j g_{imn}}{g}d\omega \ . \qquad \text{(A-29)}$$

The integral in (A-29) is independent of x. Therefore, we have verified Eshelby's key result in that the strain (and therefore the stress) is uniform inside the inclusion.

It is convenient to write (A-29) as

$$\varepsilon_{ij} = S_{ijkl}\varepsilon^*_{kl} \ , \qquad \text{(A-30)}$$

where S_{ijkl} is called the Eshelby tensor; S_{ijkl} takes on the general form

$$S_{ijkl} = \frac{1}{16\pi(1-\nu)}\int_{\Sigma}\frac{\lambda_i g_{jkl} + \lambda_j g_{ikl}}{g}d\omega, \qquad \text{(A-31)}$$

for an isotropic material with an inclusion. Note that the Lame's constants correspond to the matrix since the isotropic inclusion is assumed to have the same elastic properties as the matrix but with an eigenstrain introduced in Ω. The Eshelby tensor is not symmetric in general.

A.6 Eshelby's Tensor for Spherical Inclusions

In our analysis of spherical particle-reinforced composites, we utilize the form of the Eshelby tensor for spherical inclusions. When the inclusions are spherical in

shape, $a_1=a_2=a_3$, and **(A-31)** simplifies dramatically. The equations for the non-zero components of the Eshelby tensor are:

$$S_{1111} = S_{2222} = S_{3333} = \frac{7 - 5\nu}{15(1 - \nu)},$$

$$S_{1122} = S_{2233} = S_{3311} = S_{1133} = S_{2211} = S_{3322} = \frac{5\nu - 1}{15(1 - \nu)}, \qquad \textbf{(A-32)}$$

$$S_{1212} = S_{2323} = S_{3131} = \frac{4 - 5\nu}{15(1 - \nu)}.$$

A.7 Eshelby's Tensor for Continuous Fibers

If the inclusions are elliptical cylinders (i.e., $a_3 \rightarrow \infty$) as is the case with continuous fibers, then the non-zero components of the Eshelby tensor are:

$$S_{1111} = \frac{1}{2(1-\nu)}\left\{\frac{a_2^2 + 2a_1a_2}{(a_1+a_2)^2} + (1-2\nu)\frac{a_2}{a_1+a_2}\right\},$$

$$S_{2222} = \frac{1}{2(1-\nu)}\left\{\frac{a_1^2 + 2a_1a_2}{(a_1+a_2)^2} + (1-2\nu)\frac{a_1}{a_1+a_2}\right\},$$

$$S_{1122} = \frac{1}{2(1-\nu)}\left\{\frac{a_2^2}{(a_1+a_2)^2} - (1-2\nu)\frac{a_2}{a_1+a_2}\right\},$$

$$S_{2233} = \frac{1}{2(1-\nu)}\frac{2\nu a_1}{a_1+a_2},$$

$$S_{1133} = \frac{1}{2(1-\nu)}\frac{2\nu a_2}{a_1+a_2},$$

(A-33)

$$S_{2211} = \frac{1}{2(1-\nu)}\left\{\frac{a_1^2}{(a_1+a_2)^2} - (1-2\nu)\frac{a_1}{a_1+a_2}\right\},$$

$$S_{1212} = \frac{1}{2(1-\nu)}\left\{\frac{a_1^2 + a_2^2}{2(a_1+a_2)^2} + \frac{1-2\nu}{2}\right\},$$

$$S_{2323} = \frac{a_1}{2(a_1+a_2)}, \qquad S_{3131} = \frac{a_2}{2(a_1+a_2)}.$$

It should be emphasized that ν in (A-32) and (A-33) pertains to the Poisson's ratio of the matrix material.

APPENDIX B

INCREMENTAL THEORIES OF PLASTICITY

B.1 Introduction

The purpose of this appendix is to summarize the incremental plasticity theories used to calculate the increment of matrix plastic strain, $\Delta\varepsilon_{ij}^{pm}$. Two theories were utilized: a nonlinear kinematic hardening theory with backstress decomposition and an incremental isotropic hardening theory.

B.2 Nonlinear Kinematic Hardening Theory

The nonlinear kinematic hardening theory selected in this work for representation of matrix behavior is along the lines of that employed by Chaboche and co-workers (1978, 1983a, 1983b) and further developed by McDowell (1985) and McDowell and Moosbrugger (1989) for nonproportional cyclic plasticity. The kinematical hardening variable or backstress, α_{ij}, is decomposed into an arbitrary number of components representative of dislocation interaction at corresponding size scales. This permits accurate description of complex plasticity phenomena. Defining the yield surface in the von Mises form

$$F = \frac{3}{2}\left(\sigma_{ij}^{m'} - \alpha_{ij}\right)\left(\sigma_{ij}^{m'} - \alpha_{ij}\right) - R^2 \qquad \text{(B-1)}$$

where $\sigma_{ij}^{m'} = \sigma_{ij}^{m} - (1/3)\sigma_{kk}^{m}\delta_{ij}$ and α_{ij} is assumed to be deviatoric, we can write the flow rule as

$$\dot{\varepsilon}_{ij}^{pm} = \frac{1}{h}\left(\dot{\sigma}_{kl}^{m} n_{kl}\right) n_{ij} \text{ if } F=0 \text{ and } \dot{\sigma}_{kl}^{m} n_{kl} \geq 0$$
$$\dot{\varepsilon}_{ij}^{pm} = 0 \text{ otherwise.} \qquad \text{(B-2)}$$

By the consistency condition, if $\dot{F}=0$ during plastic flow, we may write

$$\dot{F} = 0 = \frac{\partial F}{\partial \sigma_{ij}^{m}}\dot{\sigma}_{ij}^{m} + \frac{\partial F}{\partial \alpha_{ij}}\dot{\alpha}_{ij} - 2R\dot{R} \qquad \text{(B-3)}$$

The nonlinear kinematic hardening rule is of the form

$$\dot{\alpha}_{ij}^{(n)} = C^{(n)}\left[b^{(n)} n_{ij} - \alpha_{ij}^{(n)}\right]\dot{p} \qquad \text{(B-4)}$$

where n = 1,2,...,M is the total number of decomposed backstresses, i.e.

$$\dot{\alpha}_{ij} = \sum_{n=1}^{M} \dot{\alpha}_{ij}^{(n)} \qquad \text{(B-5)}$$

and

$$\dot{p} = \left(\dot{\varepsilon}_{ij}^{pm}\dot{\varepsilon}_{ij}^{pm}\right)^{\frac{1}{2}}.$$

In equation **(B-2)** and **(B-4)**,

$$n_{ij} = \frac{\dfrac{\partial F}{\partial \sigma^m_{ij}}}{\left|\dfrac{\partial F}{\partial \sigma^m_{kl}}\right|} = \frac{\sigma'_{ij} - \alpha_{ij}}{\left|\sigma'_{kl} - \alpha'_{kl}\right|} = \sqrt{\frac{3}{2}}\frac{\left(\sigma'_{ij} - \alpha_{ij}\right)}{R} \qquad \text{(B-6)}$$

and $C^{(n)}$ and $b^{(n)}$ are material constants. In this study, we assume pure kinematic hardening ($\dot{R}=0$). Using **(B-1)**, **(B-4)**, and **(B-5)**, **(B-3)** leads to

$$h = \sum_{n=1}^{M} C^{(n)}\left[b^{(n)} - \alpha^{(n)}_{ij} n_{ij}\right] \qquad \text{(B-7)}$$

For the aluminum in this study, M=2, $C^{(1)}$ = 12, $C^{(2)}$ = 1400, $b^{(1)}$ = 15, $b^{(2)}$ = 5.6, and R = 2.0 ksi.

B.3 Incremental Isotropic Hardening Theory

Weng (1988) tested his secant modulus theory on a composite with an epoxy resin matrix reinforced with silica particles. He gives the following information to represent the behavior of the epoxy matrix:

$$\bar{\sigma}^m = \sigma^m_y + H(\bar{\varepsilon}^{pm})^n \qquad \text{(B-8)}$$

where σ_y^m = 11 ksi ≡ uniaxial yield strength; H = 4.67 ksi; n = 0.26;

the effective matrix stress is

$$\bar{\sigma}^m = \sqrt{\frac{3}{2}\sigma^{m\prime}_{ij}\sigma^{m\prime}_{ij}}; \qquad \text{(B-9)}$$

effective matrix plastic strain is

$$\bar{\varepsilon}^{pm} = \sqrt{\frac{2}{3}\varepsilon_{ij}^{pm}\varepsilon_{ij}^{pm}} \; ; \tag{B-10}$$

and the deviatoric matrix stress is

$$\sigma_{ij}^{m'} = \sigma_{ij}^{m} - \frac{1}{3}\sigma_{kk}^{m}\delta_{ij} \; . \tag{B-11}$$

We use isotropic hardening plasticity with the yield surface (i.e. no backstress)

$$F = \frac{3}{2}\sigma_{ij}^{m'}\sigma_{ij}^{m'} - Y^2. \tag{B-12}$$

The flow rule for determining plastic matrix strain is

$$\begin{aligned} \dot{\varepsilon}_{ij}^{pm} &= \frac{1}{h}(\dot{\sigma}_{kl}^{m}n_{kl})n_{ij} \quad \textit{if } F=0 \textit{ and } \dot{\sigma}_{kl}^{m}n_{kl} \geq 0 \\ \dot{\varepsilon}_{ij}^{pm} &= 0 \textit{ otherwise,} \end{aligned} \tag{B-13}$$

where

$$n_{ij} = \frac{\dfrac{\partial f}{\partial \sigma_{ij}^{m}}}{\left|\dfrac{\partial f}{\partial \sigma_{ij}^{m}}\right|} = \frac{\sigma_{ij}^{m'}}{|\sigma_{ij}^{m'}|} = \sqrt{\frac{3}{2}}\frac{\sigma_{ij}^{m'}}{\bar{\sigma}^{m}}. \tag{B-14}$$

The yield surface radius, Y, is

$$Y = \sigma_y^m + H\left(\sqrt{\frac{2}{3}}p\right)^n , \tag{B-15}$$

where

$$\sqrt{\frac{2}{3}}p = \int_0^t \sqrt{\frac{2}{3}}\left(\dot{\varepsilon}_{ij}^{pm}\dot{\varepsilon}_{ij}^{pm}\right)^{\frac{1}{2}}dt = \int_0^t \dot{\bar{\varepsilon}}^{pm}dt = \bar{\varepsilon}^{pm}. \tag{B-16}$$

This theory is valid only for proportional loading. By the consistency condition, $\dot{F}=0$ during plastic flow; therefore, h, the plastic hardening modulus, is given by

$$h = \frac{2}{3}Hn(\bar{\varepsilon}^{pm})^{n-1} = \frac{2}{3}Hn\left(\frac{\bar{\sigma}^m-\sigma_y^m}{H}\right)^{\frac{n-1}{n}} = \frac{2}{3}\frac{d\bar{\sigma}^m}{d\bar{\varepsilon}^{pm}} . \tag{B-17}$$

APPENDIX C

FLOWCHARTS FOR COMPUTER PROGRAMS

The purpose of this appendix is to outline the logic in the various FORTRAN programs employed to calculate the theoretical results presented in this thesis. This appendix includes flowcharts for the three analytical methods presented in Chapters II and III. These were the EIAS Method with Elastic Constraint (Program BALNIT); the EIAS Method-Tangent Stiffness Formulation (Program TAN1); and the EIAS Method-Tangent Stiffness Formulation with β parameter and χ function (Program CSTAR).

The main program reads in the stress rate and time step from an input file called BALIN. The applied stress increment is calculated by two subroutines called SETUP and INTEG (for INTEGration). The SCM (for Self-Consistent Method) subroutine is then called to calculate the output variables. These output variables were:

$\bar{\sigma}_{ij}$ the composite stress;

$\bar{\varepsilon}_{ij}$ the composite strain;

ε^{pm}_{ij} plastic matrix strain;

σ^{m}_{ij} matrix stress;

and $\Delta\varepsilon_{ij}^{pm}$ increment of plastic matrix strain.

After returning to the main program, the stress and strain state for that particular time step is written to an output file called BALOUT. The program continues this cycle until the loading history is exhausted.

The SCM subroutine varies for each of the three programs. In the BALNIT program, the SCM subroutine is based on the EIAS Method with Elastic Constraint detailed in Chapter II of the main thesis. The flowchart for this SCM subroutine is shown in Figure C-1. The SCM subroutine for the TAN1 program is based on the EIAS Method Tangent Stiffness formulation presented in § 3.1, and its flowchart is shown in Figure C-2. Finally, the SCM subroutine for the CSTAR program, which incorporates the ß parameter and χ function into the EIAS Method Tangent Stiffness Formulation, is shown in the flowchart in Figure C-3.

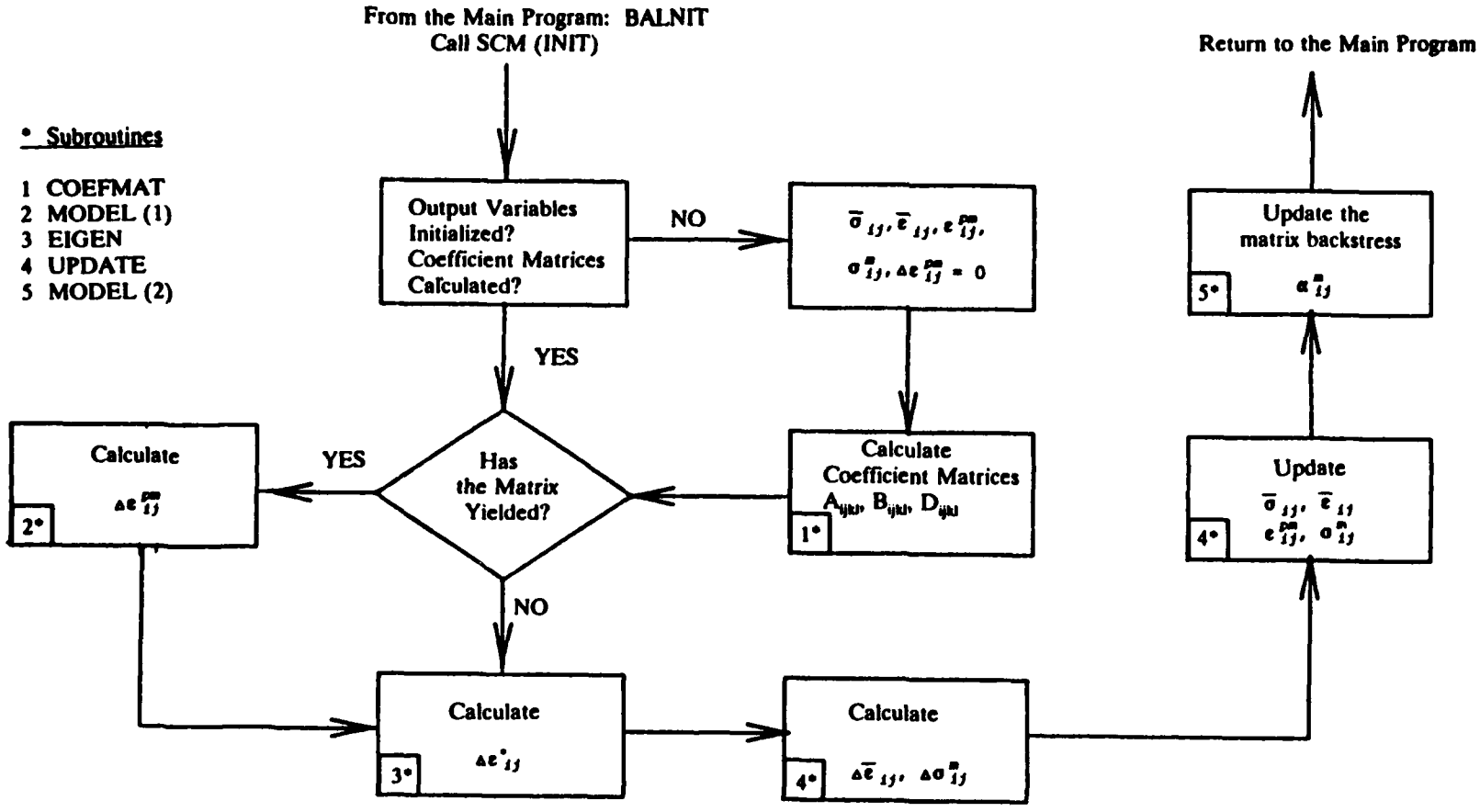

Figure C-1. Flowchart for SCM subroutine in Program BALNIT.

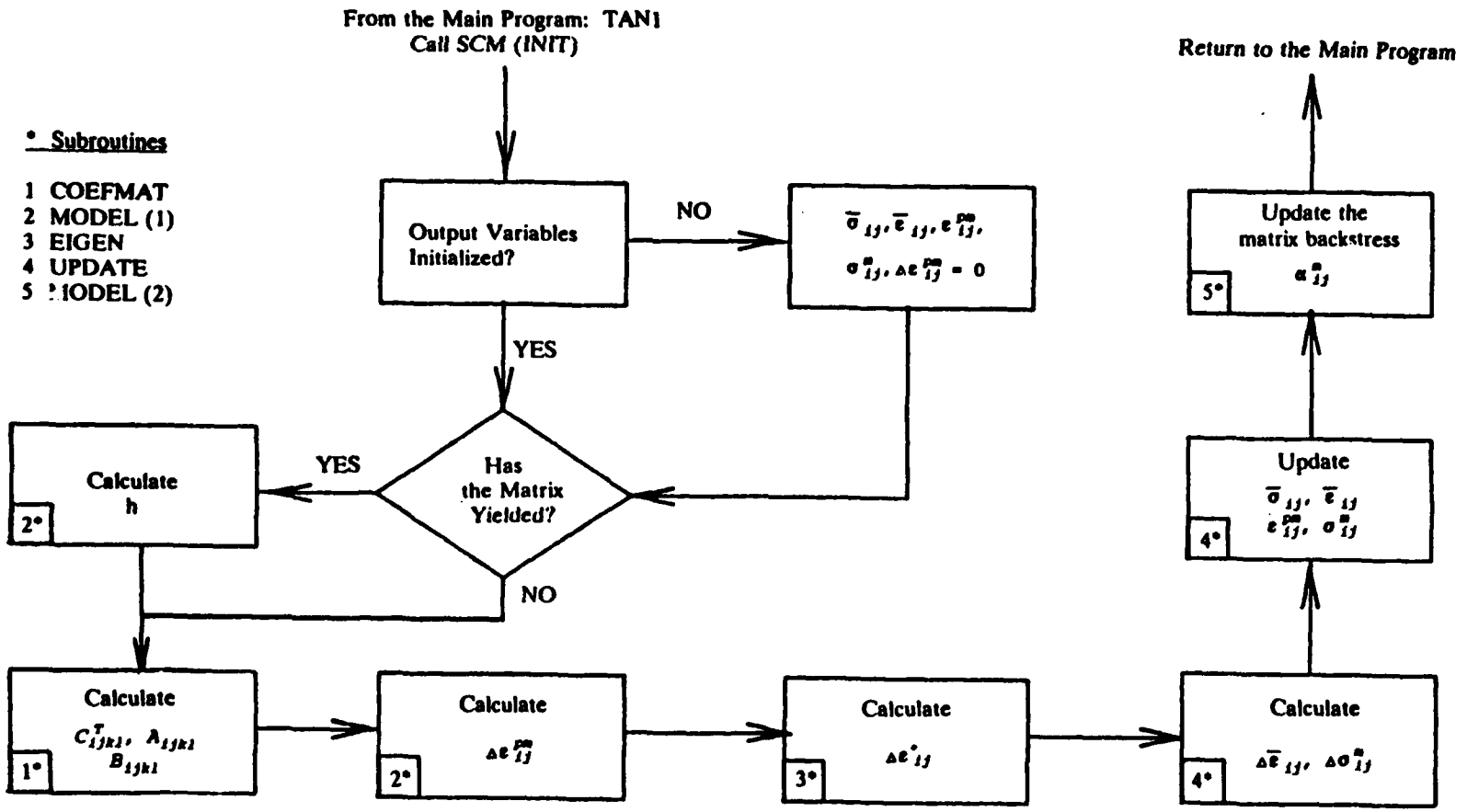

Figure C-2. Flowchart for SCM subroutine in Program TAN1.

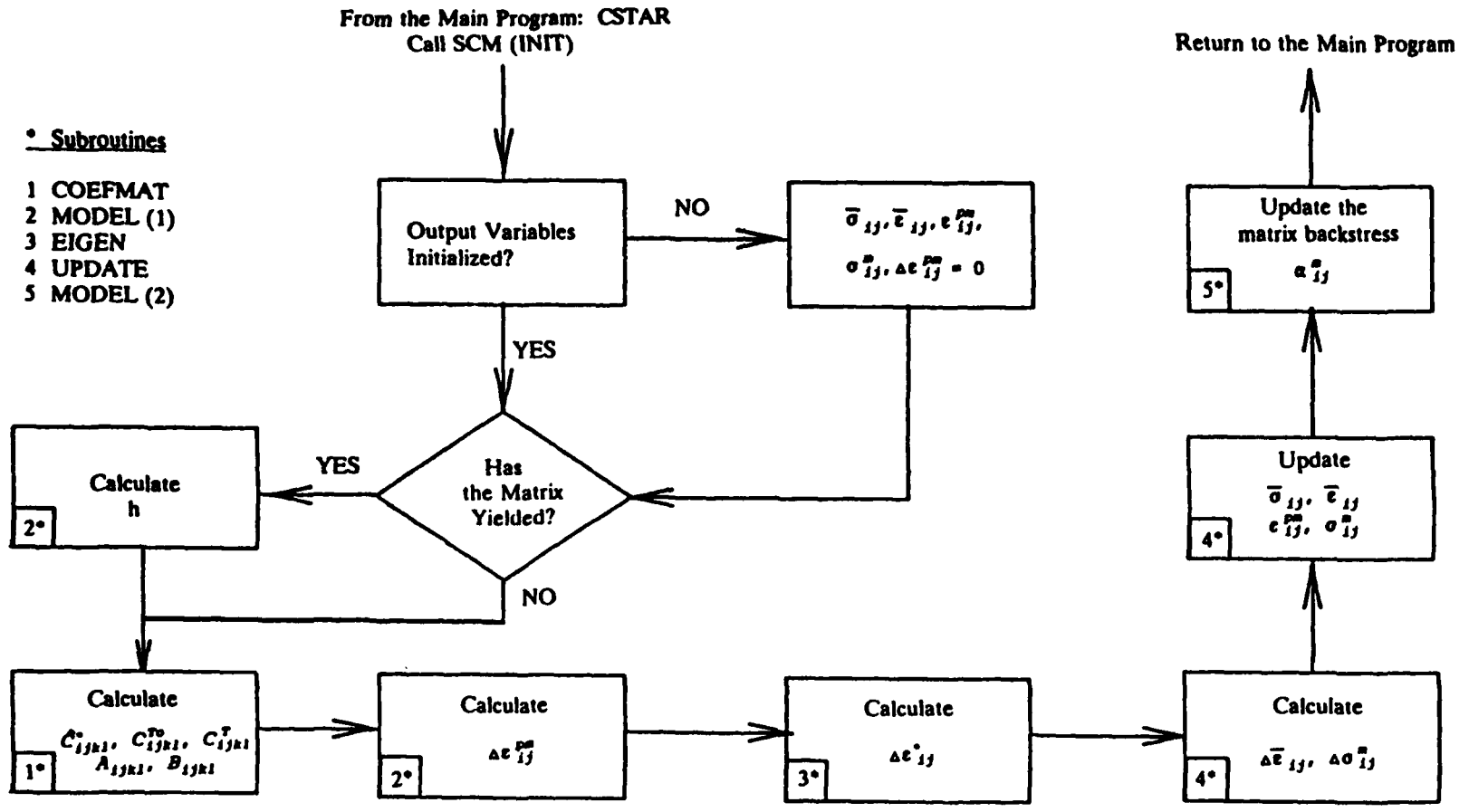

Figure C-3. Flowchart for SCM subroutine in Program CSTAR.

APPENDIX D

COMPARISON OF THE TANGENT STIFFNESS APPROACH WITH THE SECANT STIFFNESS APPROACH

According to the Eshelby approach, secant stiffness method (Weng, 1988),

$$C^{*}_{ijkl}\left(\Sigma\varepsilon^{n}_{kl}\right) = C^{s}_{ijkl}\left(\Sigma\varepsilon^{n}_{kl} - \varepsilon^{*}_{kl}\right); \quad n = 1,2,3 , \tag{D-1}$$

where $\varepsilon_{kl}{}^{1} = \varepsilon_{kl}{}^{o}$, the comparison material strain; $\varepsilon_{kl}{}^{2} = \varepsilon_{kl}{}^{I}$, the image strain, $\varepsilon_{kl}{}^{3} = \varepsilon_{kl}{}^{pt}$, the perturbation strain; and $\varepsilon_{kl}{}^{*}$ is the eigenstrain. Here, $C_{ijkl}{}^{s}$ is the matrix secant modulus.

Now, at the next stage of deformation, we again apply the secant stiffness method, i.e.,

$$\begin{aligned} &C^{*}_{ijkl}\left[\Sigma\varepsilon^{n}_{kl} + \delta\left(\Sigma\varepsilon^{n}_{kl}\right)\right] \\ &\qquad = \left(C^{s}_{ijkl} + \delta C^{s}_{ijkl}\right)\left(\Sigma\varepsilon^{n}_{kl} - \varepsilon^{*}_{kl} + \delta\Sigma\varepsilon^{n}_{kl} - \delta\varepsilon^{*}_{kl}\right) . \end{aligned} \tag{D-2}$$

Subtracting state (D-1) from state (D-2) gives

$$\begin{aligned} C^{*}_{ijkl}\delta\left(\Sigma\varepsilon^{n}_{kl}\right) = \delta C^{s}_{ijkl}\left(\Sigma\varepsilon^{n}_{kl} - \varepsilon^{*}_{kl}\right) + C^{s}_{ijkl}\left(\delta\Sigma\varepsilon^{n}_{kl} - \delta\varepsilon^{*}_{kl}\right) \\ + \delta C^{s}_{ijkl}\left(\delta\Sigma\varepsilon^{n}_{kl} - \delta\varepsilon^{*}_{kl}\right) \end{aligned} \tag{D-3}$$

or

$$C^{*}_{ijkl}\delta\left(\Sigma\varepsilon^{n}_{kl}\right) = \delta\left[C^{s}_{ijkl}\left(\Sigma\varepsilon^{n}_{kl} - \varepsilon^{*}_{kl}\right)\right] + \delta C^{s}_{ijkl}\left[\delta\left(\Sigma\varepsilon^{n}_{kl}\right) - \delta\varepsilon^{*}_{kl}\right] . \tag{D-4}$$

But, noting that the tangent stiffness approach is given by

$$C^{T}_{ijkl}\left[\delta\left(\Sigma\varepsilon^{n}_{kl}\right) - \delta\varepsilon^{*}_{kl}\right] = \delta\left[C^{s}_{ijkl}\left(\Sigma\varepsilon^{n}_{kl} - \varepsilon^{*}_{kl}\right)\right] , \tag{D-5}$$

where $C_{ijkl}{}^{T}$ is the tangent stiffness of the matrix, it is clear that **(D-4)** may be written as

$$\underbrace{C^{*}_{ijkl}\delta\left(\Sigma\varepsilon^{n}_{kl}\right) = C^{T}_{ijkl}\left(\delta\Sigma\varepsilon^{n}_{kl} - \delta\varepsilon^{*}_{kl}\right)}_{\text{tangent stiffness approach}} + \delta C^{s}_{ijkl}\left[\delta\left(\Sigma\varepsilon^{n}_{kl}\right) - \delta\varepsilon^{*}_{kl}\right]. \tag{D-6}$$

Equation **(D-6)** infers that the tangent stiffness approach, *in principle, differs from* successive application of the secant stiffness approach by only a second order term which can be taken as arbitrarily small for small increments, provided the loading is proportional. Hence, the tangent stiffness approach is the logical analog of the secant stiffness method for incremental matrix plasticity.

A subtle difference, however, is introduced if the assumption is made in the tangent stiffness method that the stress-strain relationship of the comparison matrix material is given by

$$\dot{\sigma}^{o}_{ij} = C^{T}_{ijkl}\dot{\varepsilon}^{o}_{kl} \tag{D-7}$$

such that $C_{ijkl}{}^{To} = C_{ijkl}{}^{T}$ is assumed. By differencing the results of parallel solutions

from the current state employing C_{ijkl}^{To} and C_{ijkl}^{T}, respectively, in **(D-7)**, it can be shown that the error, ΔE, of the tangent stiffness approach with assumption **(D-7)** relative to successive application of the secant stiffness approach is given by

$$\Delta E = O\Big[\left|\left(C^{*}_{ijkl} - C^{T}_{ijkl}\right)\delta\left(C^{T\,-1}_{ijkl}\sigma^{o}_{ij} - C^{To\,-1}_{ijkl}\sigma^{o}_{ij}\right)\right| + \left|\delta C^{s}_{ijkl}\delta\left(\Sigma\varepsilon^{i}_{kl} - \varepsilon^{*}_{kl}\right)\right|\Big] . \qquad \textbf{(D-8)}$$

The notation O[*] denotes that the error is "on the order of" the quantity enclosed in the brackets. Clearly, the error is second order provided that either $C_{ijkl}^{*} = C_{ijkl}^{T}$, which is highly improbable, or that $C_{ijkl}^{T} = C_{ijkl}^{To}$, which is perhaps obvious. Hence, the assumption $C_{ijkl}^{To} = C_{ijkl}^{T}$ in the tangent stiffness approach will lead to first order error in representing the secant stiffness results unless

$$\left|\left(C^{*}_{ijkl} - C^{T}_{ijkl}\right)\delta\left(C^{T\,-1}_{ijkl}\sigma^{o}_{ij} - C^{To\,-1}_{ijkl}\sigma^{o}_{ij}\right)\right| \qquad \textbf{(D-9)}$$

is of second order.

There are several important regimes where **(D-9)** is satisfied, including elastic behavior of both phases and low volume fraction of reinforcement or phase property mismatch such that the matrix stress differs little from the average composite stress. Perhaps the most prevalent and important case is where the matrix work hardening behavior is slight which is common for ductile matrix materials. In this case, the variation of the magnitude of C_{ijkl}^{T} is small across a wide range of matrix plastic strain.

It must be emphasized that in a fully incremental approach, the matrix behavior is permitted to be path history dependent, unlike in the secant stiffness approach. Precise assignment of C_{ijkl}^{To} is therefore an impossible task in the general case. This is the basis for introducing the parameter β in the tangent stiffness approach, e.g. equation (3-14).

For situations where the constraint of the fibers on the matrix is high enough in the plastic regime to result in $\|\sigma_{ij}^{o}\| >> \|\sigma_{ij}^{m}\|$, β is introduced to effectively force the tangent stiffness toward values less than the actual matrix plastic stiffness, even in the transient yielding regime. This effect is perhaps most relevant in off-axis and shear loadings since matrix plasticity has little influence on behavior for loading nearly aligned with the fiber direction.

In summary, it appears that the tangent stiffness model in its general form is a quite simple, versatile and accurate approach for incremental elastic-plastic composite deformation. It requires no iteration at each loading increment and requires only constituent properties for user input.

APPENDIX E

CONSTITUENT PROPERTIES

E.1 Introduction

We investigated the inelastic behavior of two composite systems. The boron-aluminum system is a unidirectional, continuous fiber-reinforced composite for which the fibers are boron and the matrix is aluminum. The silica-epoxy system is a spherical particle-reinforced composite where the spherical particles are made of silica and the matrix is an epoxy resin. Listed below are the elastic properties of these constituent materials which were used in our investigation.

E.2 Constituent Properties of the Boron-Aluminum System

The boron fibers are considered elastic while the aluminum matrix is elastic-plastic in the B/Al system. Both the aluminum matrix and boron fibers were assumed isotropic. Their respective elastic properties are shown below.

	E_A (10^6psi) [GPa]	G_A (10^6psi) [GPa]	ν_A	E_T (10^6psi) [GPa]	G_T (10^6psi) [GPa]
6061 Al	10.5 [72.5]	3.95 [27.2]	0.33	10.5 [72.5]	3.95 [27.2]
Boron	58.0 [400.0]	24.2 [166.8]	0.20	58.0 [400.0]	24.2 [166.8]

where the subscript A corresponds to the 33 (fiber) or the "aligned" direction and the subscript T corresponds to the 12 or the "transverse" plane. E, G, and ν are the Young's modulus, shear modulus, and elastic Poisson's ratios, respectively. These properties were obtained from Dvorak and Bahei-El-Din (1987). The material properties used to characterize the flow of the matrix are listed in Appendix B.

E.3 Constituent Properties of the Silica-Epoxy System

In the silica-epoxy system, the silica is elastic and the epoxy is elastic-plastic. Both phases are assumed to be isotropic. From Weng (1988), the elastic properties are as follows:

	E (10^6psi) [GPa]	ν
Silica	10.6 [73.1]	0.18
Epoxy	0.458 [3.16]	0.35

The material properties used to characterize the flow of the matrix are listed in Appendix B.

APPENDIX F

ANISOTROPIC CONSTRAINT HARDENING AND THE χ FUNCTION

F.1 Introduction

In this thesis, we conducted a theoretical analysis of the inelastic behavior of metal-matrix composites reinforced with aligned, continuous fibers and attempted to model the experimental response of the Boron-Aluminum system. Due to the anisotropy associated with the aligned nature of the reinforcement and the high transverse shear stiffness of the boron fiber, constraint hardening is highly anisotropic in the boron-aluminum composite system.

In our tangent stiffness model (§ 3.1), we observed a hardening response in the plastic regime for off-axis loading because we did not take this constraint hardening phenomenon into consideration. Further investigation revealed that relief of constraint hardening in this composite system was due to rotation of the matrix plastic strain rate vector away from the fiber direction towards the transverse direction (which is the direction of least constraint). We incorporated this mechanism for constraint relief into our model via the χ function. With this χ function we computed an effective fiber stiffness which ensured a continuous transition to matrix-dominated behavior as is observed in the plastic regime for the boron-aluminum

composite system.

The purpose of this appendix is to explain this phenomenon of constraint hardening as it relates to composites reinforced by aligned, continuous fibers and provide a justification for the form of our proposed χ function. Furthermore, we will discuss how it might apply to different types of composite systems.

F.2 Anisotropic Constraint Hardening

To understand constraint hardening, let us consider an element of matrix material which is bounded on two sides by fibers (see Figure F-1). For an applied stress in the X_3-direction, the matrix material cannot contract laterally in the X_2-direction due to the high transverse shear stiffness of the boron fibers. This lateral constraint results in a stiffer response for loads applied in the fiber (X_3) direction. However, when a stress is applied in the transverse (X_2) direction, the matrix deforms "naturally" or in a matrix-dominated mode since there is no constraining effect on the top and bottom surfaces of the element. We can see that the level of constraint varies considerably between the fiber and transverse directions. Therefore, we say that the constraint hardening is anisotropic. It is important to realize that the fiber direction is the direction of greatest constraint while the transverse direction is the direction of least constraint.

F.3 Relief Mechanism for Anisotropic Constraint

It has been experimentally observed for off-axis loadings that boron-aluminum exhibits a transition to the so-called "matrix-dominated mode" of deformation in the plastic regime. Therefore, it is evident that there is a relief of constraint hardening effects associated with the presence of the stiff boron fibers. We must identify the mechanism responsible for this relief of constraint in order to successfully model the experimental behavior.

Dvorak and Bahei-El-Din (1988) observed that even for proportionally applied off-axis loadings there is nonproportionality of the plastic strains in the matrix. For an off-axis loading, the plastic strain rate vector, $\dot{\varepsilon}_{ij}^{pm}$, is initially collinear with the matrix stress rate (see Figure F-2). However, as plastic flow develops, $\dot{\varepsilon}_{ij}^{pm}$ rotates away from the fiber direction towards the direction of least constraint. This rotation of $\dot{\varepsilon}_{ij}^{pm}$ accounts for the observed nonproportionality of the plastic matrix strains. At this point, there is sufficient rationale to conclude that the rotation of $\dot{\varepsilon}_{ij}^{pm}$ is responsible for the observed relief of constraint hardening. To confirm this rationale, we analyzed the rotation of the matrix plastic strain rate vector, the results of which were presented in § 4.5 of the main thesis. We will restate those results here.

We utilized the results from our tangent stiffness model to analyze the rotation of $\dot{\varepsilon}_{ij}^{pm}$. It is important to remember that the tangent stiffness model accurately approximated the response of the composite in the initial yielding regime. Therefore, it is accurate up to approximately 0.1 or 0.2 % strain. Hence, we are justified in

using the results of this model in our analysis of $\dot{\varepsilon}_{ij}^{pm}$.

Referring to Figure 8, we see that in the 0° orientation the plastic strains remain proportional as indicated by the linearity of the plot of ε_{33}^{pm} versus ε_{22}^{pm}. However, in the off-axis orientations, there is curvature of the plot indicating increasing dominance of ε_{22}^{pm} and rotation of $\dot{\varepsilon}_{ij}^{pm}$ away from the fiber direction towards the direction of least constraint, the transverse direction. This analysis confirms our hypothesis that rotation of $\dot{\varepsilon}_{ij}^{pm}$ is the mechanism responsible for the relief of constraint hardening and the transition to a matrix-dominated response in the boron-aluminum composite system.

F.4 Analyzing Constraint Hardening Utilizing Wang's Representation Theorem

At this point, we have established that there is decreasing constraint hardening in the boron-aluminum composite associated with the development of plastic flow in the matrix due to rotation of $\dot{\varepsilon}_{ij}^{pm}$. If we define ψ_{ij} as

$$\psi_{ij} = \frac{\partial \sigma_{kk}^{m}}{\partial \varepsilon_{ij}^{pm}}, \tag{F-1}$$

then ψ_{ij} is clearly the rate of change of the hydrostatic constraint stress, σ_{kk}^{m}, with plastic matrix strain. In general, we may represent ψ_{ij} as an isotropic tensor function of the form

$$\psi_{ij} = \psi_{ij}\left(\hat{e}_3, \alpha_{kk}^{m}; \beta, \chi\right). \tag{F-2}$$

The unit vector $\hat{e}_3$ represents constraint hardening due to the anisotropy in the composite due to fiber reinforcement while α_{kl}^m represents constraint hardening in the matrix due to the impedance of dislocation motion by the presence of the reinforcement. The semicolon indicates implicit dependence of ψ_{ij} on the functions β and χ which are our proposed methods of representing constraint hardening effects in the composite. Using Wang's representation theorem, ψ_{ij} may be expressed in terms of the irreducible functionality basis of the pair $(\hat{e}_3, \alpha_{kl}^m)$ (Wang, 1970) as follows:

$$\psi_{ij} = \varphi_1(\alpha_{kl}^m, \hat{e}_3; \beta, \chi)\delta_{ij} + \varphi_2(\hat{e}_3, \alpha_{kl}^m; \chi)\hat{e}_3 \otimes \hat{e}_3 + \varphi_3(\alpha_{kl}^m; \beta)\alpha_{ij}^m + \varphi_4(\alpha_{kl}^m; \beta)\alpha_{ik}^m \alpha_{kj}^m \quad \text{(F-3)}$$

Here, ψ_{ij} is expressed as the sum of four isotropic tensor functions whose arguments are as shown above. The first term in the expression, φ_1, is included based on the formality of the representation but will drop out since the first invariant of ε_{ij}^{pm} is equal to zero. The second term, φ_2, represents constraint hardening in fiber-reinforced composites. The third and fourth terms, φ_3 and φ_4, represent constraint hardening in particle-reinforced composites. Since the second term and the third and fourth terms are representative of two completely different classes of composite materials, cross terms in the representation have been omitted. Also, joint invariants of α_{kl}^m have been omitted as second order.

We will now take a closer look at constraint hardening in fiber-reinforced

composites using Wang's representation theorem. For fiber-reinforced composites, we may in general express ψ_{ij} using the second term in (F-3) as

$$\psi_{ij} = \psi_{ij}\left(\hat{e}_3, \alpha_{kl}^{m}; \beta, \chi\right) . \tag{F-4}$$

From § 3.2 of the main thesis, we recall that constraint hardening due to α_{kl}^{m} is isotropic and that constraint hardening associated with $\hat{e}_3$ is anisotropic. We may think of β as the function utilized to represent isotropic constraint hardening while χ is the function utilized to represent anisotropic constraint hardening. If we refer to Figure F-3, we can see that the anisotropic constraint hardening due to β and χ is dominant over isotropic constraint hardening for fiber-reinforced composites. This graphical illustration in combination with our analysis in § 3.2 leads us to conclude that isotropic constraint hardening is of second order importance in the fiber-reinforced composite.

F.5 Development of the χ Function

We have shown that relief of constraint in the fiber-reinforced composite is associated with the rotation of $\dot{e}_{ij}^{pm}$ of away from the fiber direction during off-axis loadings. Furthermore, we have shown that constraint hardening is an anisotropic phenomenon in this class of composites.

From § 3.2, the hydrostatic constraint stress rate is

$$\dot{\sigma}_{kk}^{m} = \xi \left| \dot{e}_{kl}^{pm} \right| n_{33} = \xi \dot{e}_{33}^{pm} , \tag{F-5}$$

where n_{33} is the component of n_{ij}, the unit normal vector in the direction of $\dot{\varepsilon}_{ij}^{pm}$, in the fiber direction, $\hat{e}_3$ and χ is an isotropic scaler function of $\hat{e}_3$ and α_{kl}^{m}. As plastic flow in the matrix develops and $\dot{\varepsilon}_{ij}^{pm}$ rotates away from $\hat{e}_3$, n_{33} decreases in magnitude. We also know from experimental evidence that the boron-aluminum system demonstrates a rapid transition to matrix-dominated behavior (see experimental data plotted in Figure 10, for example).

Utilizing these facts, we are able to model constraint relief by effectively reducing the stiffness of the fiber utilizing the χ function as follows:

$$\hat{C}_{ijkl}^{*} = \left(C_{ijkl}^{*} - C_{ijkl}^{T}\right)\chi + C_{ijkl}^{T} \qquad \text{(F-6)}$$

where χ takes on the form

$$\chi = \exp\left[-\left\{\frac{h_o}{h}\left(1-\frac{n_{33}}{\sqrt{2/3}}\right)\right\}^{N}\left(1 - \frac{a}{c}\right)\right]. \qquad \text{(F-7)}$$

The idea here is to facilitate the transition to matrix-dominated behavior (the tangent stiffness, C_{ijkl}^{T}) by effectively reducing the fiber stiffness from C_{ijkl}^{*} in the elastic regime to C_{ijkl}^{T} in the inelastic regime.

Some explanation of the terms in (F-7) is required. The asymptotic plastic hardening modulus, h_o, is indicative of the asymptotic plastic behavior of the matrix material. Therefore, the ratio h_o/h is representative of the plastic strain state of the matrix. In the elastic regime, where $h \to \infty$, $h_o/h \to 0$ and $\chi \to 1$. However, as plastic flow develops, $h_o/h \to 1$ and contributes to the overall value within the brackets.

The component of n_{ij} in the $\hat{e}_3$ direction, n_{33}, is indicative of the rotation of $\dot{\varepsilon}_{ij}^{pm}$. As plastic flow develops and constraint is relieved, $n_{33} \rightarrow 0$. As indicated by the experimental data, matrix-dominated behavior is realized earlier on for more off-axis orientations (e.g. 45°) than for off-axis orientations closer to the fiber direction (e.g. 10°). This is because n_{33} is initially greater for the 10° orientation say than the 45° orientation. Therefore, it takes longer for matrix-dominated behavior to develop in the 10° orientation.

As stated above, the boron-aluminum system exhibits a rapid transition to matrix-dominated behavior. This may not be the case for other composite systems. The exponent N allows us to dictate the rate of transition to matrix-dominated behavior. In general, the higher the transverse shear stiffness of the fiber, the faster the transition. For the boron-aluminum system, we fitted to the 15° orientation using N=4.

The aspect ratio a/c is included to take into account the nature of the reinforcement. For aligned, continuous fibers, a/c = 0. For spherical, particle reinforcement, a/c = 1.

Taking the above factors into consideration, we can see that the χ function generally behaves as shown in Figure F-4. When there is no plastic flow, $\chi = 1$ and $\hat{C}_{ijkl}^{\bullet} = C_{ijkl}^{\bullet}$ for all off-axis orientations. As plastic flow develops, χ exponentially decays to zero at a rate which is dependent on the loading orientation and the transverse shear stiffness of the fiber. Figure F-4 is intended to give a general

representation of this behavior and is not indicative of a particular system.

F.6 Conclusion

In summary, the χ function is a mathematical means of modeling the relief of anisotropic constraint hardening in fiber-reinforced composites. It is theoretically based on the fact that constraint is relieved by rotation of $\dot{e}_{ij}^{pm}$ away from $\hat{e}_3$ during the development of plastic flow of the matrix and that matrix-dominated behavior is exhibited in the plastic regime.

Its development was based solely on our attempts to model the inelastic behavior of boron-aluminum. Applications to other systems such as graphite-aluminum have as yet to be investigated. Isotropic constraint hardening in the boron-aluminum composite was neglected as second order because of the dominance of anisotropic constraint due to the high shear transverse stiffness and anisotropy of the reinforcement. Therefore, the β parameter and the concept of the comparison matrix material were not incorporated into our attempts to model boron-aluminum. We recognize that for other systems, this may indeed not be the case. A combination of β and χ may be required to successfully model the inelastic behavior of systems with more compliant reinforcement.

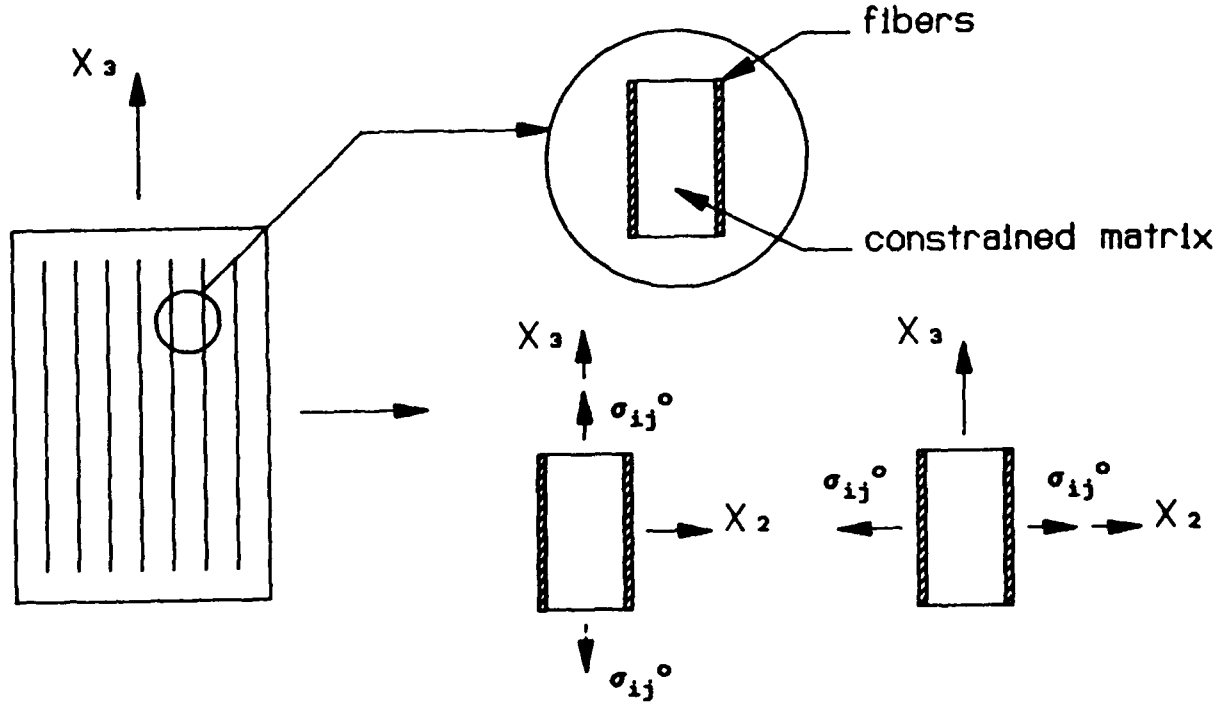

Figure F-1. Constraint hardening in fiber-reinforced composites.

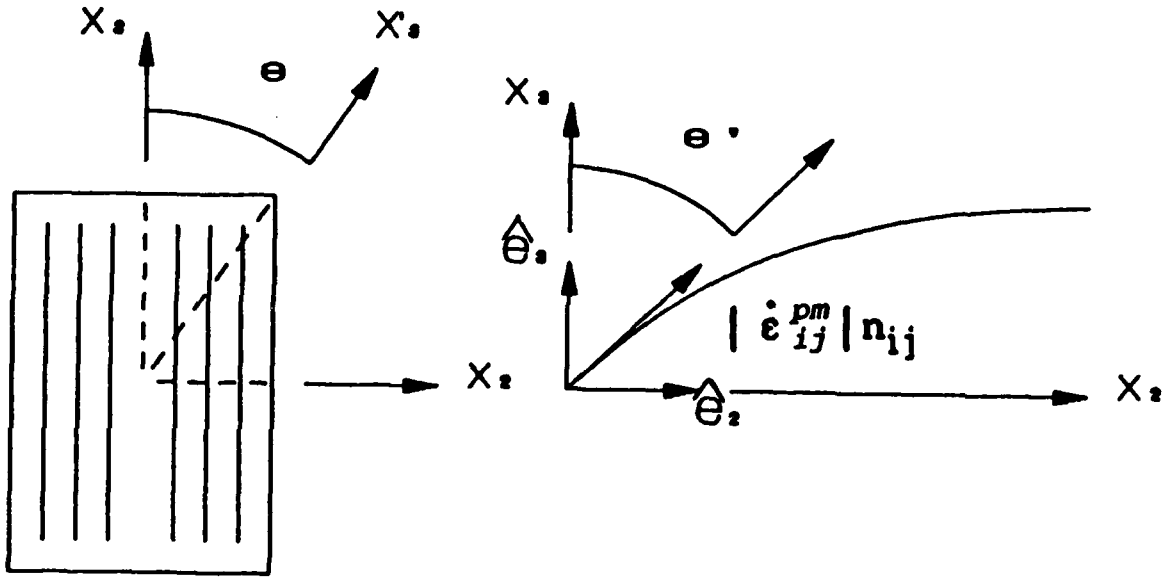

Figure F-2. Rotation of the matrix plastic strain rate vector away from the fiber direction during the development of plastic flow in the matrix material.

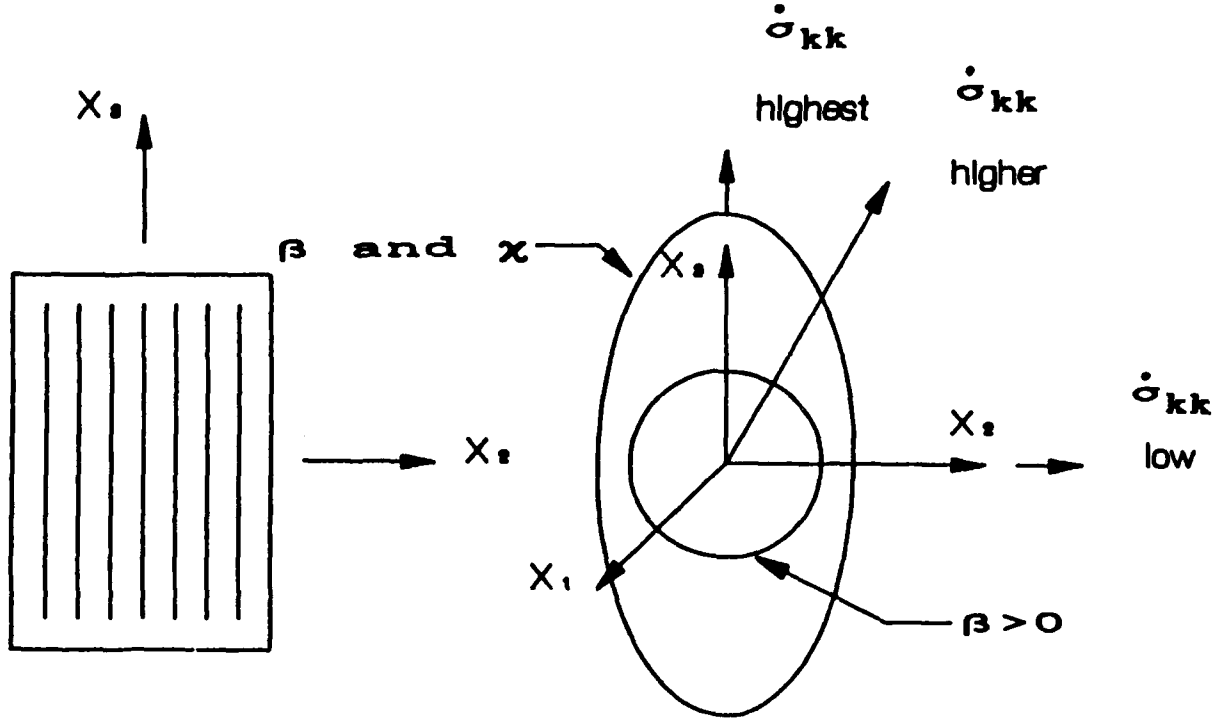

Figure F-3. Anisotropic constraint hardening in fiber-reinforced composites.

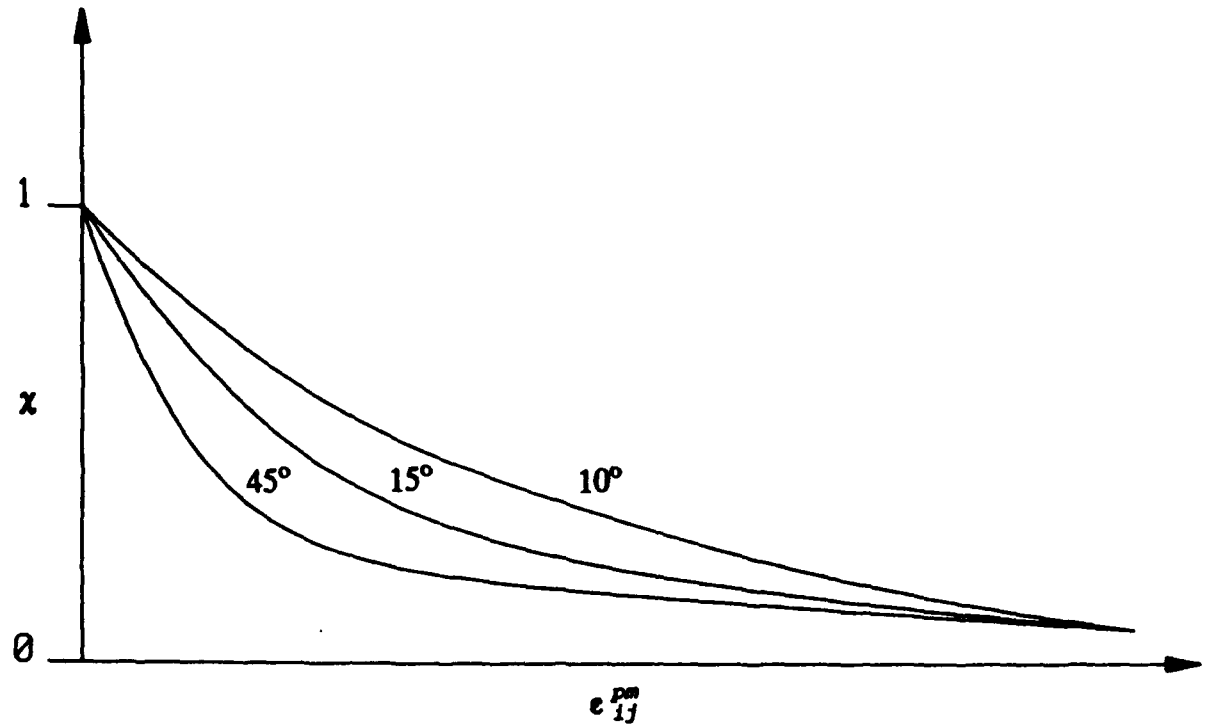

Figure F-4. Rate of decay of χ for various off-axis orientations as a function of plastic matrix strain.